2010

Investigating the Effects of Various Crowd Characteristics on the Dynamic Properties of an Occupied Structure

Robert Joseph Firman III
Bucknell University

Follow this and additional works at: https://digitalcommons.bucknell.edu/honors_theses

Part of the Civil Engineering Commons

Investigating the Effects of Various Crowd Characteristics on the Dynamic Properties of an Occupied Structure

by

Robert J. Firman III

A Proposal Submitted to the Honors Council

For Honors in Civil & Environmental Engineering

May 3, 2010

Approved by:

Adviser: Kelly A. Salyards

Department Chairperson: Jeffrey C. Evans

**Investigating the Effects of Various Crowd Characteristics
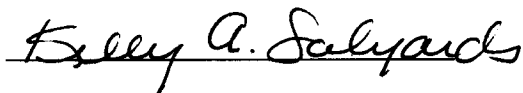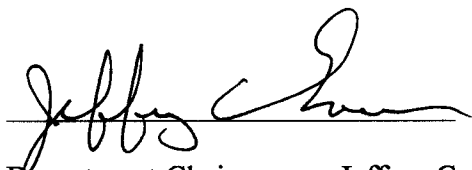on the Dynamic Properties of an Occupied Structure**

by

Robert J. Firman III

A Proposal Submitted to the Honors Council

For Honors in Civil & Environmental Engineering

May 3, 2010

Approved by:

_____

Adviser: Kelly A. Salyards

_____

Department Chairperson: Jeffrey C. Evans

ACKNOWLEDGEMENTS

TABLE OF CONTENTS

LIST OF TABLES

LIST OF FIGURES

Figure	Title	Page

Figure   Title   Page

ABSTRACT

One of the challenges for structural engineers during design is considering how the structure will respond to crowd-induced dynamic loading. It has been shown that human occupants of a structure do not simply add mass to the system when considering the overall dynamic response of the system, but interact with it and may induce changes of the dynamic properties from those of the empty structure. This study presents an investigation into the human-structure interaction based on several crowd characteristics and their effect on the dynamic properties of an empty structure. The dynamic properties including frequency, damping, and mode shapes were estimated for a single test structure by means of experimental modal analysis techniques. The same techniques were utilized to estimate the dynamic properties when the test structure was occupied by a crowd with different combinations of size, posture, and distribution.

The goal of this study is to isolate the occupant characteristics in order to determine the significance of each to be considered when designing new structures to avoid crowd serviceability issues. The results are presented and summarized based on the level of influence of each characteristic. The posture that produces the most significant effects based on the scope of this research is standing with bent knees with a maximum decrease in frequency of the first mode of the empty structure by 32 percent at the highest mass ratio. The associated damping also increased 36 times the damping of the empty structure. In addition to the analysis of the experimental data, finite element models and a two degree-of-freedom model were created. These models were used to

gain an understanding of the test structure, model a crowd as an equivalent mass, and also to develop a single degree-of-freedom (SDOF) model to best represent a crowd of occupants based on the experimental results. The SDOF models created had an average frequency of 5.0 Hz, within the range presented in existing biomechanics research, and combined SDOF systems of the test structure and crowd were able to reproduce the frequency and damping ratios associated with experimental tests.

Results of this study confirmed the existence of human-structure interaction and the inability to simply model a crowd as only additional mass. The two degree-of-freedom model determined was able to predict the change in natural frequency and damping ratio for a structure occupied by multiple group sizes in a single posture. These results and model are the preliminary steps in the development of an appropriate method for modeling a crowd in combination with a more complex FE model of the empty structure.

CHAPTER 1: INTRODUCTION AND LITERATURE REVIEW

1.1 Introduction

As the engineering industry continues to progress into the future with technological advances and a desire to maximize efficiency, structural engineers are faced with many challenges. One such challenge, related to the current trend of longer spans and the use of lightweight materials, is increased flexibility and potential dynamic serviceability concerns involving the perception and comfort associated with vibration. The increased flexibility tends to reduce the fundamental natural frequency and it is more probable that external excitations will be able to initiate resonance or a near-resonance condition. Resonance occurs when the excitation frequency (or one of its harmonics) matches, or nearly matches, the natural frequency of the structure and can result in serviceability issues associated with excessive vibration. Serviceability design of structures to be occupied by large crowds such as stadium structures is especially important because excessive vibration could lead to panic within the crowd and jeopardize safety.

The challenge for structural engineers begins during design when considering how the structure will respond to crowd-induced dynamic loading. It has been shown that human occupants of a structure do not simply add mass to the system when considering the overall dynamic response of the system, but interact with it and may induce changes in the dynamic properties, such as frequency, damping, and mode shapes, from those of the empty structure. Dynamic measurements taken from occupied structures that have shown signs of potential serviceability issues suggest that the change

in dynamic properties can be significant and vary greatly. Because the dynamic response and performance of a structure can be influenced considerably by a change in properties, the effects of human-structure interaction need to be incorporated into design to avoid future serviceability issues while still allowing for the most efficient design.

1.2 Purpose of research

The purpose of this research is to improve the understanding of relationships between the empty structure dynamic properties and occupied structure dynamic properties with respect to varying crowd characteristics and ascertain if a simple model of a crowd can be used to predict these relationships for design purposes. The crowd characteristics that are studied include the crowd distribution, the mass ratio of the empty to occupied structure, and the stationary posture of the crowd.

1.3 Overview of research

To accomplish the objectives of this research, a test structure specifically designed for a previous vibration serviceability research project, was selected to ensure a sufficient dynamic response (Raebel, 2000). The dynamic properties of the structure were experimentally determined for a variety of human-occupancy configurations. Each configuration involved a different combination of the crowd characteristics of distribution, mass ratio, and posture of the crowd. Relationships among the dynamic properties derived experimentally from each of these scenarios and the dynamic properties derived experimentally from the empty structure are presented herein. An appropriate crowd single degree-of-freedom crowd model is also presented.

1.4 Literature review

1.4.1 Overview of dynamic load-induced vibration serviceability

Structures are designed for two types of limit states, strength and serviceability; where a limit state is a set of criteria that must be satisfied when a structure is in operation. Strength limit states are more commonly recognized and relate to the safe carrying capacity of a structure. If not properly designed to meet strength limit states, a structure could fail catastrophically. The other type of limit state that is less commonly known by the general population is a serviceability limit state. Serviceability limit states involve maintaining an acceptable level for perception, comfort, or functionality in areas including deflection or vibration (Geschwindner, 2008). Dynamic load-induced vibration is a specific serviceability concern referring to a potential level of discomfort associated with unexpected vibrations generated by the occupants of a structure.

Dynamic load-induced vibration serviceability can affect a large number of people. Crowds can be synchronized to produce large dynamic loads on a structure and generate excessive vibration that may produce panic or discomfort. Common structures in this category include stadium structures, grandstands, and any other long span structure. These structures are often the most susceptible to excessive vibrations because they have low mass and damping and are easily excited by the dynamic motion of occupants. The first step in understanding dynamic load-induced vibration is understanding how stationary occupants can affect the dynamic properties of a structure.

1.4.2 Existing serviceability guidance

The majority of design standards in the United States, and worldwide, are primarily concerned with addressing strength limit states and avoiding structural failure in its most catastrophic form (Ebrahimpour & Sack, 2005). There is, however, limited guidance available for vibration serviceability. In the US, the most widely recognized source of vibration serviceability guidance exists within AISC's Design Guide 11: Floor Vibrations Due to Human Activity (Murray & Allen, 1997). Guidelines in this document include references to human comfort, design for walking excitation, and design for rhythmic excitation. However, no reference is made to the interaction that exists between occupants and the structure, a phenomenon that allegedly can drastically alter the dynamic properties. This may be in part because Design Guide 11 was first released over a decade ago but is also due to the fact that Design Guide 11 is not specifically intended to be used for heavily occupied structures. Similar guidance exists in the United Kingdom through interim guidance titled Dynamic Performance Requirements for Permanent Grandstands Subject to Crowd Action. This reference places a limit on the natural frequency of structures where vibration serviceability should be considered in design (IStructE, 2001).

Human-structure interaction is one of the missing components in all of the current guidelines for dynamic serviceability throughout the world. Despite the potential for serviceability problems, limited resources have been spent in developing a method to investigate, understand, and quantify the effects that occupants can have on structural dynamic properties. The few attempts at incorporating the human component into design

that have been made are vague or unproven. For example, in the UK, the *Guide to Safety at Sports Grounds* suggests incorporating occupants simply as an additional mass in design (Bernan, 2008). Other research suggests that occupants must be considered as single or multiple degree of freedom systems and not just as mass alone (Sachse & Pavic, 2003).

1.4.3 Human-structure interaction

The effects of human-structure interaction are most prevalent in civil engineering structures consisting of lightweight materials and long, unsupported spans. By incorporating these two components into design, structures are likely to have lower natural frequencies, around the range of 2 to 6 Hz (Harrison & Yao, 2008). This frequency range is well within the range which can be excited by occupants and also within the range of the natural frequency of the human body, as will be discussed in Section 1.4.5.

The participation of occupants in these structures can be considered as passive or active, but for live events it is often a combination of both. Passive occupant participation exists when occupants are relatively stationary on a structure. Two of the most common forms of passive activity are sitting and standing. In each form, the occupants' position does not change substantially in time. In contrast, active occupant participation encompasses all other forms of rhythmic movement where the occupants' position varies in time. These movements, including jumping and bobbing, are often in synchronization with other occupants or an audio or visual stimulus (Sim, 2006). Unlike

passive participation, active participation does not affect the dynamic properties of the structure unless the occupants remain in constant contact with the structure (i.e. bobbing).

This study focused exclusively on the effects of passive occupants on a structure. The purpose is to gain a better understanding of the passive component before exploring the more realistic combined component of both passive and active.

1.4.4 Relevant dynamic studies

One of the first mentions of human-structure interaction appeared in a research study conducted by Lenzen in 1966. This research involved verifying a commonly used mass-only system to model a human occupant. As expected the mass-only model decreased the natural frequency of the test structure. However, the damping was increased when a human occupant was used instead of its equivalent mass. Because of these differences, it was suggested that the equivalent mass model is too simplistic and does not account for the dynamic properties and complexities of the human body. This research that took place over half a century ago was one of the first acknowledgements of the existence of human-structure interaction and sparked a slow but growing interest (Lenzen, 1966).

A more recent example occurred at Twickenham Stadium in the UK in the early 1990s, where the first natural frequency of an occupied section of the stadium was reduced by more than 3 Hz due to the presence of occupants. Also, an additional mode

was created with a frequency slightly higher than the original unoccupied, first natural frequency (Ellis & Ji, 1997). The results, shown in

Table **1**, are from several different frames in the stadium, all having an average unoccupied first natural frequency of 7.70 Hz. Similar results in frequency reduction were also seen with an occupied temporary grandstand with a much higher empty natural frequency of 16 Hz (Ellis & Ji, 1997).

Table 1: Frequency results from study of Twickenham Stadium (Ellis & Ji, 1997).

	Frequency (Hz)		
Example	Empty 1st mode	Occupied 1st mode	Occupied 2nd mode
Frame 5	8.55	5.44	8.72
Frame 9	7.32	5.41	7.91
Frame 11	7.24	5.13	7.89

The authors of the Twickenham Stadium study continued their research with laboratory tests performed on a simply supported, reinforced concrete beam. Dissimilar to the results obtained from both in-service structures, the laboratory results revealed an increase in natural frequency when one individual occupied the beam. Although the natural frequency of this test structure, 18.68 Hz, was much higher than the stadium frames, the unexpected results provide further motivation to develop a better understanding for the human-structure interaction. From these examples, it appears that the unoccupied natural frequency of the structure can influence the characteristics of the structure when occupied. This is helpful in understanding that different structures will respond differently when occupied, but there is currently no method for predicting which effect will be encountered to allow it to be taken into account for serviceability design.

Similarly to the first set of results from Twickenham Stadium, Littler observed a decrease in the first natural frequency of a retractable grandstand (Littler, 2000). Not only did the natural frequency of the occupied structure decrease, but also the decrease in this example varied based on the posture of the occupants. In this example, seated occupants reduced the natural frequency slightly more than when occupants were standing. However, this study is based on a single structure and results may or may not be typical for all structures, thus the need to perform similar studies on structures with different empty natural frequencies. Also, there is no description of specific standing posture which will be proven to be important in this study per Chapter 4.

Laboratory results for a single person test rig, as shown in Figure 1, resulted in an increase in natural frequency as concluded by Duarte and Ji (2009). The rig was designed to be single degree-of-freedom test structure consisting of a circular steel plate supported by three identical, equally spaced steel springs. This study was conducted by comparing fifteen different human-rig setups with the properties obtained from the empty rig (Duarte & Ji, 2009). The results of this study are limited because they only include the effects of one person on the test rig, a scenario that is unlikely to exist or even cause concern in a real structure. Also, the mass of the test subject is more than twice that of the test rig, a value inconsistent with typical properties of in-service structures (Dougill, 2005). The small-scale nature of this study does not provide particularly relevant guidance for human-structure interaction when considering civil engineering structures, but it does indicate that the results for an individual on small test rig cannot simply be extrapolated to a larger group size.

Figure 1: Single person test rig consisting of two steel plates and three stiff springs (Duarte & Ji, 2009).

Separate studies by Brownjohn, Hothan, and Falati expanded upon the posture component of the human-structure interaction (Brownjohn, 1999; Hothan, 2008; Falati, 1999). Each study showed that crowd posture affected the change in natural frequency and damping, but experimental testing was only performed with one or two occupants. Each study also experimented with equivalent mass and the results confirmed Lenzen's original observation.

From these examples and others, several general observations can be made (Sachse & Pavic, 2003). First, the occupied natural frequency is dependent on several factors including the natural frequency of the empty structure, the mass ratio of the empty to occupied structure, and the occupant posture. Second, laboratory tests performed on small-scale test rigs generally result in an increase in natural frequency when occupied. This is either due to the high natural frequency of the test rig or the small-scale configuration that is not realistic for actual structures.

1.4.5 Biomechanics

There has been a considerable amount of research conducted in the area of biomechanics for industries such as aerospace and transportation. From these industries, various single and multiple degree-of-freedom systems have been proposed as methods to model the human body. However, these industries and the corresponding research focus mainly on vibrations and deflections of large amplitudes for a single individual. In contrast, vibrations in civil structures are limited to smaller amplitudes and must consider groups of individuals or crowds. For this reason, the validity of these models for structural engineering applications is debatable. Two of these models are shown in Figure 2 including a simple and more complex human-body model.
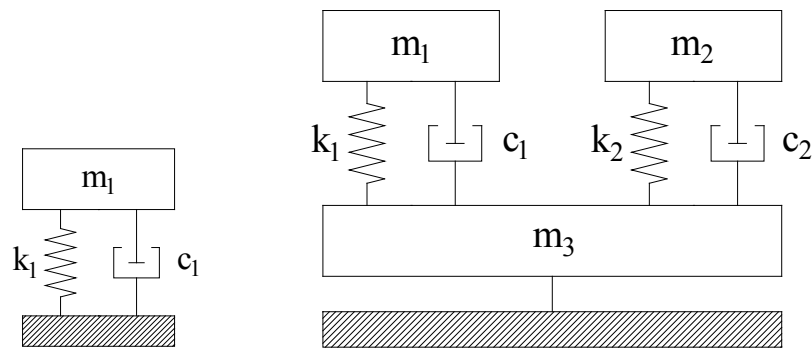
Figure 2: Human body models, single degree-of-freedom system (left), two degree-of-freedom system with non-vibrating mass (right) (Sachse & Pavic, 2003).

One piece of information from these industries that can be utilized is the average natural frequency of the human body in the vertical direction. This range lies between 4 and 6 Hz depending on an individual's age, gender, body type, and posture (Wasserman & Wasserman, 2002). This range helps to explain the complexity and difficulty in understanding crowd dynamics and the resulting human-structure interaction.

It is also important to note that the average natural frequency of the human body is within the range of the frequency of most structures when human-structure interaction is involved. The human body is more sensitive to vibration within this range, increasing the potential for uneasiness and the occurrence of widespread panic. There has been much written elsewhere on human sensitivity to vibrations and human level of comfort that will not be discussed here, mainly because human discomfort was not measured during this study (Ebrahimpour & Sack, 2005).

1.5 Thesis overview

Chapter 2 outlines the experimental methodology applied in this research, including details of the experimental test structure, experimental equipment, measurement placement, and the various crowd characteristics. The experimental testing procedure for each of the given test days is outlined.

Experimental analysis methods are presented in Chapter 3 aiming to show the progression of the methods employed throughout the research process and specifically the steps taken in estimating the dynamic properties from experimental test results. Experimental modal analysis techniques, data acquisition procedures, curve-fitting approach using the ME'scope software package, and general data organization are discussed.

Chapter 4 discusses the results obtained from the experimental procedures beginning with the dynamic properties of the empty structure. The results for the first

mode of the system in terms of crowd distribution, the mass ratio of the empty to occupied structure, and the posture of the crowd are presented. These results are further discussed in terms of design considerations and the limitations of these results.

The modeling techniques in this research are used to gain a preliminary understanding of the test structure, model a crowd as an equivalent mass, and also to develop a single degree-of-freedom (SDOF) model representing a crowd are discussed in Chapter 5. A finite element model of the test structure was created using SAP2000 and a simplified model was created in MASTAN2. Additionally, a single degree-of-freedom (SDOF) system representing the test structure was modeled in Matlab. The results and limitations associated with the modeling are discussed.

Chapter 6 presents a summary of the results from this study including the conclusions from estimating the dynamic properties of the test structure based on varying crowd characteristics and the conclusions pertaining to the modeling. Recommendations for future work are also presented.

CHAPTER 2: EXPERIMENTAL METHODOLOGY

2.1 Preliminary activities

2.1.1 Selection and description of experimental test floor

The test floor selected for this research, located at The Pennsylvania State University, was specifically designed as a flexible floor for vibration serviceability research. Figure 3 and Figure 4 show structural drawings of the test structure and an image taken during testing is shown in Figure 5. The floor system consists of five equally spaced 14K4 joists supported at each end by a W8x13 girder. The overall dimensions of the floor are 27 feet by 11 feet, including a 6-inch overhang on all edges. The steel joists support a 2.5-inch normal weight concrete slab on 1-inch form deck. The entire structure is supported by pipe columns located in each corner that are not intended to participate in the dynamic response of the floor. The first natural frequency of the floor, as determined by the methods outlined in AISC's Design Guide 11, is 6.82 Hz. Corresponding calculations are presented in Appendix A. Previous experimental research determined a first natural frequency of 7.04 Hz (Raebel, 2000).
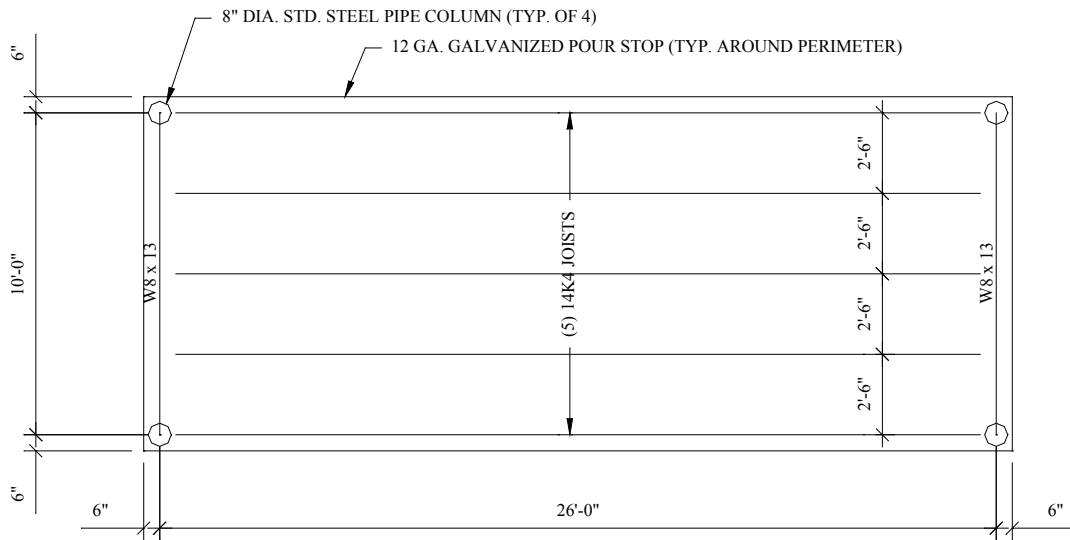
Figure 3: Plan view of test structure (Raebel, 2000).
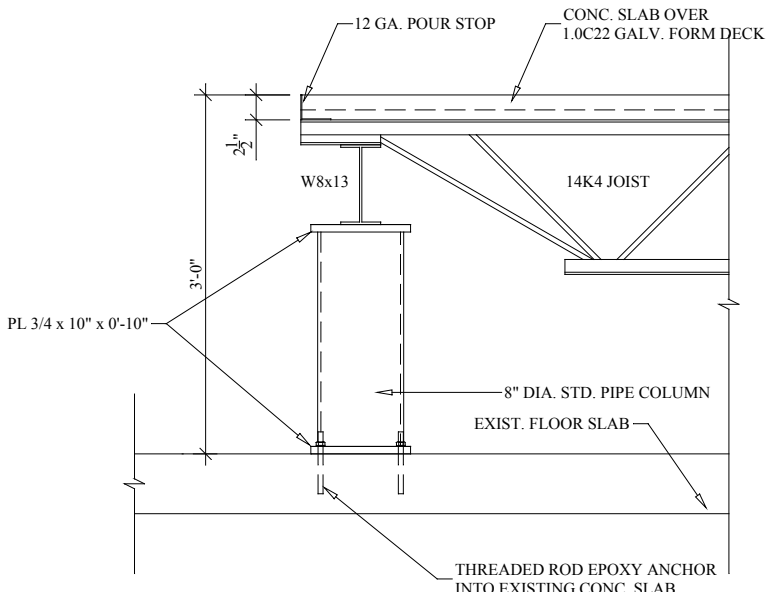
Figure 4: Section view through beam (Raebel, 2000).

Figure 5: Empty structure with electrodynamic shaker and accelerometers shown.

2.1.2 Description of experimental equipment and software

Data collection utilized a personal computer and eZ-Analyst, a real-time vibration and acoustic analysis software package produced by Measurement Computing Corporation's IOtech line of products. Two eight-channel dynamic signal conditioning modules, IOTech's model WBK18, were connected to the main acquisition unit, a WaveBook516/E. This configuration allowed for the use of a maximum of sixteen acceleration input channels and also two output channels. Refer to Chapter 3 for details and capabilities of eZ-Analyst. A diagram of the full equipment setup can be seen in Appendix B.

One of the output channels of the WaveBook was used to send a voltage signal generated within the eZ-Analyst software to an amplifier. The amplifier from APS Dynamics, model 145, amplifies the voltage signal and sends it to the electrodynamic

shaker, also from APS, model 400. The force output by the shaker was measured by the combined signal of four load cells that were part of a custom force plate. The signals from each load cell were combined in a junction box and one force signal was returned to and recorded by the data acquisition system.

The response of the structure was measured by seismic accelerometers from PCB Piezotronics, model 393A03. These accelerometers are capable of recording frequency responses within the range of 0.5 to 2000 Hz. The accelerometers were secured to the surface of the test structure using modeling clay and duct tape, as recommended by the manufacturer when more permanent attachment is not possible, and were connected to the data acquisition system by means of insulated cables. Calibration factors for the force plate and accelerometers are presented in Appendix C.

Modal parameters of the test results were estimated using Vibrant Technology's ME'scopeVES 5.0. This software package allows for frequency response functions (FRFs), defined in Chapter 3, to be directly imported from the eZ-Analyst software used for data acquisition. Using FRFs from test results and a simple model that was constructed within ME'scope, natural frequencies, damping ratios, and mode shapes were estimated. The ME'scope software package utilizes various methods of curve fitting a function to the experimentally measured FRFs from each measurement location for a specific test. This curve-fitting process is often referred to as an art integrated with the science behind the analysis methods. Details pertaining to the analysis methods performed with ME'scope are discussed in Chapter 3.

A finite element model of the test structure was created in Computer & Structures, Inc.'s SAP2000 (Computers and Structures, 2005). This model is used as a preliminary model to verify the location of nodal lines and also estimate the stiffness of the test structure. The first five mode shapes from the finite element model are shown in Figure 6 and were used to determine the measurement locations discussed in Section 2.1.3 and 2.1.4. MASTAN2, an interactive structural analysis program, was also utilized to create a simpler finite element model to explore the effects of an equivalent mass on the test structure (MASTAN2, 2010).

An additional single degree-of-freedom (SDOF) system was created in Matlab to model the test structure as a simple system and facilitate the combination of a crowd model with the empty structure and estimate the effects of human-structure interaction. The results from the combined model will be compared to those from experimental testing. Chapter 5 provides additional modeling information.
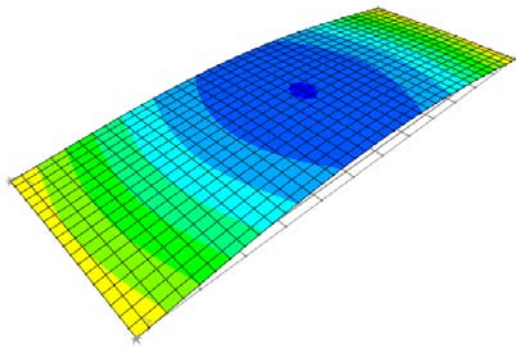
a. SAP Mode 1
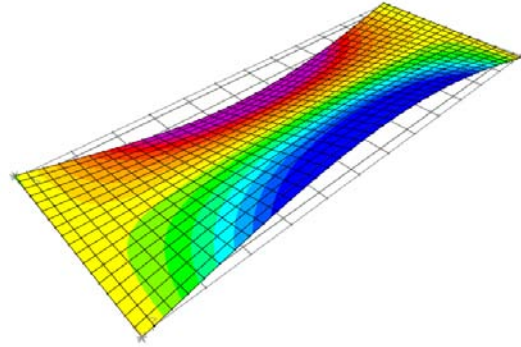
b. SAP Mode 2
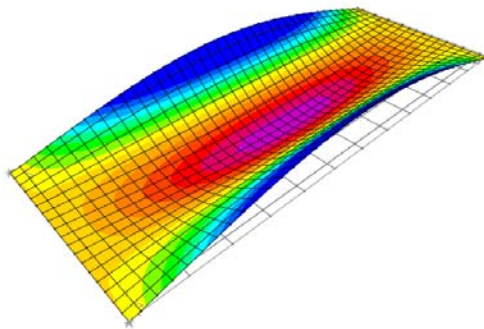
c. SAP Mode 3
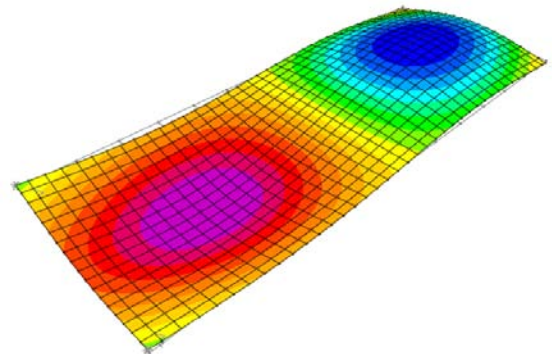
d. SAP Mode 4
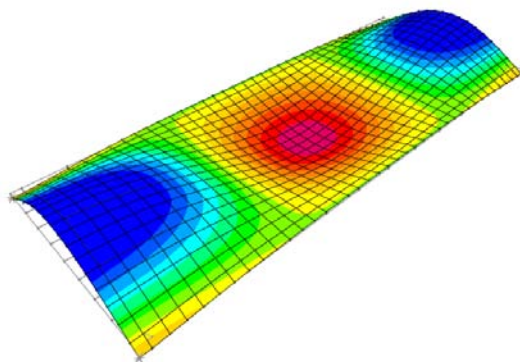
e. SAP Mode 7

Figure 6: First five mode shapes from SAP finite element model.

2.1.3 Location and description of excitation

The electrodynamic shaker was placed at a location on the test structure that would be able to properly excite the first five modes. For a simple rectangular floor, this location is slightly offset from the center of the floor in both the longitudinal and transverse directions. The offset eliminates the chance that the shaker is placed on a nodal line of one of the first several modes. If the shaker were to be placed on one of these nodal lines, the structure would not be excited at that particular frequency and the associated mode shape would not appear in the results.

The electrodynamic shaker received a signal that is known as a chirp or swept sine signal. This signal consists of a sinusoidal signal with varying and increasing frequency over a specified frequency bandwidth for a finite time interval. For this research, an 8-second signal was utilized with a starting frequency of 1 Hz and an ending frequency of 50 Hz.

Each individual test consists of five 8-second chirp signals and the results from each test were combined using statistical averages. By averaging the results from five chirp signals into one test, the experimental data was able to be compared. One way that this was done was by the use of a coherence function. The coherence is the measure of how well the output is linearly related to the input and requires multiple individual signals to be combined (Raebel, 2000). A coherence value will always be between zero and one, where a value of unity suggests that two FRFs are identical. For this study, the

minimum acceptable value of coherence is 0.80 which is reasonable for civil engineering structures.

2.1.4 Location and description of response measurement

Fourteen measurement locations were distributed evenly across the entire test structure as shown in Figure 7.   Accelerometers were placed in a pattern similar to the one presented by Raebel that proved to provide a sufficient representation of the test structure for analysis purposes (Raebel, 2000).   In general, the accelerometer locations were along the centerline of both of the edge joists and the center joist.   One accelerometer was moved from the center joist and placed at the location of the shaker. The purpose of this was to provide a driving point FRF. At this location all resonances are separated by anti-resonances, one of the several characteristics of this particular FRF that is useful during analysis (Avitabile, 2001). Figure 7 also shows the location of the shaker and force plate.
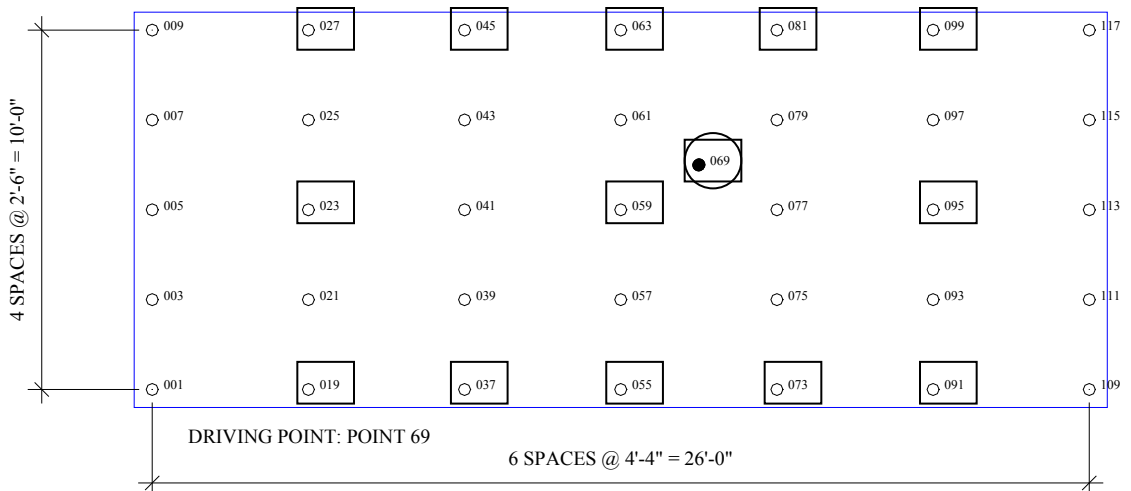
Figure 7: Test grid. Accelerometer locations are boxed. Electrodynamic shaker location is circled (Raebel, 2000).

2.2 Participant information

There were a total of thirty-three participants that volunteered for experimental testing, while the maximum used at any given time was nineteen. Of these individuals, five were female and twenty-eight were male. See Table 2 for additional information in regards to testing participants. The majority of the volunteer participants were students at Penn State University, either undergraduate or graduate. Research personnel from Bucknell University also acted as test subjects. Each participant was given a brief overview of the purpose for research and the overall testing procedure prior to experimental testing.

Table 2: Summary of occupant information.

	Height (ft-in)	Weight (lbf)	Age
Average	5-11	187.6	23
Minimum	5-4	123.4	20
Maximum	6-6	314.8	49
Female	5		
Male	28		

Research involving human subjects requires an approval from the Institutional Review Board (IRB). An online training course was completed and a proposal summarizing the experimental procedure and subject participation was also submitted and approved. Participants were required to complete a pre-approved consent form in accordance with the approved IRB regulations for this research. A sample consent form can be seen in Appendix D.

2.3 Occupant characteristics

2.3.1 Posture

There were three different postures used throughout this study. For all postures, participants were instructed to remain as still as possible throughout the duration of each individual test. By remaining still throughout the entire duration of a test, irregularities in response data could be minimized and unwanted vibrations not associated with the natural frequencies of the structure could be limited as well. The testing personnel would notify participants when measurements were being recorded to help eliminate excess movement during a particular test. To avoid any possible balance problems or other excess movement, participants were instructed to set their sight directly at the wall in front of them.

The three individual postures are discussed briefly and examples of each can be seen in Figure 8.

1. <u>Standing (straight knees)</u> – standing upright with hands directly at the side of the body, palms facing inward. Knees not locked, but in a casual resting position.
2. <u>Standing (bent knees)</u> – standing upright with hands directly at the side of the body, palms facing inward. Knees slightly bent in a position that can be sustained for a minute's duration.
3. <u>Seated</u> – sitting on bench comfortably with knees forming a 90-degree angle. Feet planted firmly and flat on the ground. Hands placed palms down on thighs.
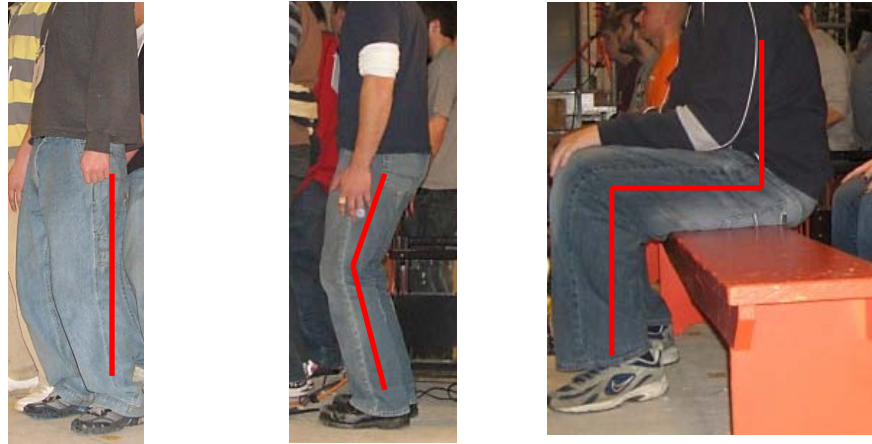
| a. Straight knees | b. Bent knees | c. Seated |
| (posture a) | (posture b) | (posture c) |

Figure 8: Examples of postures used for experimental testing.

2.3.2 Crowd distribution

The distribution of the occupants on the test structure was also varied. Two different distributions were selected not to exceed the design load of the floor of 78 psf (Raebel, 2000). Based on several assumptions, the maximum allowable distribution for this structure was estimated to be 2.25 ft^2 per person. This value is greater than the minimum suggested value for maximum crowd distribution of 1.78 ft^2 per person (Kappos, 2002). The maximum allowable distribution for this structure allowed participants a greater level of comfort during testing and was increased to 2.78 ft^2 per person when considering the combined effects of both static and dynamic loading. This distribution is thus referred to as the "dense" case for the remainder of this document and provides a 20-inch by 20-inch area for each occupant. The second distribution used was selected to be less dense than the first but not to exceed the dimensions of the test structure based on the greatest number of occupants. This distribution will be referred to as the "sparse" case and provides a 28-inch by 28-inch area for each occupant. Table 3

shows the different distributions used. Distribution calculation can be found in Appendix E.

Table 3: Summary of distributions selected for experimental testing.

Distribution Condition	Grid spacing (in x in)	Distribution (ft^2/person)	Load (psf)
Maximum suggested (Kappos, 2002)	16x16	1.78	100.2
Maximum allowable	18x18	2.25	78
Dense	20x20	2.78	64.8
Sparse	28x28	5.44	33.1

2.3.3 Mass ratio

The mass ratio of occupants to empty structure is the third crowd characteristic that is varied. The desired mass ratios were in the range of 0.25 to 0.75 for typical stadium structures at full capacity (Dougill, 2005). However, due to the strength of the floor and availability of participants, the higher mass ratios were unattainable. Table 4 shows the different mass ratios that were used in this study. For each of the first three lowest mass ratios used, equivalent mass tests were also performed. For these tests, mass was added to the structure in the form of lead weights and bags of dry mortar along the same grid as used for human testing and with approximately the same mass as the equivalent human occupants.

Table 4: Summary of mass ratios used for experimental testing.

Test	Total people	Occupant weight (lbf)	Mass ratio (occupant/empty)	Equivalent weight (lbf)
1	1	193	0.022	200
2	4	720	0.082	670
3	8	1370	0.157	1323
4	16	2900	0.332	--
5	19	3760	0.431	--
Structure weight (lbf)			8730	

2.4 Experimental testing procedure

There were four separate testing days in which experimental data were collected. Each day, at least one different mass ratio was tested for each posture and distribution. After initial setup and installation, the general procedure for each session began with preliminary checks of equipment to ensure that the shaker was receiving the output signal and that each accelerometer was measuring a response. For a baseline comparison, initial empty-structure tests were also performed and the response recorded. The experimental tests with occupants would then be conducted as instructions were given for the posture and distribution to be used. To ensure that the properties of the test structure were not altered during the tests with occupants, empty structure tests were performed at the end of each test day for verification. For a more detailed description of testing procedure, see Appendix F.

CHAPTER 3: EXPERIMENTAL ANALYSIS

3.1 Experimental modal analysis

The purpose of experimental testing in this study is to estimate the dynamic properties of the structure in an empty condition and when occupied by crowds demonstrating a variety of crowd characteristics. This is accomplished through the techniques of experimental modal analysis where a known excitation force is applied to the structure while simultaneously measuring the response at various locations. The application of fast Fourier transforms to both the reference and response signals, as recorded by the force plate and accelerometers respectively, leads to the generation of a frequency response function, a powerful tool in dynamic property prediction. The methods outlined here are considerably simplified and further information can be found in other literature (Ewins, 2000). The following sections discuss the steps followed in estimating the dynamic properties, including frequency, damping, and mode shapes, of the unoccupied structure.

3.2 Data acquisition using eZ-Analyst

IOTech's eZ-Analyst software served several functions in the experimental portion of this study. It generated the forcing function for the electrodynamic shaker; it recorded the reference signal from the force plate, and it recorded the response signal from the accelerometers. The recording settings used are shown in Table 5. Although only the response of the structure at low frequencies was of interest, a frequency bandwidth of 0 to 50 Hz was used. The upper bound of this range was selected to be able to compare results with previous research conducted within the same range (Raebel,

2000). As discussed in Chapter 2, the chirp signal consisted of an 8 second signal that was repeated five times for each test. From preliminary testing, five chirp signals were determined adequate to provide the necessary levels of coherence when averaging.

Table 5: eZ-Analyst acquisition settings for experimental testing.

Analysis frequency (Hz)	50.00
Spectral lines	400
Nyquist factor	2.56
Frame width (s)	8.000
Delta time (s)	0.00781
Delta frequency (Hz)	0.1250
Averaging type	Linear
Number of averages	5

The eZ-Analyst software allows for real-time observation of both the reference and response signals in both time and frequency domains. In addition, it also generates the FRF and the coherence function corresponding to a given test in real time. Figure 9 shows the time history of the reference signal as it would be exported from eZ-Analyst. The FRF and coherence of an empty structure test are shown in Figure 10. Because the eZ-Analyst software functions in real-time, the computer operator is able to observe and interpret the data as it is being collected. This helps to identify flawed data and is especially important when under time constraints.
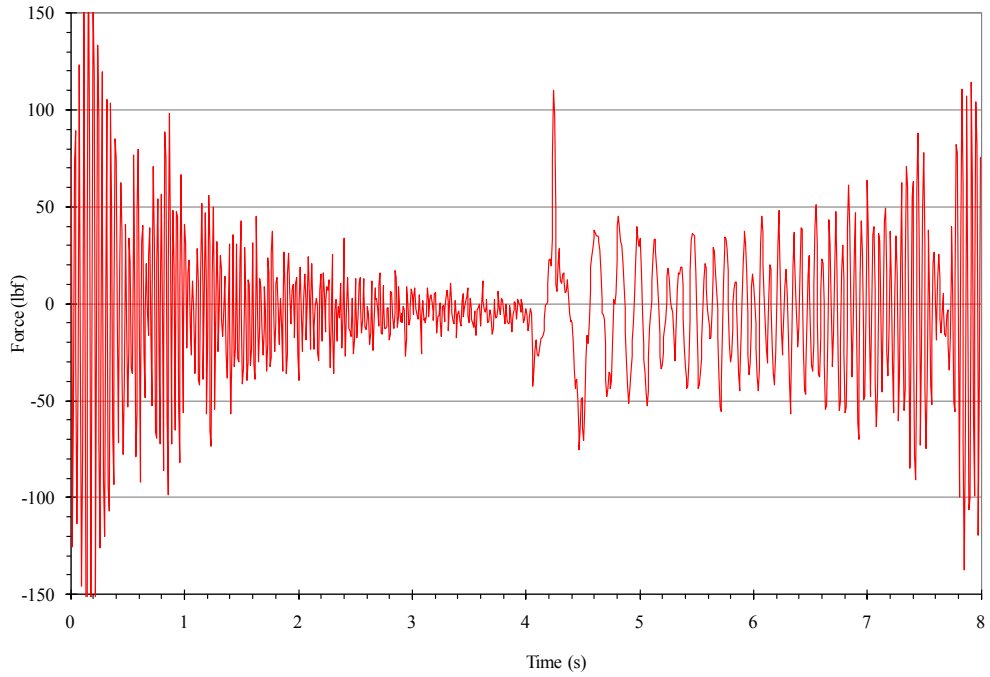
Figure 9: Example of force signal generated by electrodynamic shaker.
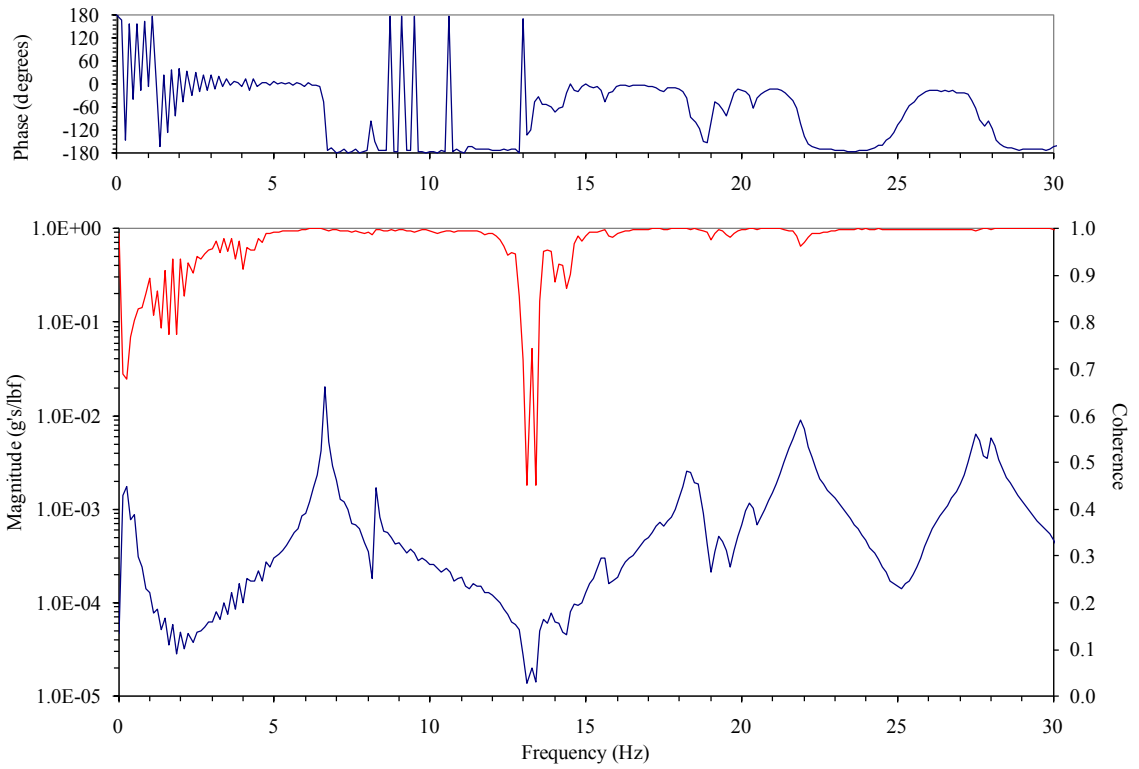
Figure 10: Driving point FRF for empty structure test.

3.3 Estimation of dynamic structural properties using ME'scope

The estimation and visualization of the frequency, damping, and mode shapes using ME'scope can be divided into three different phases. The first phase involves constructing a model of the test structure within the software. The second phase includes importing the FRFs into ME'scope and applying the curve-fitting algorithms. The final phase involves confirming the results from the curve fitting process by means of visual inspection of the curve fits and mode shapes.

The model created in ME'scope is a simple model that incorporates only the geometry of the test structure. The model is assembled using a grid identical to the locations of acceleration measurement. FRFs imported from experimental tests are paired with the nodes at the corresponding location. At nodes where measurements are not available, the response is interpolated from the surrounding nodes. Also, simple support conditions were used in each corner of the test structure. These support conditions only created stability and a reference point for viewing mode shapes and did not influence the behavior of the mode shapes themselves.

Individual data files pertaining to each experimental test were able to import directly from the eZ-Analyst software. Once imported, the curve fitting process began by first looking at an overlaying of the magnitude of each of the fourteen FRFs plotted in the frequency domain. Each analysis began by looking at the magnitude plot first to gain a general understanding of where each natural frequency was located. For the scope of this research, only the first five natural frequencies corresponding to the first five modes of

the test structure were analyzed. This is a realistic approach because the frequencies of all of the first five modes are below 30 Hz. The upper frequency range is also unlikely to be significantly affected or be the cause of any serviceability concerns.

Once the general location of each mode was determined, several checks were performed to determine the appropriate bandwidth to be used for curve fitting each mode. The real component of the FRF was checked for locations where it crossed the x-axis. A peak in the imaginary component of the FRF also corresponds with the location of a natural frequency. The imaginary component of the FRF is often considered to be the most reliable source for modal parameter estimation (Allemang, 1994). The final two checks involved checking for a phase shift in the FRF and also checking to ensure that the coherence associated with the FRF was reasonable over the curve fitting bandwidth. Once a location of a mode was determined, the automated curve fitting process was executed within ME'scope utilizing a global polynomial fit and alias free polynomial method. This process was done individually for each of the first five modes for each experimental test.

The final phase involved verifying the results of the automated curve fitting methods. The results of the curve fitting were applied to the model created within ME'scope to animate the mode shape corresponding to the selected natural frequency. The first five mode shapes for the empty structure are shown in Figure 11. The odd modes shown for this structure represent modes dominated by bending of the joists in a sinusoidal shape. The even modes for this structure represent modes that exhibit a

torsional tendency.   It should be noted that the curve fitting process executed in ME'scope is subjective to user interpretation and some visual inspection.
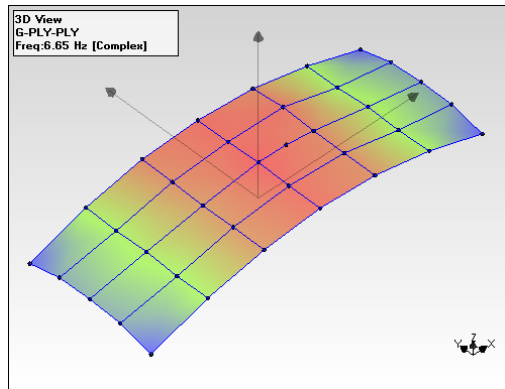
a. ME'scope empty Mode 1 (f=6.7 Hz)   b. ME'scope empty Mode 2 (f=8.2 Hz)
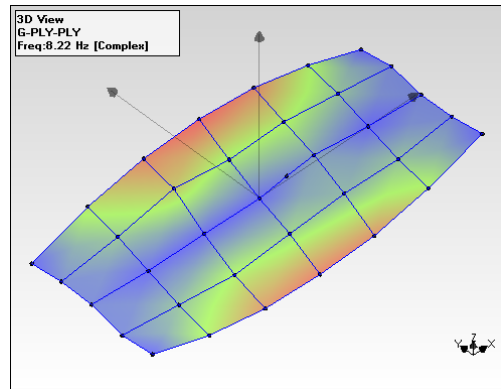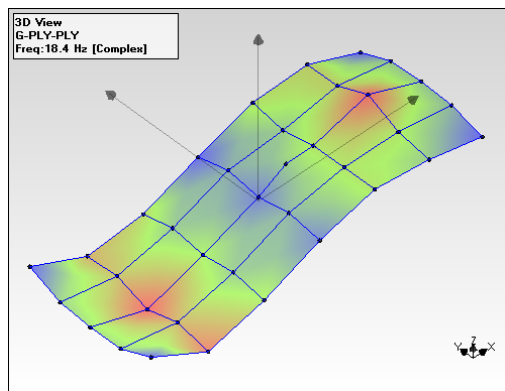
c. ME'scope empty Mode 3 (f=18.4 Hz)   d. ME'scope empty Mode 4 (f=21.9 Hz)
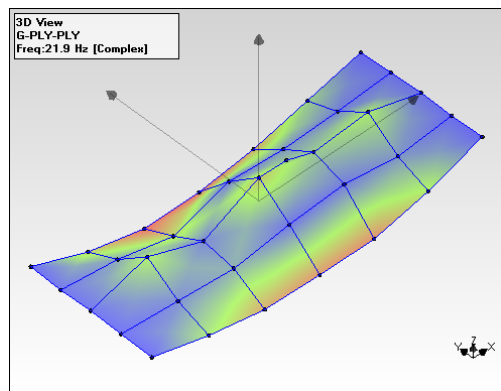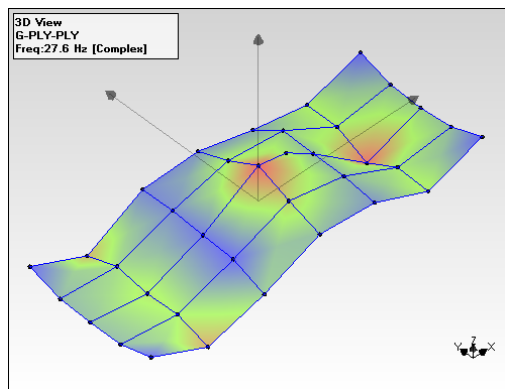
e. ME'scope empty Mode 5 (f=27.6 Hz)

Figure 11: Mode shapes and frequencies for first five modes of the empty test structure.

3.4 Organization of analysis data

The process for estimating the dynamic properties of the structure when occupied was similar to that for the empty structure. Individual data sets including FRFs and coherence functions can be found in Appendix G while a summary of the data is included in Chapter 4. Once the dynamic properties for each configuration were estimated, the frequency and damping results were organized into a spreadsheet in order to further analyze and visualize the experimental data and develop trends.

CHAPTER 4: RESULTS AND DISCUSSION

4.1 Introduction to results

The experimental results involving human occupants collected in this study provide insight into the interaction between the crowd characteristics of posture, distribution, and mass ratio, and their effects on the frequency, damping, and mode shapes of the test structure. In total, twenty-four different tests with occupants were performed which included all applicable combinations of the three postures, two distributions, and five mass ratios. Each individual type of test was duplicated to prevent analysis of flawed data and the measurement results were analyzed similar to the procedure followed for the empty structure.

The frequency values that are presented are the damped natural frequency as opposed to the undamped natural frequency. The damped natural frequency is the undamped natural frequency combined with a modification factor based on the damping ratio. Because the damping ratios discussed are relatively low, the damped natural frequency is very similar to the undamped natural frequency and thus is appropriate for this study.

Although each of the first five modes appears to exhibit a trend, only the first mode is to be discussed in detail. The trends in the remaining four modes are less significant and the uncertainty associated with the modal parameter estimation is greater than with the first mode. In addition, the response of a structure is typically dominated

by vibration in the first mode. Thus, any effects on the first mode are more noticeable to occupants. For this structure, the first natural frequency is within the frequency range that humans are most sensitive to vibrations so the potential for serviceability concerns is increased.

Before focusing on the details associated with the first mode, some of the results and trends in frequency for the second through fifth mode are presented in Figure 12, Figure 13, Figure 14, and Figure 15. For the second mode, the change in frequency for each posture decreased slightly with increase in mass ratio. However, the frequency of the third and fifth modes increased while the frequency of the fourth mode remained unchanged. Because the mass of the occupants was centered on the structure, the odd numbered modes (the bending modes for this structure) showed the greatest change in frequency. The other two torsion modes are not as affected by the occupant mass in the center. Additional data for these modes can be seen in Appendix H.
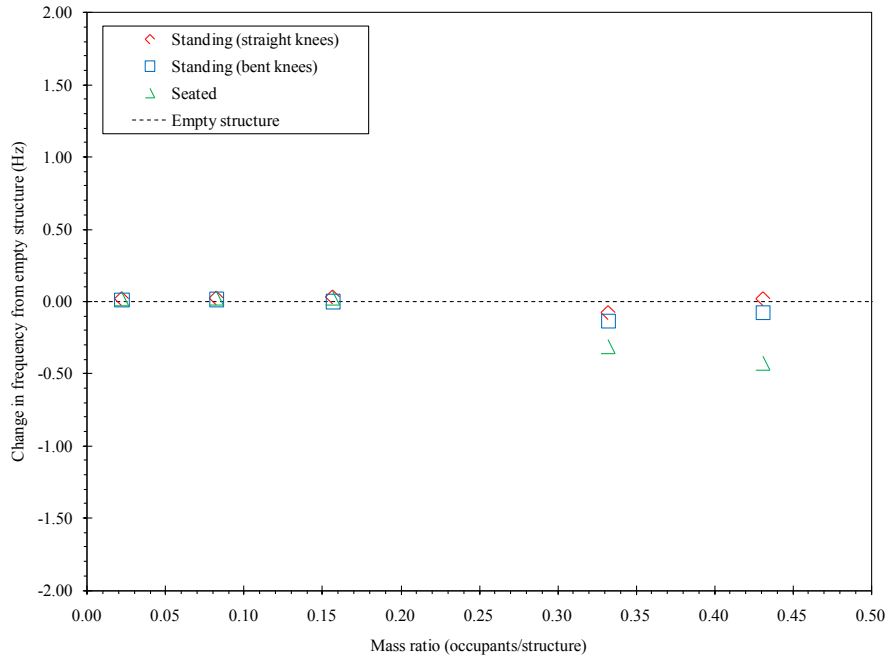
Figure 12: Experimental results for change in frequency for mode 2.
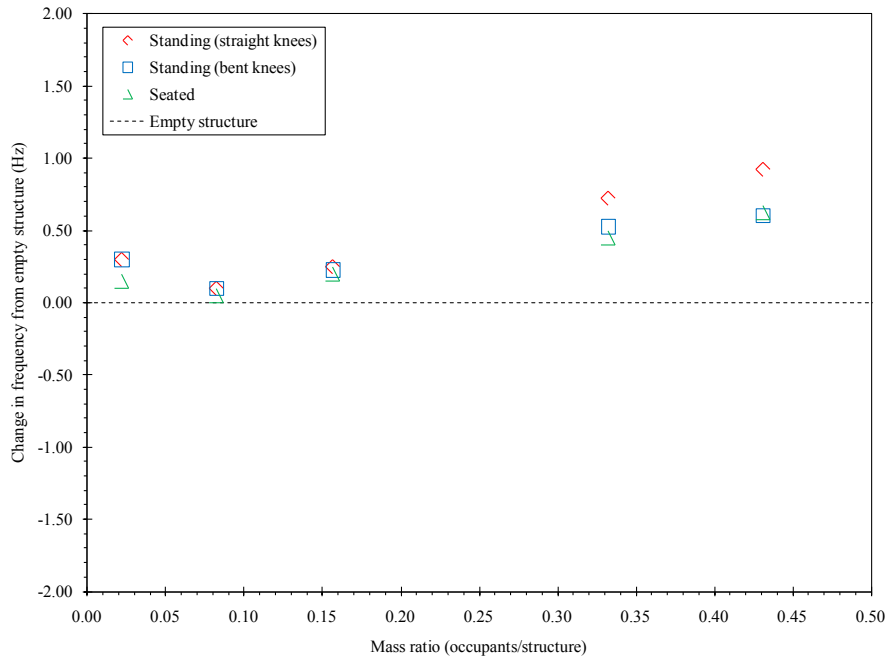
Figure 13: Experimental results for change in frequency for mode 3.
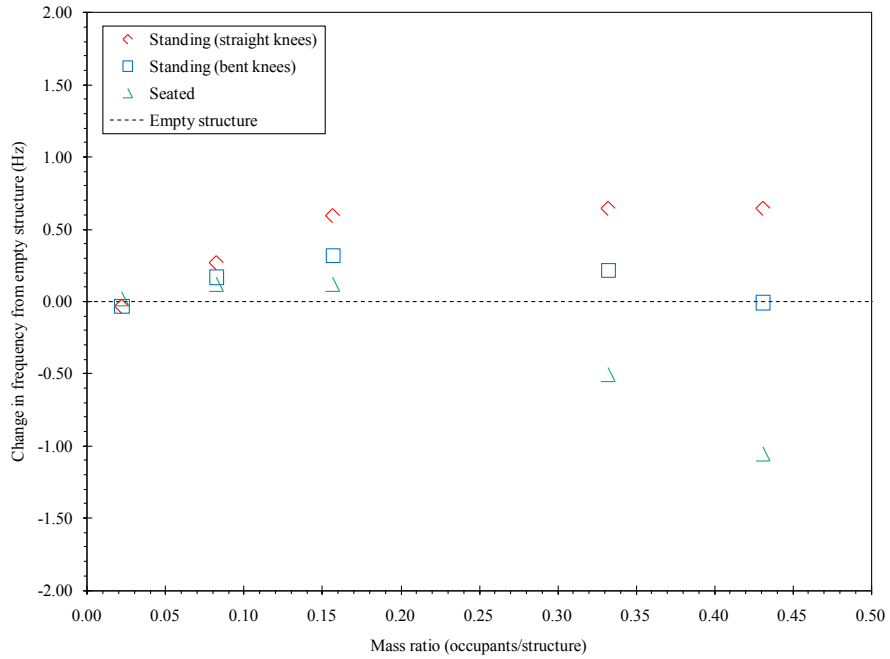
Figure 14: Experimental results for change in frequency for mode 4.
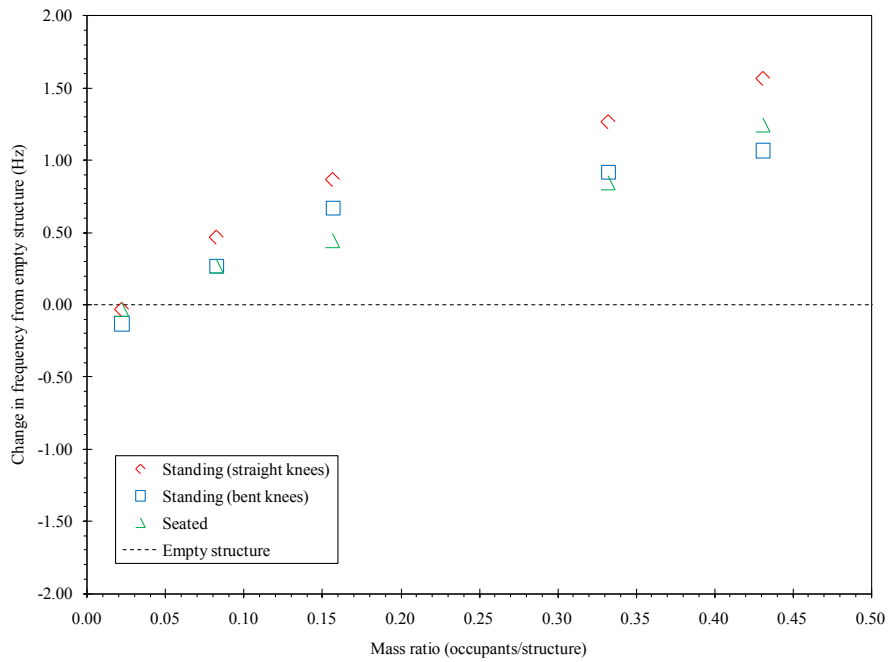
Figure 15: Experimental results for change in frequency for mode 5.

Some of the trends in damping for modes two through five are presented in Figure 16, Figure 17, Figure 18, and Figure 19. Modes three through five have a maximum increase in damping of 2.5% for all postures and mass ratios. Also, the second mode is only affected at the two highest mass ratios and only for the standing with bent knees and seated postures. Additional data for these modes can be seen in Appendix I.
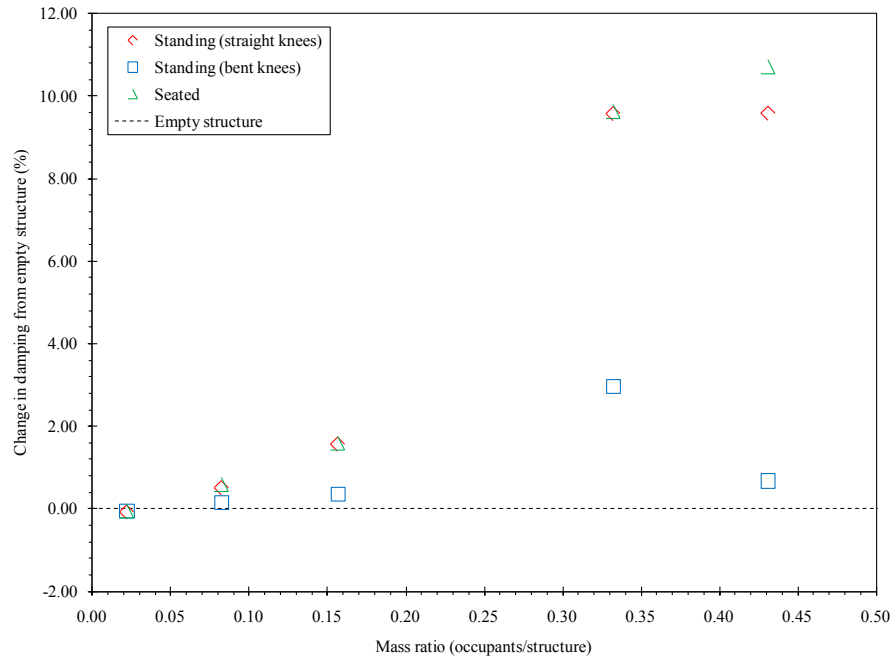
Figure 16: Experimental results for change in damping for mode 2.
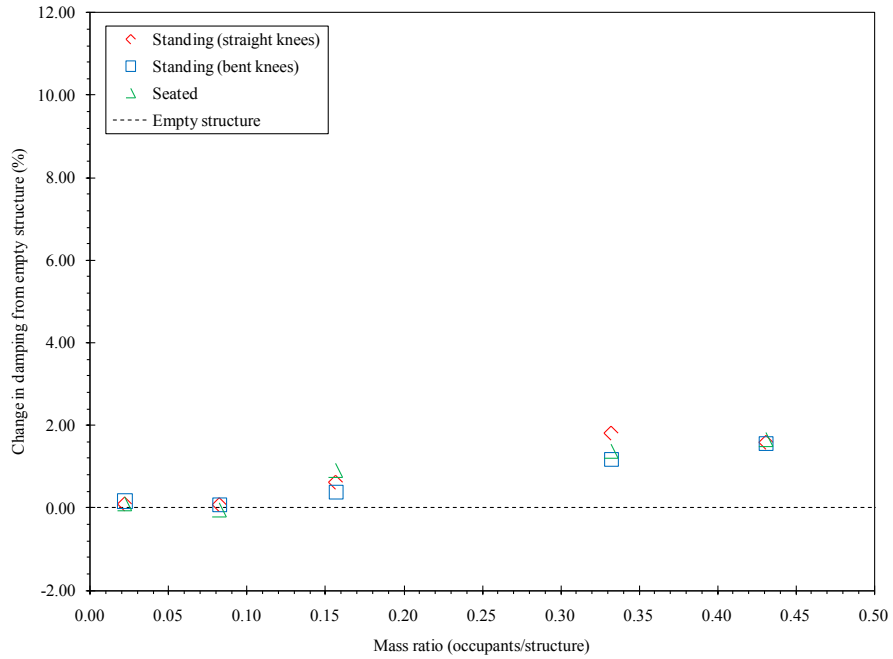
Figure 17: Experimental results for change in damping for mode 3.
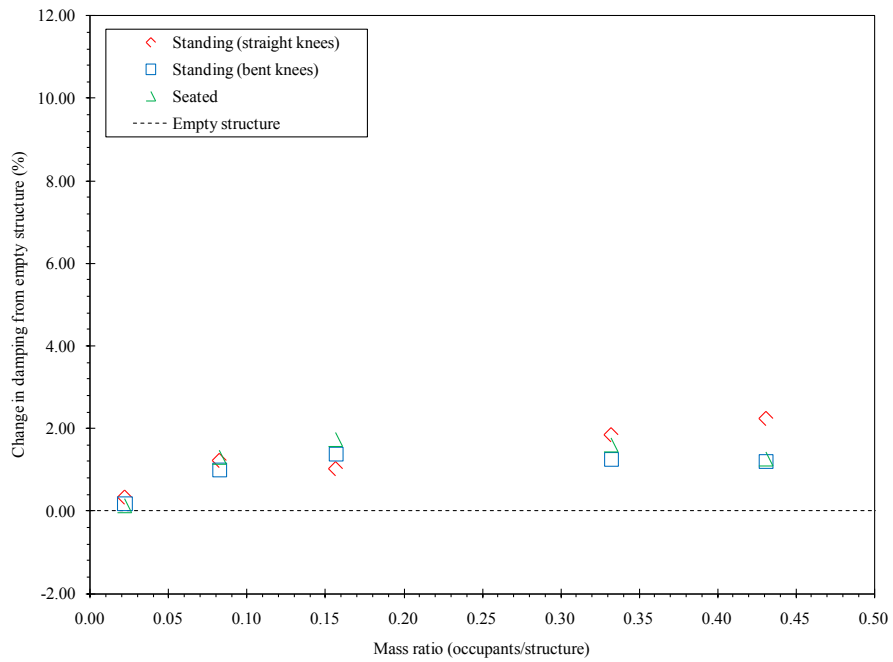
Figure 18: Experimental results for change in damping for mode 4.
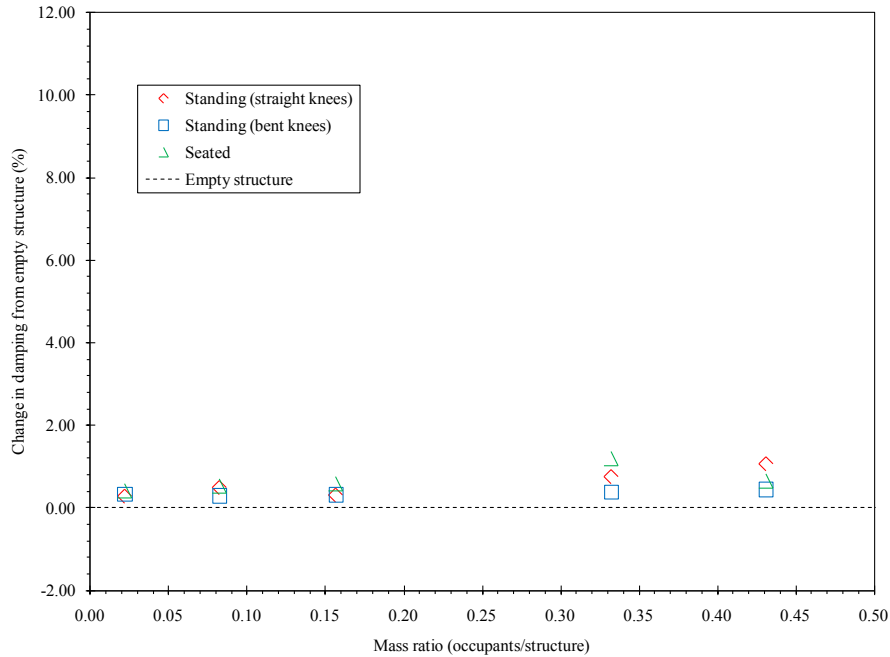
Figure 19: Experimental results for change in damping for mode 5.

As previously mentioned in Chapters 1 and 2, equivalent mass tests were performed for only the three lowest mass ratios due to availability of mass. Figure 20 shows the frequency results from the equivalent mass tests for the first mode that confirm earlier research. It also shows the theoretical basis for extending the experimental results to higher mass ratios that will be discussed in Chapter 5. Damping ratios are unchanged with the equivalent mass tests and therefore not shown. The equivalent mass tests did not create the same effect on the dynamic properties as the occupants, again confirming the results presented in other research and first by Lenzen (1966). These results suggest that the human-structure interaction cannot be simplified to an equivalent mass.
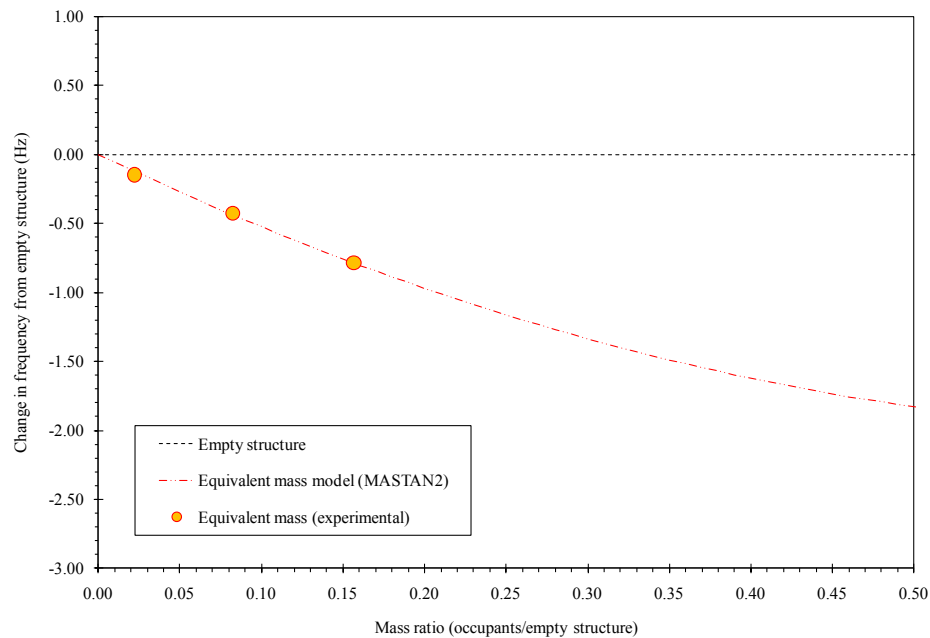
Figure 20: Experimental results for change in frequency using equivalent mass.

4.2 First mode results

4.2.1 Frequency

The frequency of the first mode is affected by two of the three crowd characteristics explored in this study. These two characteristics are posture and mass ratio. The effects of occupant distribution, however, are less noteworthy and will only be discussed briefly.

The change in natural frequency of the occupied system from the empty structure is a function of both the occupant's posture and mass ratio. These trends are identified in Figure 21, Figure 22, and Figure 22. The only exception to the trends in change in natural frequency is for the standing posture with bent knees scenario. For standing with straight knees and seated, the natural frequency decreases significantly from that of the

empty structure. However, standing with bent knees produces minimal change in the natural frequency. The decrease in natural frequency for standing with straight knees and seated becomes greater with increasing mass ratio, the other independent variable.

Figure 21: Experimental results for change in frequency for the first mode and standing with straight knees posture.

Figure 22: Experimental results for change in frequency for the first mode and standing with bent knees posture.

Figure 23: Experimental results for change in frequency for the first mode and seated posture.

The experimental results suggest that standing with straight knees produces the most significant change in frequency of all three studied postures and across all mass ratios examined in this study.

These results can all be compared to results presented by Brownjohn in which the posture controls the degree to which the frequency is affected (Brownjohn, 1999). In contrast to results from this study, Brownjohn's results show that a seated occupant reduces the natural frequency more than a standing occupant. However, the difference in frequency reduction is less than 2 percent of the empty natural frequency. The differences may be attributed to other inaccuracies and not necessarily the posture of the occupant.

The results concerning posture also differed from those presented by Littler (2000). Sitting occupants reduced the natural frequency more than standing occupants. However, Littler does not distinguish between the many different forms of standing. It is possible that Littler's standing occupants were a combination of standing with straight knees and also bent knees. A combination of the two types of standing could reduce the effects of standing with straight knees to a level less severe than seated occupants. The distinct separation of postures used in this study aids in the comparison to previous work. Also, the natural frequency of the retractable grandstand studied by Littler is twice that of the test structure used for this research. The combination of the two studies suggests that an additional factor, empty structure natural frequency, may determine which posture affects frequency more.

The two distributions used throughout this study did not produce significantly different results for the first mode. This is likely because the first mode is a bending mode in which the entire mass is generally located in the same central location for both distributions. However for the torsion modes, the occupants' mass in the sparse distribution is distributed over a larger area of the structure exhibiting the most deformation in the mode shape, therefore having a greater impact on the natural frequency associated with this mode shape.

4.2.2 Damping

The results for the damping at the first mode are less conclusive than those for frequency. The damping ratios are difficult to estimate accurately and are even more

affected by the bandwidth selected in the curve-fitting process. However, like frequency, damping is also dependent mainly on mass ratio and posture.

For the standing with straight knees posture and the seated posture, the damping ratio increased nearly linearly for the first three mass ratios. Figure 24, Figure 25, and Figure 26 show the trends in damping for the first mode. Beyond this point, the damping ratio remained within a range of 8-18%. Due to the inaccuracies discussed with estimating the damping ratios and only testing two mass ratios above 0.2, projecting this range beyond the mass ratios studied would be unsubstantiated. It appears that the standing with bent knees posture generates a less significant level of damping than the other two. This posture had a maximum increase in damping of 6%. These trends are summarized in Figure 27.
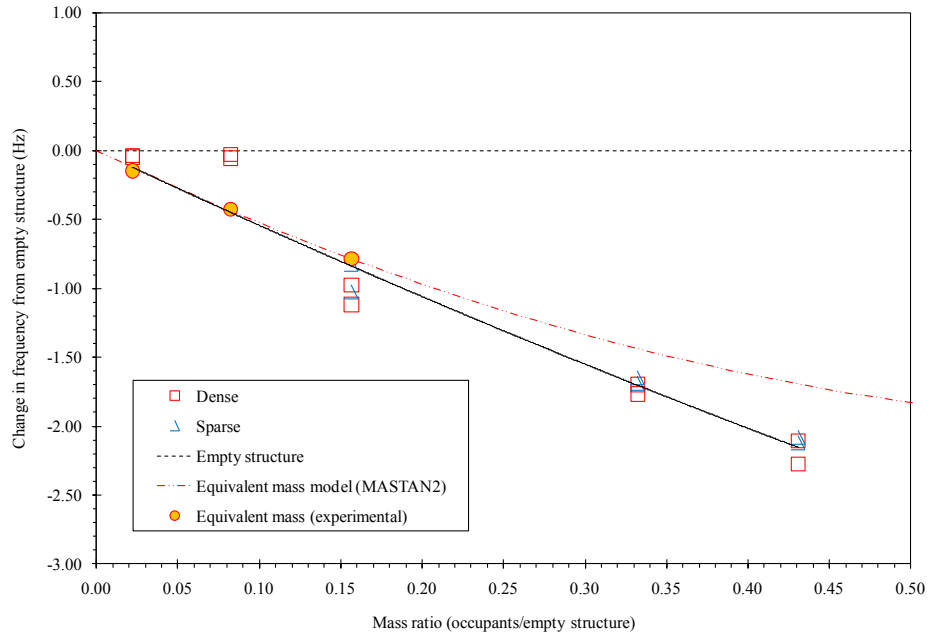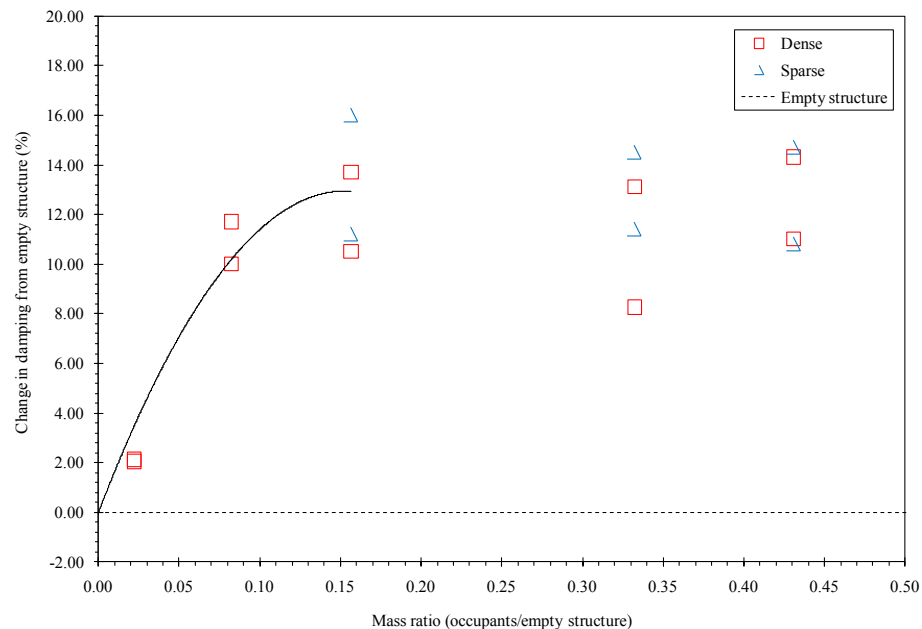

Figure 24: Experimental results for change in damping for the first mode and standing with straight knees posture.
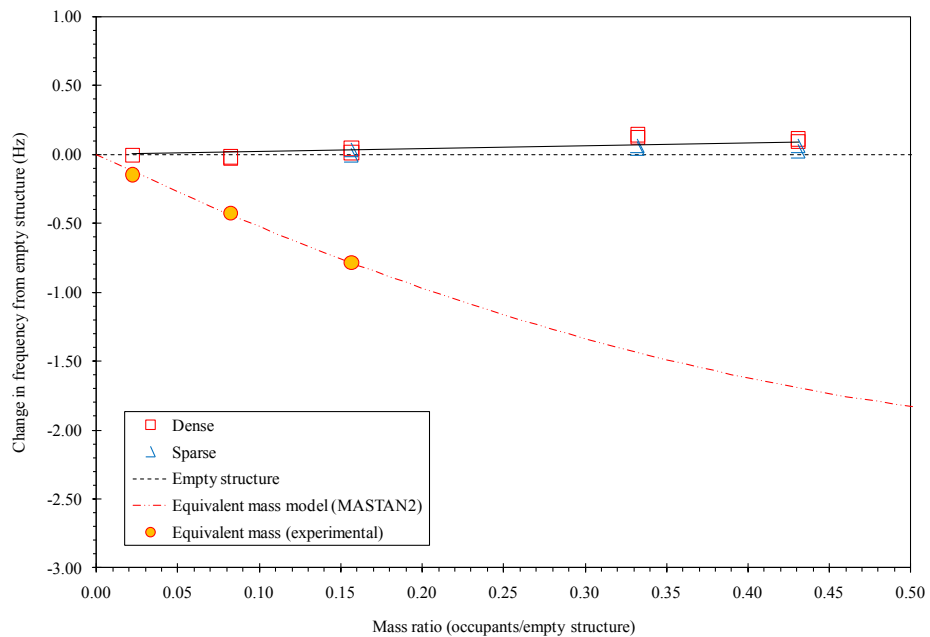
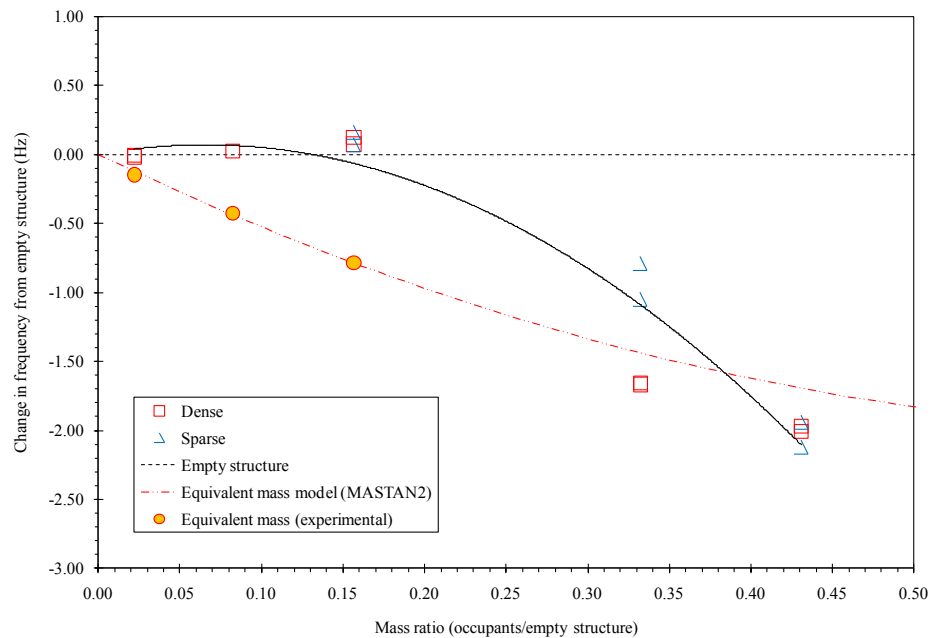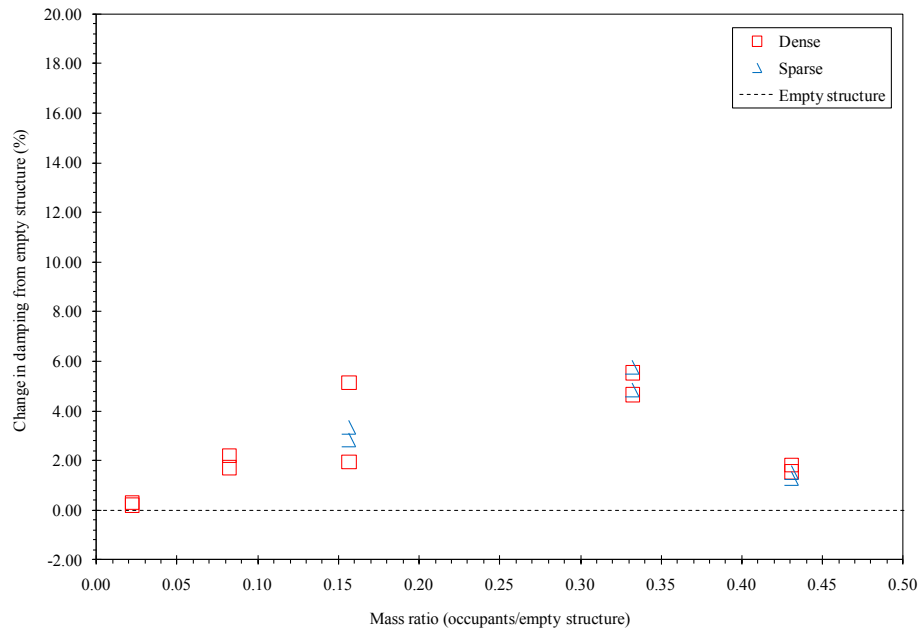Figure 25: Experimental results for change in damping for the first mode and standing with bent knees posture.
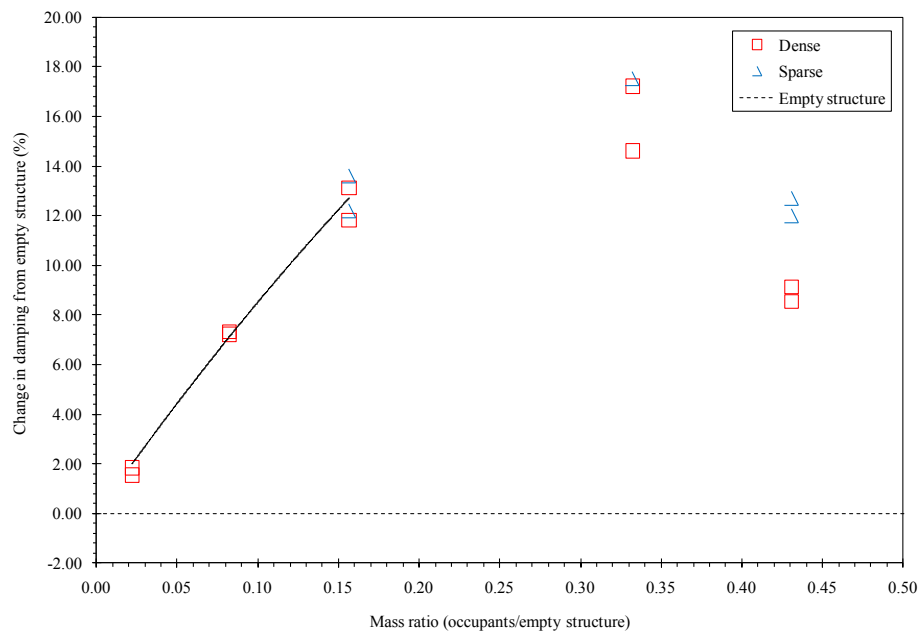
Figure 26: Experimental results for change in damping for the first mode and seated posture.
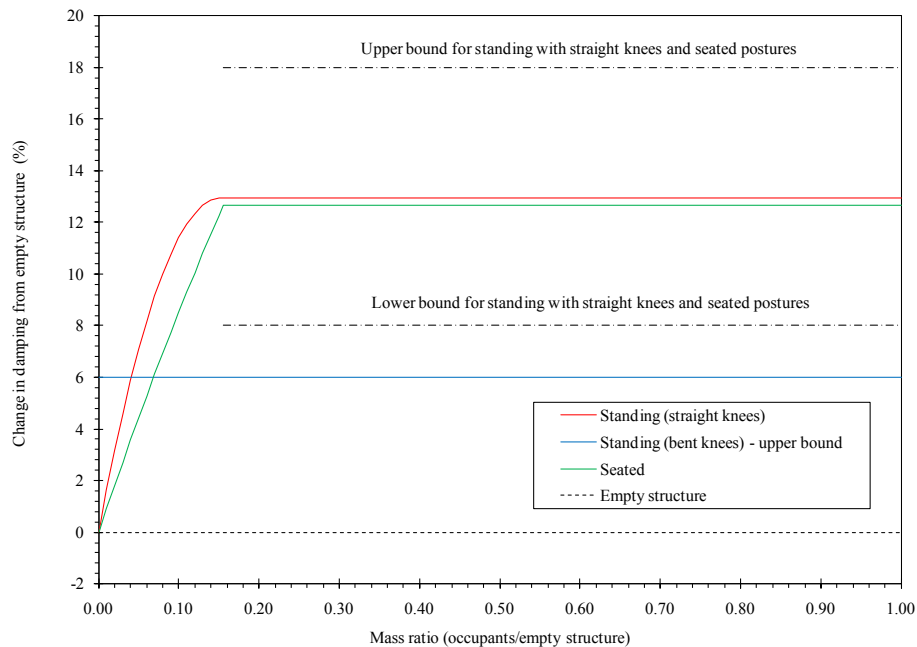
Figure 27: Trends from experimental results for change in damping for the first mode.

4.3 Design considerations

A conservative approach to design would be to consider the crowd characteristics that produce the largest change in frequency and smallest change in damping from the empty structure properties. The smallest change in damping is appropriate because a highly damped mode is not as perceivable by occupants. Assuming a higher damping ratio than the actual could lead to potential serviceability issues being overlooked. Of the variables affecting frequency and damping, only posture is unknown in real, occupied structures. Posture can vary greatly for different events in a particular structure. For these reasons, future design guidance should be based on the posture that produces the most significant changes. Based on this study, that posture is standing with straight knees.

4.4 Limitations

The results presented here are limited by several factors. The largest factor is the sample size for empty structure natural frequency. Because only one structure was tested, the results from this study may not be typical for structures with different natural frequencies. Chapter 5 offers insight into how a single degree-of-freedom model of a crowd may be able to provide insight into the response of structures with other natural frequencies.

The mass ratios that were achieved in this study are not representative of the full set of the possible mass ratios for in-service structures. Only two of the mass ratios for this research were in the common range of mass ratios for real grandstand structures but at the lower end. Because of this, the results relating change in frequency to mass ratio and posture and the proposed relationships are only applicable for systems with a mass ratio less than 0.43.

There is also uncertainty in the methods used for analyzing the experimental data as addressed in Chapter 3. The curve fitting process relies on a thorough understanding of the underlying mathematical theory and experience. The ME'scope software is intended to minimize the required theoretical understanding and experience, but it is still an uncertain process. These uncertainties can lead to variability in the frequency and damping ratio estimates that have been developed. In addition to the variability inherent in ME'scope, there is an increased level of difficulty in executing the curve fitting process on tests with larger group sizes. More occupants generally create a lower

coherence at the frequencies that are being analyzed. A larger group size presents the greater possibility of one occupant not remaining still for the duration of the test. The coherence is consequently affected negatively. Also, more occupants have the effect of altering the damping ratio of the first mode to allow the peak to be lost in an adjacent mode or simply be less pronounced. Either case makes recognizing these modes, and estimating the dynamic properties accurately, more difficult.

CHAPTER 5: MODELING

5.1 Introduction to modeling

Three different forms of modeling were explored as the first step in the determination of the appropriateness for the application of a simplified model to represent the response incorporating human-structure interaction. The first form involved creating a complex finite element model of the test structure. From this model, approximate nodal lines were determined in order to plan the placement of accelerometers and to confirm the locations presented by previous research (Raebel, 2000). The model was also used to estimate the static stiffness of the structure utilizing a unit load and corresponding deflection. In general, the ultimate goal of finite element modeling is to accurately predict the behavior of a structure when occupied, with a particular emphasis on the dynamic response for serviceability design. This can help foresee and prevent potential crowd serviceability issues by utilizing detailed FE modeling during the design phase. A second finite element model was created to model the change in frequency of the empty structure when a varying equivalent mass is applied.

A single degree-of-freedom (SDOF) model was also created to represent the test structure. This model is much less complex than either finite element models and was proven to adequately represent the first mode of the empty test structure in frequency and damping. Also, an additional SDOF system was created to represent the occupants. The properties for the occupant system were estimated from the experimental results corresponding to that occupant posture, group size, and distribution. The two SDOF

systems were combined to estimate the response of the occupied structure and compared to the experimentally measured FRF at the first mode.

5.2 Finite element model

Before a complex finite element model can be utilized for predicting the effects of human-structure interaction, the phenomenon must be more fully understood. For this reason, the first finite element model discussed is only a preliminary step in the process of modeling a crowd of occupants.

The finite element model of the full floor used in this study was created in SAP2000 as a two-dimensional structure. The model consists of only frame and area elements that are inserted in the same plane. Frame elements are used to model the joist and girder members with properties based on recommendations in Design Guide 11. Area elements are used for the concrete slab. To account for all members being in the same plane, the transformed moment of inertia of the slab is subtracted from moment of inertia for the joist and girder members. The members are meshed based on a grid corresponding to the accelerometer placement grid used for experimental testing. This grid is also subdivided into smaller sections with no dimension being larger than one foot.

An understanding of the boundary conditions is important to properly predict the behavior of the modeled structure. Proper boundary conditions are as important to modeling the real structure as the section and material properties of the individual members. The boundary conditions for the structure are based on research presented by

Beaver (1998). A diagram of the boundary conditions can be seen in Figure 28. One corner of the structural frame is restrained from translation in the x, y, and z directions. The nearest corner, along the width of the structure, is restrained from translation in the x and z directions. The remaining two corners are restrained in only the z direction. Two corners of the slab overhangs are also restrained.
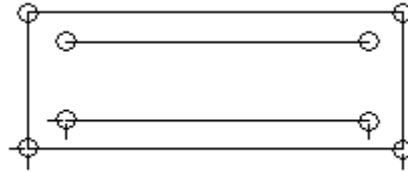
Figure 28: Boundary conditions used in finite element model; a dash represents a restraint, circle a roller support (Beaver, 1998).

The frequency of the first mode and the subsequent four modes estimated in the FE model is higher than those estimated from experimental data. Table 6 shows the differences in frequency between the experimental results and the SAP model. This model was used to estimate the static stiffness of the floor, albeit slightly higher than the experimentally determined value presented in Section 5.3, for use in the SDOF model of the empty structure. An improved understanding of the dynamic behavior and modeling of joist systems is needed before this type of a complex finite element model can be used for accurately predicting dynamic response of the system. Additional limitations of this model are discussed in Section 5.4.

An even simpler finite element model was created in MASTAN2 that eliminates the uncertainty of modeling composite joist systems by modeling the floor as an equivalent beam system. The purpose of this model was to determine the effects of an equivalent mass on the empty structure and create a simplified theoretical equivalent

mass curve. The model consisted of a single member in two dimensions. Properties of the member were determined based on the actual mass of the empty test structure and an equivalent stiffness which yielded a first natural frequency similar to experimental testing. The member was simply supported at either end and divided into segments along its length in order to match the spacing of human occupants that was for experimental testing. A uniform distributed load was then applied to the model over a specified length corresponding to a given mass ratio. The frequency associated with each configuration was determined and the results are presented in Figure 29 along with the experimental equivalent mass results. Although simplistic, this model illustrates that the changes in frequency associated with an equivalent mass are less than those associated with human occupants.

Table 6: Comparison of frequency between experimental testing and SAP model.

Mode			Damped Frequency (Hz)			Difference (%)	
Exp.	SAP	Raebel Model	Exp.	SAP	Raebel Model	SAP	Raebel Model
1	1	1	6.6	7.4	7.5	11.5	12.5
2	2	2	8.2	9.3	9.4	13.4	14.5
3	4	4	18.4	25.1	23.3	36.1	26.6
4	3	3	21.8	19.4	18.5	-11.1	-15.2
5	7	6	27.5	41.3	35.7	50.1	29.6
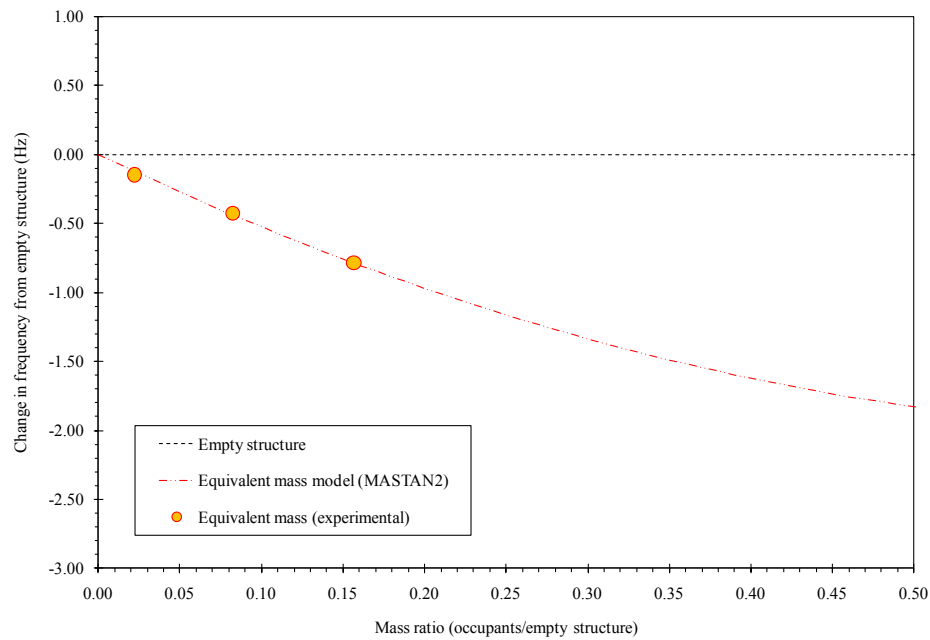
Figure 29: MASTAN2 equivalent mass results.

5.3 Single degree-of-freedom model

The purpose of the single degree-of-freedom model is to try and model the effect of a crowd on a structure in its simplest form for crowd serviceability design as a precursor to utilizing the more complex finite element mode. The SDOF model that was created is the most simplistic model and includes a mass (m), stiffness (k), and damping factor (c). The behavior of this model is represented by Equation 1. The model shown in Figure 30 includes a combination of two SDOF systems, one used to model the empty structure and the other to model the occupants.

$$m\ddot{x} + c\dot{x} + kx = f(t) \tag{1}$$

Figure 30: Two SDOF systems combined in series. 1-structure, 2-occupants.

Utilizing experimental data collected for the empty structure, the creation of an appropriate SDOF system representing the empty structure is possible. The mass of the structure is a constant value as determined from material properties of each individual member and it is assumed that the majority of this mass is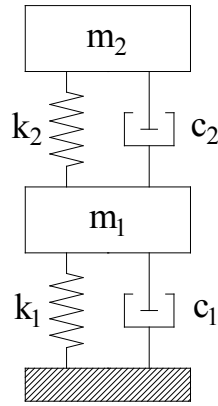 participating in the first mode. Stiffness values were determined from calculations relating natural frequency and mass. The damping ratio of approximately 0.5% was determined based on the results from Chapter 4. Equations 2-4 were used to transform the damping ratio into the units appropriate for the SDOF model in Matlab (Avitabile, 2009) and to calculate stiffness from the known mass and frequency of the structure. Sample calculations are presented in Appendix J.

$$c_c = 2mw_n \tag{2}$$

$$\zeta = c/c_c \tag{3}$$

$$k = w_n^2 m \tag{4}$$

Where:
    c_c = critical damping
    m = mass
    w_n = natural frequency
    ζ = percent critical damping

As mentioned in Section 2.1.2, the stiffness value determined from the finite element model was used to confirm the value calculated from Equation 4. Because the natural frequency of the preliminary finite element model created in SAP2000 is slightly higher than the value determined from experimental testing, the finite element model should have a higher stiffness than the stiffness calculated for the SDOF model. This assumption was confirmed, and the stiffness value calculated from experimental test data was determined to be a reasonable approximation.

The properties for the SDOF system representing the crowd are not as simple to determine. As discussed in Section 1.4.5, past literature has provided many different possible values of frequency, damping, and stiffness to represent a human or crowd (Sachse & Pavic, 2003). These properties are not consistent amongst authors with damping ratios ranging from 32 to 50 percent and stiffness values greater than 5000 lbf/ft, suggesting that there is not a single solution and that a range of reasonable models exists (Sachse & Pavic, 2003).

Modeling the crowd as a SDOF system was performed for only the standing with straight knees posture. This posture was selected because it produced the most significant changes in both frequency and damping at the four highest mass ratios studied.

In order to model the occupants, the mass associated with each standing test was known based on recorded values of the occupants, but the frequency, stiffness, and damping associated with each crowd configuration needed to be determined. To do this,

an iterative approach was utilized which applied a simplistic curve fitting method to an experimental FRF from an occupied test. This method was created and executed in Matlab, combining all possible combinations of frequency, stiffness, and damping within a specified range for each variable. The curve fitting itself utilized a three-point approach, analyzing the peak of the experimental FRF at the natural frequency and one point with a lower frequency and one with a higher frequency than the natural frequency. See Appendix K for the Matlab script files used to execute this curve fit.

Figure 31 shows a comparison of an FRF generated from the combination of the two SDOF systems representing the empty structure and the crowd into a single 2DOF system with an experimentally measured FRF at the corresponding center point of the structure. The 2DOF system represents the interaction between the occupants and the structure and how this interaction affects the dynamic properties of the entire system as indicated by the experimental measurements. Similar to the SDOF system used to recreate the empty structure, the 2DOF system shown exhibits a frequency similar to the experimental measurement and relatively similar peak width representing the system damping for the first mode. A summary of the properties used to represent the crowd as a SDOF for each selected test is shown in Table 7. For each test, the damped natural frequency of the human body was determined to be within the range presented in Chapter 1. Also, the damping ratios of the crowd were consistent between 25 and 35 percent. Although the damping values between the experimental results of the occupied system and the 2DOF model are slightly different, this can be attributed to the variability in the estimation of the damping ratio associated with the crowd. Additional FRFs comparing

experimental results with the 2DOF for all mass ratios used in this study can be found in Appendix L.

Similar to the discussion presented in Section 5.1, using the damped natural frequency of the human occupants is an appropriate assumption. Although the damping ratios associated with the human body are considerably greater than those corresponding to the structure, using the undamped natural frequency does not alter the 2DOF FRF drastically.
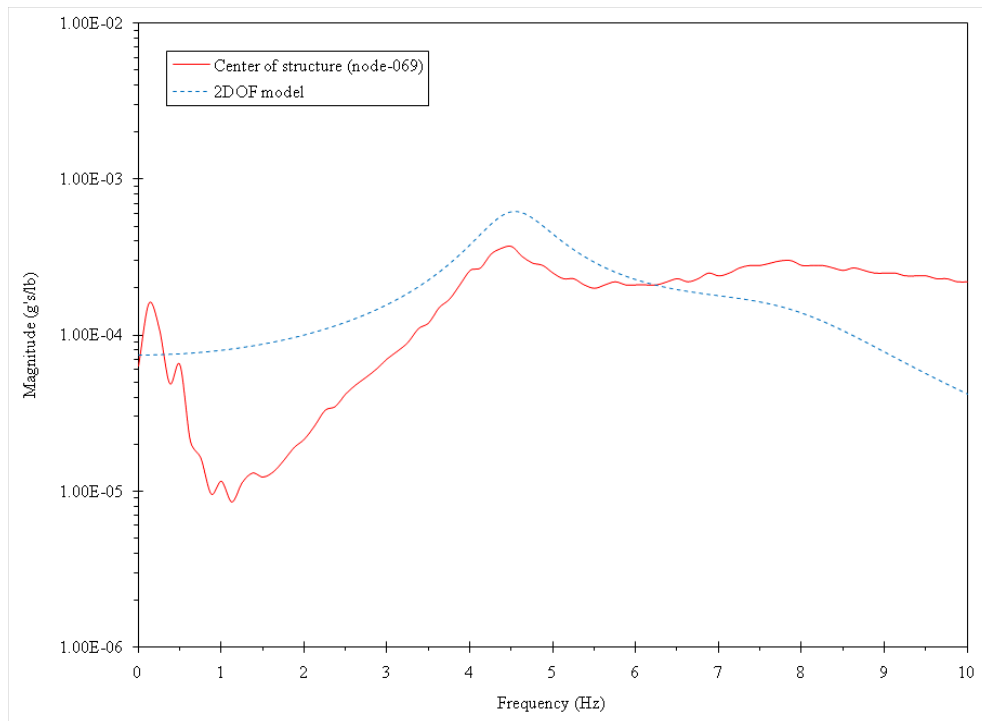

Figure 31: FRF comparison between experimental results and 2DOF model for a mass ratio of 0.43.

Table 7: Summary of 2DOF model properties.

Mass ratio	Damped Freq. (Hz)		Damping (%)		Crowd Properties		
	Exp.	Model	Exp.	Model	Damp. Freq. (Hz)	Damp. (%)	Stiff. (lbf/ft)
0.02	6.58	6.57	2.59	2.77	5.4	35	250
0.08	6.60	6.63	11.35	5.76	4.6	35	450
0.16	5.50	5.47	13.35	11.64	4.4	30	1550
0.33	4.88	4.95	12.32	8.84	5.8	25	3250
0.43	4.54	4.54	13.20	9.91	4.2	30	3450

5.4 Summary of modeling

Overall, the results of the modeling study are the first steps in a much larger effort to model the effects of human-structure interaction. The results from the MASTAN2 model confirm the experimental results for equivalent mass and illustrate the differences between human occupants and an equivalent mass as shown in Chapter 4.

This study also shows that a combined system of two SDOF systems can be used represent the interaction between structure and occupants. Although there are still many complexities associated with the variety of crowd characteristics still to be explored, the results suggest that this method of modeling occupants could potentially produce adequate results in conjunction with a complex finite element model.

The single degree-of-freedom model provides some insight into the study of human-structure interaction. One of the most noteworthy results is that the damped frequency of the human body determined for each example that was studied is within the range discussed in Chapter 1 with an average frequency of 4.9 Hz. Also, the occupant

stiffness increased linearly with increasing mass ratio, as expected based on the method used for determining stiffness.

Similar to the results for the natural frequency of the occupants, the damping ratio of the occupants was also consistent across the range of 25-35%. These values are also within the range of previous literature (Sachse & Pavic, 2003). The combined system including the frequency of the human body, occupant stiffness, and damping ratios was able to accurately predict the change in both frequency and damping of the combined system for a variety of mass ratios with a similar posture.

Many combinations of crowd properties identified through the curve fitting method that was utilized produce a visually acceptable curve fit to the experimental results. The results for the examples shown are based on the lowest combined percent error for all criteria when compared to the experimental FRF. In some cases, the percent error between the occupant properties selected in the second best solution is less than two percent.

There are several improvements that could be done to the curve fitting method to produce more reliable results. First, smaller increments could be used for each variable to allow for a more refined and accurate solution. Also, the tolerance placed on the conditions to determine the appropriateness of each variable could also be reduced to eliminate less accurate combinations of occupant properties. Finally, the curve fitting method could be expanded to include more than just three points.

The series of SDOF models provide some useful information in their ability to accurately reproduce the natural frequency, stiffness, and damping of the occupied structure for the first mode. Because the dynamic properties of these SDOF models are similar, they can be the basis for developing a consistent SDOF model to be applied across the entire range of mass ratios. For example, the natural frequency of all the occupant models is between 4.2 and 5.8 Hz. A SDOF model of a crowd with an average natural frequency of 5.0 Hz is likely to be appropriate for all cases. Similar relationships exist for determining the stiffness and mass properties from the number of people in the crowd being modeled.

5.5 Limitations

There are several limitations associated with the results presented for the finite element models and SDOF model. First, the finite element model created in SAP2000 is based on conservative design guidance not specifically intended for use within a finite element model. A steel joist and concrete slab structure is a complex system to model. Other research presents some of the complexities in understanding and attempting to model structures similar to the test structure (Beaver, 1998). Also, the existing test structure contains a large crack in the concrete spanning the width of the structure that may affect the stiffness of the model. This flaw is not incorporated into the finite element model because the complexity involved in recreated it is outside the scope of this study. Similarly, The MASTAN2 model is simplistic and it only models the first mode of the actual floor.

The SDOF model also contains limitations. This model only considers the first mode of the individual and combined systems. However, the higher modes can also have an effect on the magnitude, stiffness, and damping associated with the first mode and alter the current estimations. Also, the test structure and occupants are more complex than the assumptions made for the SDOF system. The masses of the structure and occupants are distributed across an area and not a lumped mass located at one individual point. Also, human properties vary for each individual, suggesting that one value of stiffness and damping may also be an oversimplification and instead, a range of properties associated with a design model is more appropriate. The complexity of the overall problem and the inherent variability in both modeling methods and human occupant characteristics limit the development of a single, detailed model. An approximation, like the one presented here, that is fairly accurate and rather simple to apply may be most appropriate.

The magnitude of the FRF for the 2DOF model is different than that of the experimental for all tests shown but most noticeably in the empty structure. This modeling technique can lead to either an overestimation or underestimation of the actual response at lower frequencies. In addition to the difference in magnitude at the natural frequency, the slope leading up to this point is also substantially different. This may be attributed to the variability in experimental data within the low frequency range and the inability to accurately apply a curve fit within this range.

CHAPTER 6: SUMMARY AND CONCLUSIONS

6.1 Summary and conclusions

Human-structure interaction is an underdeveloped component of existing serviceability design guidelines. Previous studies have suggested the existence of this interaction but none have attempted to isolate the effects of various crowd characteristics in order to determine the level of interaction generated by combinations of these characteristics. By varying multiple characteristics, this study confirmed the existence of human-structure interaction and its dependency on several factors. This study, like others, also confirmed that the application of an equivalent mass does not produce the same results as an actual crowd of occupants. Confirmation of these two components is the foundation for the need to improve existing design guidance and utilize the information collected from this study in regards to the effect that distribution, mass ratio, and posture have on the dynamic response of a structure.

Previous research has often been limited to single data points from in-service events without the ability to identify possible trends. These studies are good in providing specific case by case examples of human-structure interaction, but are limited with only one crowd size and often an unknown description of crowd posture. In this regard, they fail to present a thorough examination and understanding of human-structure interaction. Similarly, traditional laboratory tests are not an accurate representation of real structures because they are limited by factors including scale and the natural frequency of the empty structure. For these reasons, the methodology and test structure used in this study offer a

unique example of an investigation into human-structure interaction based on crowd distribution, the mass ratio of the empty to occupied structure, and the posture of the stationary crowd and evaluating each variable independently when applied on a more realistic test structure.

Based on the three variables studied, it was determined that changes in both natural frequency and damping ratios of an occupied structure are related to not only posture but also the mass ratio of the occupants to the structure. These changes are most noticeable in the first mode. The changes produced by varying the distribution of occupants, however, are less significant. The subsequent four modes of vibration of the occupied structure show trends similar to those seen in the first mode but are also less significant and less critical in considering serviceability design. The average maximum frequency change in modes two through five for all mass ratios is 15 percent as compared to a maximum frequency change in the first mode of 32 percent. Similarly, the average maximum change in damping was only 8 times greater than the empty structure for modes two through five, whereas for the first mode, the maximum change in damping was 36 times greater than the empty structure. These results indicate that continued research should focus primarily on the effect of human-structure interaction on the first mode because it is the most significant and the dynamic response of most structures is dominated by vibration in the first mode.

The results presented for the first mode can be further evaluated based on the three postures used in the study. Independent of mass ratio, the average change in

frequency was most significant for the standing with straight knees and seated postures with decreases in the natural frequency of the occupied structure of 15 and 10 percent respectively. Damping was also 20 times greater for each of the same postures than of the empty structure. In general, as the mass ratio increases for a given posture the magnitude of change increases as well. It is important to understand these trends relating mass ratio and posture to the change in structural properties so that they can be utilized in the development of future studies that will incorporate the additional variables identified herein, as well as in the development of interim guidance for predicting the effects of human-structure interaction during design.

This study also provides a starting point for a simple method for modeling a combined system of a structure and crowd. The structure was able to be modeled as a single degree-of-freedom system with the frequency and damping of the first mode similar to the values determined from experimental testing. Also, the series of single degree-of-freedom crowd models that have been created for each of the testing scenarios in this study differ in both frequency and damping values of the occupants by approximately only 20 percent. This variation is considered acceptable based on the variability in the properties of the human body and the simplistic nature of this modeling technique. The combined system of structure and crowd models was able to accurately estimate the change in natural frequency with respect to the corresponding experimentally measured results to within an average difference of less than 4 percent for all mass ratios studied. The change in damping was less accurately predicted but still within 30 percent for all mass ratios except one. These results signify that a SDOF model

of a structure combined with a SDOF model of a crowd can produce reasonable predictions for the effects of human-structure interaction on the dynamic properties of the empty structure.

6.2 Future work

This study delineates several clear paths for future work and further improvement of the human-structure interaction phenomenon. It also generates new questions and areas of interest. First, additional mass ratios in the range associated with existing structures need to be studied. Results with different mass ratios will be able to support or enhance the understanding obtained from the mass ratios used in this study.

There are also other variables that have not been included in this study. One variable that is believed to have significance based on the results of this and previous studies is the empty structure natural frequency. The testing methods outlined in this study can be applied to another structure with a different empty natural frequency. These results will be able to provide another data point and determine whether or not the same model or a model similar to the model used in this study is an appropriate representation of a crowd.

Finally, the single degree-of-freedom models presented in this research can be expanded to more accurately model the empty structure and the crowd as well as the combined system. Refined modeling techniques can also be applied to finite element models in order to improve the accuracy. Enhancements in methods for creating finite

element models will enable the application of the SDOF crowd models to the finite element model itself.

APPENDICES

Appendix A: Design Guide 11 calculation of empty natural frequency.

Input

Concrete

Concrete weight $w_c := 150\text{pcf}$

Concrete strength $f'_c := 3000\text{psi}$

Floor total thickness $t_{fl\_tot} := 2.5\text{in}$

Deck rib thickness $t_{rib} := 1\text{in}$

Minimum concrete thickness $t_{min} := t_{fl\_tot} - t_{rib} = 1.5 \cdot \text{in}$

Effective slab thickness $t_{eff} := t_{fl\_tot} - \dfrac{t_{rib}}{2} = 2 \cdot \text{in}$

Joist properties

Joist name $\text{Joist\_designation} := \text{"14K4"}$

Type of joist (angle or bar) $\text{Joist\_type} := \text{"bar"}$

Joist weight $w_{joist} := 6.7\text{plf}$

Depth of joist $d_j := 14\text{in}$

Joist spacing $\text{space}_j := 30\text{in}$

Length of joist $L_j := 26\text{ft}$

Allowable stress of steel $f_{all} := 30\text{ksi}$ $\qquad w_{all} := 251\dfrac{\text{lbf}}{\text{ft}}$

Girder properites

Girder name $\text{Girder\_name} := \text{"W8x13"}$

Girder weight $w_{gird} := 13\text{plf}$

Cross-sectional area $A_{gird} := 3.84\text{in}^2$

Moment of intertia $I_{gird} := 39.6\text{in}^4$

Depth of girder $d_{gird} := 7.99\text{in}$

Length of girder $L_{gird} := 10\text{ft}$

Steel modulus of elasticity $E_s := 29000\text{ksi}$

Distributed loads

Live load $L_{live} := 0\text{psf}$

Slab and deck weight $L_{slab} := 25\text{psf}$

Calculations

Steps for calculating joist properties from joist table data.

1. Determine the allowable moment for joist section:

$$L_n := L_j - 0.33\text{ft} = 25.67 \cdot \text{ft}$$

$$M_{all} := \frac{w_{all} \cdot L_n^2}{8} = 2.481 \times 10^5 \cdot \text{lbf} \cdot \text{in}$$

2. Determine the effective area of the joist:

$$A_{bot\_ch} := \frac{M_{all}}{(d_j - 1\text{in}) \cdot f_{all}} = 0.636 \cdot \text{in}^2$$

$$A_{top\_ch} := 1.25 \cdot A_{bot\_ch} = 0.795 \cdot \text{in}^2$$

$$A_{tot\_ch} := A_{top\_ch} + A_{bot\_ch} = 1.431 \cdot \text{in}^2$$

$$A_{j\_eff} := 0.85 \cdot A_{tot\_ch} = 1.217 \cdot \text{in}^2$$

3. Determine the location of the neutral axis of the joist:

Note: The neutral axis of the joist is computed with the assumption that the centroid of the top chord of the joist is 0.5in from the top of the joist and the centroid of the bottom chord of the joist is 0.5in above the bottom of the joist. Measured from the top.

$$y_{j\_est} := 0.5\text{in} + \frac{A_{bot\_ch} \cdot (d_j - 1\text{in})}{A_{tot\_ch}} = 6.278 \cdot \text{in}$$

4. Determine the moment of inertia of the joist section:

$$I_{chord\_est} := A_{top\_ch} \cdot (y_{j\_est} - 0.5\text{in})^2 + A_{bot\_ch} \cdot (d_j - y_{j\_est} - 0.5\text{in})^2 = 59.726 \cdot \text{in}^4$$

Calculations

Beam mode properties

1. Calulate the dynamic concrete modulus of elasticity:

$$E_c := \left(\frac{w_c}{pcf}\right)^{1.5} \cdot \sqrt{\left(\frac{f'_c}{ksi}\right)} \cdot ksi = 3.182 \times 10^3 \cdot ksi$$

2. Calculate the modular ratio:

$$n := \frac{E_s}{1.35 \cdot E_c} = 6.751$$

3. Calculate the transformed moment of inertia using the actual chord area:

$$y_{top} := \frac{A_{tot\_ch} \cdot (t_{rib} + y_{j\_est}) - \left(\frac{space_j}{n}\right) \cdot t_{min} \frac{t_{min}}{2}}{A_{tot\_ch} + \left(\frac{space_j}{n}\right) t_{min}} = 0.669 \cdot in \qquad \text{(Below top of form deck)}$$

$$I_{comp} := I_{chord\_est} + A_{tot\_ch} \cdot (t_{rib} + y_{j\_est} - y_{top})^2$$

$$I_{comp} := I_{comp} + \left[\left(\frac{space_j}{n}\right)\frac{(t_{min}{}^3)}{12} + \left(\frac{space_j}{n}\right)(t_{min})\left(y_{top} + \frac{t_{min}}{2}\right)^2\right] = 136.912 \, in^4$$

4. Check the span-to-depth ratio:

$$Span\_depth\_check := \begin{array}{|l}
\text{"Good"} \quad \text{if} \quad \dfrac{L_j}{d_j} \leq 24 \wedge \dfrac{L_j}{d_j} \geq 6 \wedge Joist\_type = \text{"angle"} \quad = \text{"Good"} \\[3ex]
\text{"Good"} \quad \text{if} \quad \dfrac{L_j}{d_j} \leq 24 \wedge \dfrac{L_j}{d_j} \geq 10 \wedge Joist\_type = \text{"bar"} \\[3ex]
\text{"NG"} \quad \text{otherwise}
\end{array}$$

5. Calculate reduction coefficient

$$C_r := \begin{array}{|l}
\left[0.9 \cdot \left[1 - e^{-0.28 \cdot \left(\frac{L_j}{d_j}\right)^{2.8}}\right]\right] \quad \text{if} \quad Joist\_type = \text{"angle"} \quad = 0.883 \\[3ex]
\left[0.721 + 0.00725\left(\frac{L_j}{d_j}\right)\right] \quad \text{if} \quad Joist\_type = \text{"bar"}
\end{array}$$

Calculations

$$\gamma := \frac{1}{C_r} - 1 = 0.133$$

$$I_{eff} := \frac{1}{\dfrac{\gamma}{I_{chord\_est}} + \dfrac{1}{I_{comp}}} = 104.913 \cdot in^4$$

$$I_j := I_{eff} = 104.913 \cdot in^4$$

6. Calculate the uniform distributed live load:

$$w_j := space_j \cdot \left(L_{live} + L_{slab}\right) + w_{joist} = 69.2 \cdot plf$$

7. Calculate the corresponding deflection:

$$\Delta_j := \frac{5 \cdot w_j \cdot L_j^4}{384 \cdot E_s \cdot I_j} = 0.234 \cdot in$$

8. Calculate the fundamental frequency of the joist:

$$f_j := 0.18 \cdot \sqrt{\frac{g}{\Delta_j}} = 7.314 \cdot Hz$$

Calculations

Girder mode properties

1. Calculate the effective slab width:

$$\text{slab}_{\text{eff}} := \min\left(0.2 \cdot L_{\text{gird}} + 6\text{in}, L_j\right) = 30 \cdot \text{in}$$

2. Calculate the distance from the bottom of the effective slab thickness:

$$y_{\text{top\_g}} := \frac{A_{\text{gird}} \cdot \left[\left(t_{\text{fl\_tot}} - t_{\text{eff}}\right) + t_{\text{fl\_tot}} + \dfrac{d_{\text{gird}}}{2}\right] - \left(\dfrac{\text{slab}_{\text{eff}}}{n}\right) t_{\text{eff}} \cdot \dfrac{t_{\text{eff}}}{2}}{A_{\text{gird}} + \left(\dfrac{\text{slab}_{\text{eff}}}{n}\right) t_{\text{eff}}} = 1.412 \cdot \text{in}$$

3. Calculate the transformed moment of inertia:

$$I_{g\_1} := A_{\text{gird}} \cdot \left[\left(t_{\text{fl\_tot}} - t_{\text{eff}}\right) + t_{\text{fl\_tot}} + \frac{d_{\text{gird}}}{2} - y_{\text{top\_g}}\right]^2$$

$$I_{g\_2} := \frac{\text{slab}_{\text{eff}}}{n} \frac{\left(t_{\text{eff}}^3\right)}{12} + \frac{\text{slab}_{\text{eff}}}{n}\left(t_{\text{eff}}\right)\left(y_{\text{top\_g}} + \frac{t_{\text{eff}}}{2}\right)^2$$

$$I_g := I_{\text{gird}} + I_{g\_1} + I_{g\_2} = 213.961 \cdot \text{in}^4$$

4. Account for flexible in joist seats by reducing girder moment of inertia:

$$I_g := I_{\text{gird}} + \frac{\left(I_g - I_{\text{gird}}\right)}{4} = 83.19 \cdot \text{in}^4$$

5. Calculate the equivalent uniform load for each girder:

$$w_g := \frac{\left[L_j \cdot \left(\dfrac{w_j}{\text{space}_j}\right)\right]}{2} + w_{\text{gird}} = 372.84 \cdot \text{plf}$$

6. Calculate the corresponding girder deflection:

$$\Delta_g := \frac{5 \cdot w_g \cdot L_{\text{gird}}^4}{384 \cdot E_s \cdot I_g} = 0.035 \cdot \text{in}$$

7. Calculate the girder mode fundamental frequency:

$$f_g := 0.18 \sqrt{\frac{g}{\Delta_g}} = 18.967 \cdot \text{Hz}$$

Calculations

Combined mode properties

1. Calculate combined fundamental frequency:

$$f_n := 0.18 \sqrt{\frac{g}{\left(\Delta_j + \Delta_g\right)}} = 6.824 \cdot Hz$$

Appendix B: Experimental equipment setup.
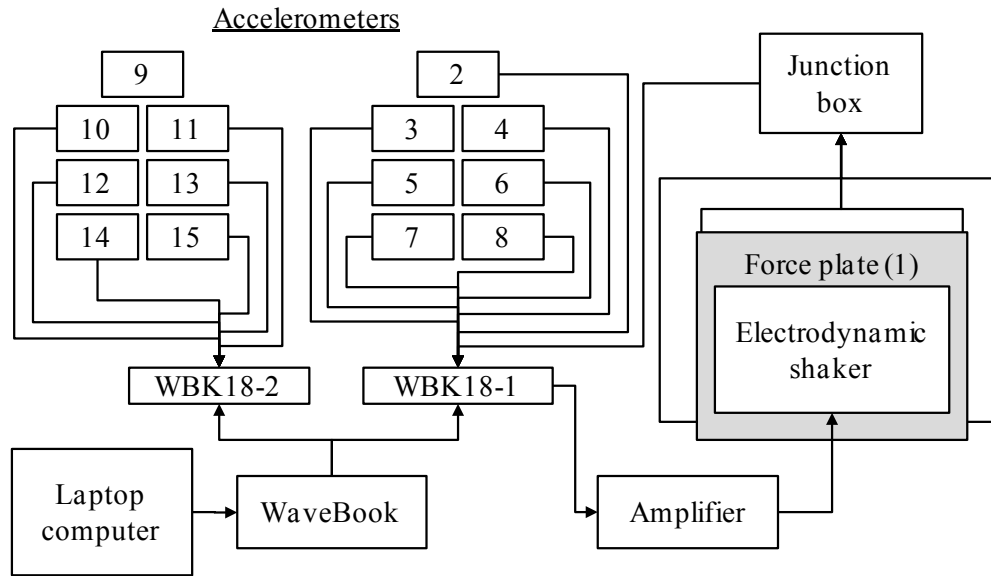
Figure 32: Experimental equipment setup.

Appendix C: Calibration factors for data acquisition system for accelerometers and force plate.

Table 8: Calibration coefficients used in eZ-Analyst.

Item	Node location	Calibration Coefficient (mV/g)
Force plate	069	-5.38 (mV/lbf)
Accelerometer #1	019	980.0
Accelerometer #2	023	1016.0
Accelerometer #3	027	1015.0
Accelerometer #4	037	1020.0
Accelerometer #5	045	1021.0
Accelerometer #6	055	985.0
Accelerometer #7	059	988.0
Accelerometer #8	063	1025.0
Accelerometer #9	073	1026.0
Accelerometer #10	069	1047.0
Accelerometer #11	081	1024.0
Accelerometer #12	091	1035.0
Accelerometer #13	095	1031.0
Accelerometer #14	099	952.0

Appendix D: Participant informed consent form.

<p style="text-align:center">Participation in Research Study involving Human-Structure Interaction
<u>Informed Consent Form</u></p>

1. **Project name:** Investigating the Effects of Various Crowd Characteristics on the Dynamic Properties of an Occupied Structure
2. **Purpose of the research:** The aim of the current study is to investigate the effects of various crowd characteristics on the dynamic properties of the structure which they occupy. It is expected that the crowd characteristics, including size, density, distribution, posture, and activity, will affect the dynamic properties of the empty structure, including natural frequency, damping ratio, and possibly mode shapes.
3. **Overall research plan:** Experimental measurements will be taken and data analysis will be performed on an empty test structure and on a variety of configurations of the structure when occupied by the study participants.
4. **Research plan duration:** It is expected that experimental measurements involving study participants will be taken in 3 sessions (approximately 1/week), each lasting approximately 30 minutes.

Additional Notes
1. **<u>Participation in this study is 100% voluntary</u>**. Participants will not be compensated in any way including, but not limited to, monetarily, academically, etc. Participants may withdraw from the study at any point and for any reason without any consequences. Participants are encouraged to ask questions at any time about the study and his/her participation in the study.
2. The data gathered in this study will be maintained confidentially through secure file storage. Data will only be used by the PI or research assistant involved with this study, unless written permission is given to do otherwise.
3. There is a small but unlikely risk of discomfort or loss of balance due to dynamic motion of structure being occupied. If you feel a loss of balance or are uncomfortable with the motion, you are to stop the activity and immediately inform the PI or research assistant so that the testing can be halted.
4. It is regarded as extremely unlikely that any physical harm would come to any research participant. The activities performed during the experimental measurement sessions are not believed to increase your risk more than what you would experience in everyday activities. In the event of physical injury resulting from the subject's participation in the research, emergency medical treatment will be immediately called for the subject. The subject should immediately notify the investigator if s/he is injured. If the subject requires additional medical treatment, s/he will be responsible for the cost. No other compensation will be provided if s/he sustains an injury resulting from the research.

I have read the above description of the research and any uncertainties were satisfactorily explained to me by Kelly Salyards or Robert Firman. I agree to participate in this research, and I acknowledge that I have received a personal copy of this signed consent form.

By signing below, I affirm that I am at least 18 years of age or older.

Printed name: _____

Signature of Subject: _____ Date: _____

Appendix E: Crowd distribution calculations.

Density Calculations

Given:

Maximum density (Kappos, 2002)
$$d_{max} := 4800 \frac{N}{m^2}$$

Maximum crowd size (Kappos, 2002)
$$max\_c := \frac{6}{m^2}$$

Floor maximum design load (Raebel, 2000)
$$w_{max} := 78 \frac{lbf}{ft^2}$$

Calculations:

1. Calculate maximum suggested dimensions per person

$$d_{max\_a} := max\_c = 0.557 \cdot \frac{1}{ft^2}$$

$$dim_{max} := \sqrt{\frac{1}{d_{max\_a}}} = 16.073 \cdot in$$

2. Calculate assumed human weight

$$w_h := \frac{d_{max}}{psf} \cdot \frac{1}{d_{max\_a} \cdot ft^2} = 179.847$$

$$w_h := w_h \cdot lbf = 179.847 \cdot lbf$$

3. Calculate allowable density

$$a_{all} := \frac{w_h}{w_{max}} = 2.306 \cdot ft^2$$

$$dim_{all} := \sqrt{\frac{a_{all}}{in^2}} \cdot in = 18.222 \cdot in$$

4. Select appropriate densities

$$dim_{dense} := 20in \qquad \text{(greater than the minimum allowable)}$$

$$dim_{sparse} := 28in \qquad \text{(greatest dimension not to exceed floor dimensions)}$$

Appendix F: Experimental testing sheets for testing sessions.

	Project title:	Investigating the Effects of Various Crowd Characteristics on the Dynamic Properties of an Occupied Structure
	Date(s):	2/21/10, 2/28/10
	Location:	Penn State University
	Test operator(s):	Kelly Salyards, Robert Firman
	Assistants:	none

Equipment

	Item	Quantity	Start	End
1	Wavebook	1	X	X
2	WBK18 modules	2	X	X
3	Wavebook power cords	2	X	X
4	Wavebook connection cables	(assortment)	X	X
5	Computer and power cord	1	X	X
6	Computer mouse	1	X	X
7	Extra computer	1	X	X
8	Accelerometer	8	X	X
9	Accelerometer mounting plate	20	X	X
10	Accelerometer mounting plate screw	21, 12	X	X
11	BNC accelerometer cable (assorted length)	12	X	X
12	Extension cord	1	X	X
13	Power strip	2	X	X
14	Ethernet cord	1	X	X
15	Hex key set	0	X	X
16	Adjustable wrench (8in Craftsman)	1	X	X
17	Tape measure	2	X	?
18	Utility knife	1	X	X
19	Phillips head screwdriver/flat head	2 (each)	X	X
20	Roll of duct tape	3	X	2y, 2r, 2b, 1w
21	Accelerometer putty (modeling clay)	--	X	X
22	IRB request form	--	X	X
23	Participant grid layout	--	X	X
24	Numbers for participants	50	X	X
25	Digital camera	1	X	X
26	BNC-BNC extension cables (long)	8	X	X
27	BNC-BNC extension cables (short)	1	X	X
28	Coupler	7	X	X
29	T-connector	4	X	X
30				
31				

- **DAY 1**
    - Layout participant grid for Day 2
    - Install accelerometers

- o Secure accelerometer cabling
  - o Preliminary tests (see below)
  - o Empty tests
- **DAY 2**
  - o Single person test
- **DAY 3**
  - o Distribute consent forms (2 copies per participant)
  - o 3 group sizes
- **DAY 4**
  - o 1 group size
  - o Equivalent mass

Procedure

Preliminary phase

Task	File Name (see Excel sheet)	Status
Excitation/response check	HSI_prelim_mm-dd-yyyy_test01	
Immediate repeatability check	HSI_prelim_mm-dd-yyyy_test02	
Homogeneity check	HSI_prelim_mm-dd-yyyy_test03	
Reciprocity check	HSI_prelim_mm-dd-yyyy_test04	
Coherence function check	--	
FRF shape check	--	
End of test repeatability check	HSI_prelim_mm-dd-yyyy_test05	

Measurement phase

- Chirp excitation setup

Input voltage to shaker, RMS (v)	0.05 – 0.28 (0.20 is reasonable)
Record length	1024
Bandwidth frequency (Hz)	30 (50 is the best available)
Time step (s)	0.0078
Nyquist frequency (Hz)	64
Number of averages (#)	3
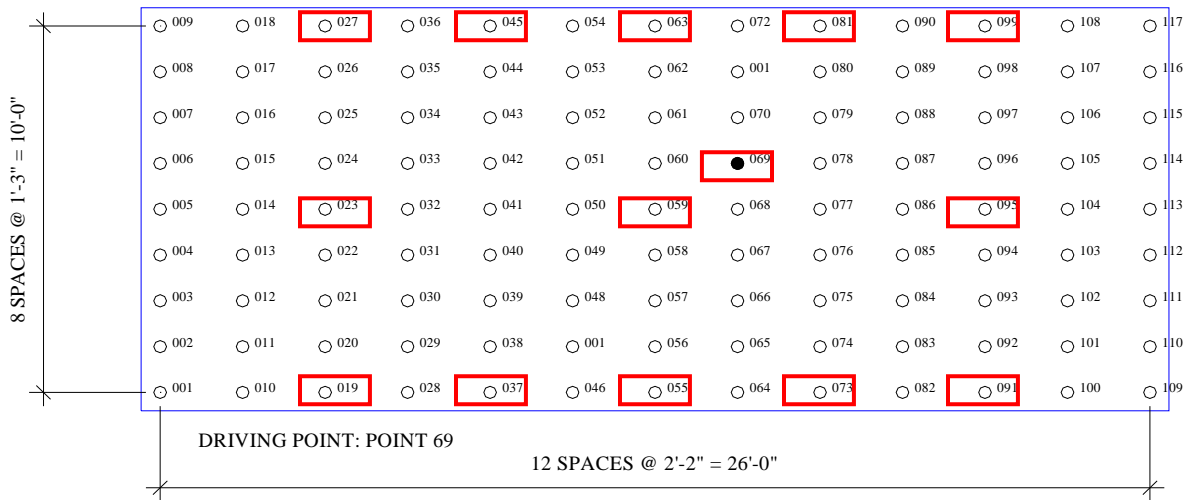
Figure 1: Dense accelerometer grid of 117 points.

Additional Notes
- IRB limitations
  - Only 3 measurement sessions
  - Less than 30 sec per measurement
  - Each activity will be performed less than 5 times in a measurement session
  - No longer than 3 hrs a session
  - Entire series of tests will occur within a 3 week time frame
  - Each participant will receive a number and subject information is to be stored in a password-protected file in a private research folder
  - No compensation
- From Raebel's Thesis
  - Shaker setup
    - The input voltage to the shaker – 0.28v root-mean-squared (RMS) which produces maximum stroke of the shaker armature at very low frequencies (but the 0.20v RMS excitation provides a reasonable level to use for analysis).
  - Sampling rate
    - Four factors influencing the sampling rate of the data acquisition system: record length, bandwidth, frequency step, and time window length.
    - For a 1024 record length and 50 hertz bandwidth, the time window is 8 seconds. This means that Δt = 8/1024, or 0.0078 seconds. Thus, the Nyquist frequency f_A = 1/(2 x 0.0078), or 64 hertz. If the frequency content of the signal collected remains lower than the Nyquist frequency, aliasing will not occur. Because of the imperfection of filtering, the bandwidth is further reduced from 64 to 50 hertz, which is 78% of the Nyquist frequency.
    - The modal parameters extracted are very similar for both 1024 and 2048 record lengths. It is concluded that either record length is acceptable for chirp excitations.
  - Averaging
    - The frequency and damping values extracted show that <u>three</u> averages of chirp data is acceptable for data collection when analyzing the experimental floor.
  - Accelerometer grid layout
    - It has been found that seven accelerometers equally spaced along the length of the joist is adequate discretization to define the mode shapes for the first five modes.
    - The results of the sparse grid also prove that instrumentation between the joists on the experimental floor is unnecessary to define the mode shapes
    - The center-to-center spacing of the accelerometers in the short direction of the bay should not exceed the spacing in the long direction.
    - The placement of the accelerometers in the short direction should include the midspan point. For both directions, the accelerometers should be placed directly over structural members.

	Project title:	Investigating the Effects of Various Crowd Characteristics on the Dynamic Properties of an Occupied Structure
	Date(s):	3/2/10
	Location:	Penn State University
	Test operator(s):	Kelly Salyards, Robert Firman
	Assistants:	Carl Anderson, Will Peterson, Jonathon Powanda

Table 1 – Checklist of supplies.

	Item	Quantity	Start	End
1	Computer and power cord	2	X	X
2	Computer mouse	2	X	X
3	Clipboard	5	X	X
4	Paper plates	100	X	X
5	Napkins	~250	X	ALL
6	Bag of pens	10	X	9
7	Duct tape	3	X	X
8	Numbers for participants	50	X	X
9	Digital camera (and charger)	1	X	X
10	Participant grid layout	--	X	X
11	Tape measure	1	X	X
12	IRB request form	--	X	X
13	Sign-in form	1	X	X
14	Consent forms (2 each) and folder	50	X	X
15				
16				
17				
18				
19				
20				
21				
22				
23				
24				
25				
26				
27				
28				
29				
30				
31				

Test schedule:

4:00	Depart Lewisburg
5:30	Arrive at State College
5:30-5:45	Unload benches and other supplies
	Order pizza
5:45-6:00	Setup accelerometers
	Setup Wavebook and secure all connections
6:00-6:15	Setup check-in station and organize material for participants
	Ensure equipment is functioning properly and at the appropriate settings
6:15-6:20	Other preparations steps needed
6:20-6:35	Participants and arrive, consent forms are distributed, data is recorded into the computer
6:35-7:02	Perform testing with participants

1. (5:00) <u>Maximum number of people</u> seated on benches (2 tests, possibly at both densities depending on space)
2. (2:00) Remove benches from floor
3. (2:30) Dense grid, knees bent
4. (2:30) Dense grid, straight legs
5. (2:30) Dense grid, knees bent
6. (2:30) Dense grid, straight legs
7. (2:30) Sparse grid, knees bent
8. (2:30) Sparse grid, straight legs
9. (2:30) Sparse grid, knees bent
10. (2:30) Sparse grid, straight legs

Total time: 27:00

7:02-7:15	Distribute pizza
	Answer any post test questions or discussion
	Any closing remarks to remaining participants
7:15-7:25	Put benches back onto the floor
7:25-7:52	Perform testing with participants

1. (5:00) <u>Four people</u> seated on benches (2 tests, possibly at both densities depending on space)
2. (2:00) *Remove benches from floor*
3. (2:30) Dense grid, knees bent
4. (2:30) Dense grid, straight legs
5. (2:30) Dense grid, knees bent
6. (2:30) Dense grid, straight legs
7. (2:30) Sparse grid, knees bent
8. (2:30) Sparse grid, straight legs
9. (2:30) Sparse grid, knees bent
10. (2:30) Sparse grid, straight legs

Total time: 27:00

7:52-8:00	Break
8:00-8:15	Find mass in basement of lab
8:15-8:30	Add <u>four person</u> mass to structure
8:30-8:43	Perform testing with mass
	(4:00) Dense grid (2 tests)
	(5:00) *Move mass to sparse grid*
	(4:00) Sparse grid (2 tests)
	Total time: 13:00
8:43-9:00	Return mass to proper location in lab

9:00-9:05	Repeat empty structure test (2 tests)
9:05-9:20	Disconnect Wavebook
	Remove accelerometers
9:20-9:30	Additional clean-up steps

Posture descriptions:

> For all postures, participant should remain as still as possibly throughout the duration of each individual test. The testing personnel will notify participants when measurements are being recorded. Sight should be set at the wall directly in front of participants.

1. **Seated** – sitting on bench comfortably with knees forming a 90 degree angle. Feet planted firmly and flat on the ground. Hands should be placed palms down on thighs.
2. **Standing (straight legs)** – standing upright with hands directly at the side of the body, palms facing inward. Knees are not locked, but in a casual resting position.
3. **Standing (bent knees)** – standing upright with hands directly at the side of the body, palms facing inward. Knees are slightly bent in a position that can be sustained for a minute's duration.

Table 2 – Filename checklist.

	No	Filename (## - participants)	Grid	Posture	Participants	SAVED?
	1	HSI__03-02-2010 startempty1	--	--	0	X
	2	HSI__03-02-2010 startempty2	--	--	0	X
	3	HSI__03-02-2010 D16c1	Dense	Seated	16	X
	4	HSI__03-02-2010 D16c2	Dense	Seated	16	X
	5	HSI__03-02-2010 S16c1	Sparse	Seated	16	X
	6	HSI__03-02-2010 S16c2	Sparse	Seated	16	X
	7	HSI__03-02-2010 D16b1	Dense	Bent	16	X
	8	HSI__03-02-2010 D16a1	Dense	Straight	16	X
	9	HSI__03-02-2010 D16b2	Dense	Bent	16	X
	10	HSI__03-02-2010 D16a2	Dense	Straight	16	X
	11	HSI__03-02-2010 S16b1	Sparse	Bent	16	X
	12	HSI__03-02-2010 S16a1	Sparse	Straight	16	X
	13	HSI__03-02-2010 S16b2	Sparse	Bent	16	X
	14	HSI__03-02-2010 S16a2	Sparse	Straight	16	X
SP	15	HSI__03-02-2010 D8c1	Dense	Seated	8	X
SP	16	HSI__03-02-2010 D8c2	Dense	Seated	8	X
S	17	HSI__03-02-2010 S8c1	Sparse	Seated	8	X
S	18	HSI__03-02-2010 S8c2	Sparse	Seated	8	X
S	19	HSI__03-02-2010 D8b1	Dense	Bent	8	X
S	20	HSI__03-02-2010 D8a1	Dense	Straight	8	X
S	21	HSI__03-02-2010 D8b2	Dense	Bent	8	X
S	22	HSI__03-02-2010 D8a2	Dense	Straight	8	X
SP	23	HSI__03-02-2010 S8b1	Sparse	Bent	8	X
SP	24	HSI__03-02-2010 S8a1	Sparse	Straight	8	X
SP	25	HSI__03-02-2010 S8b2	Sparse	Bent	8	X
SP	26	HSI__03-02-2010 S8a2	Sparse	Straight	8	X
	27	HSI__03-02-2010 D4c1	Dense	Seated	4	X
	28	HSI__03-02-2010 D4c2	Dense	Seated	4	X
	29	HSI__03-02-2010 D4b1	Dense	Bent	4	X
	30	HSI__03-02-2010 D4a1	Dense	Straight	4	X
	31	HSI__03-02-2010 D4b2	Dense	Bent	4	X
	32	HSI__03-02-2010 D4a2	Dense	Straight	4	X
	33	HSI__03-02-2010 D4mass1	Dense	--	0	X
	34	HSI__03-02-2010 D4mass2	Dense	--	0	X
	35	HSI__03-02-2010 S4mass1	Sparse	--	0	NO
	36	HSI__03-02-2010 S4mass2	Sparse	--	0	NO
	37	HSI__03-02-2010 endempty1	--	--	0	X
	38	HSI__03-02-2010 endempty2	--	--	0	X

	Project title:	Investigating the Effects of Various Crowd Characteristics on the Dynamic Properties of an Occupied Structure
	Date(s):	3/3/10
	Location:	Penn State University
	Test operator(s):	Kelly Salyards, Robert Firman
	Assistants:	Douglas Gabauer, Erin Heidecker, Meghan Murphy

Table 1 – Checklist of supplies.

	Item	Quantity	Start	End
1	Computer and power cord	2	X	X
2	Computer mouse	2	X	X
3	Clipboard	5	X	X
4	Paper plates	100	X	X
5	Napkins	~250	X	X
6	Bag of pens	9	X	X
7	Duct tape	3	X	X
8	Numbers for participants	50	X	X
9	Digital camera (and charger)	1	X	X
10	Participant grid layout	--	X	X
11	Tape measure	1	X	X
12	IRB request form	--	X	X
13	Sign-in form	1	X	X
14	Consent forms (2 each) and folder	50	X	X
15				
16				
17				
18				
19				
20				
21				
22				
23				
24				
25				
26				
27				
28				
29				
30				
31				

Test schedule:

4:00	Depart Lewisburg
5:30	Arrive at State College
5:30-5:45	Unload benches and other supplies
	Order pizza
5:45-6:00	Setup accelerometers
	Setup Wavebook and secure all connections
6:00-6:15	Setup check-in station and organize material for participants
	Ensure equipment is functioning properly and at the appropriate settings
6:15-6:20	Other preparations steps needed
6:20-6:35	Participants and arrive, consent forms are distributed, data is recorded into the computer
6:35-7:02	Perform testing with participants

1. (5:00) <u>Maximum number of people</u> seated on benches (2 tests, possibly at both densities depending on space)
2. (2:00) Remove benches from floor
3. (2:30) Dense grid, knees bent
4. (2:30) Dense grid, straight legs
5. (2:30) Dense grid, knees bent
6. (2:30) Dense grid, straight legs
7. (2:30) Sparse grid, knees bent
8. (2:30) Sparse grid, straight legs
9. (2:30) Sparse grid, knees bent
10. (2:30) Sparse grid, straight legs

Total time: 27:00

7:02-7:15	Distribute pizza
	Answer any post test questions or discussion
	Any closing remarks to remaining participants
7:15-7:25	Put benches back onto the floor
7:25-7:52	Perform testing with participants

1. (5:00) _____ seated on benches (2 tests, possibly at both densities depending on space)
2. (2:00) *Remove benches from floor*
3. (2:30) Dense grid, knees bent
4. (2:30) Dense grid, straight legs
5. (2:30) Dense grid, knees bent
6. (2:30) Dense grid, straight legs
7. (2:30) Sparse grid, knees bent
8. (2:30) Sparse grid, straight legs
9. (2:30) Sparse grid, knees bent
10. (2:30) Sparse grid, straight legs

Total time: 27:00

7:52-8:00	Break
8:00-8:15	Find mass in basement of lab
8:15-8:30	Add _____ mass to structure
8:30-8:43	Perform testing with mass
	(4:00) Dense grid (2 tests)
	(5:00) *Move mass to sparse grid*
	(4:00) Sparse grid (2 tests)
	Total time: 13:00
8:43-9:00	Return mass to proper location in lab

9:00-9:05	Repeat empty structure test (2 tests)
9:05-9:20	Disconnect Wavebook
	Remove accelerometers
9:20-9:30	Additional clean-up steps

Posture descriptions:

For all postures, participant should remain as still as possibly throughout the duration of each individual test. The testing personnel will notify participants when measurements are being recorded. Sight should be set at the wall directly in front of participants.

1. **Seated** – sitting on bench comfortably with knees forming a 90 degree angle. Feet planted firmly and flat on the ground. Hands should be placed palms down on thighs.
2. **Standing (straight legs)** – standing upright with hands directly at the side of the body, palms facing inward. Knees are not locked, but in a casual resting position.
3. **Standing (bent knees)** – standing upright with hands directly at the side of the body, palms facing inward. Knees are slightly bent in a position that can be sustained for a minute's duration.

Table 2 – Filename checklist.

	No	Filename (## - participants)	Grid	Posture	Participants	SAVED?
	1	HSI__03-03-2010 startempty1	--	--	0	X
	2	HSI__03-03-2010 startempty2	--	--	0	X
a1	3	HSI__03-03-2010 D24c1	Dense	Seated	24 (19)	X
a2	4	HSI__03-03-2010 D24c2	Dense	Seated	24 (19)	X
a1	5	HSI__03-03-2010 S24c1	Sparse	Seated	24 (19)	X
a2	6	HSI__03-03-2010 S24c2	Sparse	Seated	24 (19)	X
	7	HSI__03-03-2010 D24b1	Dense	Bent	24 (19)	X
c1	8	HSI__03-03-2010 D24a1	Dense	Straight	24 (19)	X
	9	HSI__03-03-2010 D24b2	Dense	Bent	24 (19)	X
c2	10	HSI__03-03-2010 D24a2	Dense	Straight	24 (19)	X
	11	HSI__03-03-2010 S24b1	Sparse	Bent	24 (19)	X
c1	12	HSI__03-03-2010 S24a1	Sparse	Straight	24 (19)	X
	13	HSI__03-03-2010 S24b2	Sparse	Bent	24 (19)	X
c2	14	HSI__03-03-2010 S24a2	Sparse	Straight	24 (19)	X
	15	HSI__03-03-2010 D###c1	Dense	Seated	--	--
	16	HSI__03-03-2010 D###c2	Dense	Seated	--	--
	17	HSI__03-03-2010 S###c1	Sparse	Seated	--	--
	18	HSI__03-03-2010 S###c2	Sparse	Seated	--	--
	19	HSI__03-03-2010 D###b1	Dense	Bent	--	--
	20	HSI__03-03-2010 D###a1	Dense	Straight	--	--
	21	HSI__03-03-2010 D###b2	Dense	Bent	--	--
	22	HSI__03-03-2010 D###a2	Dense	Straight	--	--
	23	HSI__03-03-2010 S###b1	Sparse	Bent	--	--
	24	HSI__03-03-2010 S###a1	Sparse	Straight	--	--
	25	HSI__03-03-2010 S###b2	Sparse	Bent	--	--
	26	HSI__03-03-2010 S###a2	Sparse	Straight	--	--
	27	HSI__03-03-2010 D##mass1	Dense	--	0	X
	28	HSI__03-03-2010 D##mass2	Dense	--	0	X
	29	HSI__03-03-2010 S##mass1	Sparse	--	0	--
	30	HSI__03-03-2010 S##mass2	Sparse	--	0	--
	31	HSI__03-03-2010 endempty1	--	--	0	--
	32	HSI__03-03-2010 endempty2	--	--	0	--
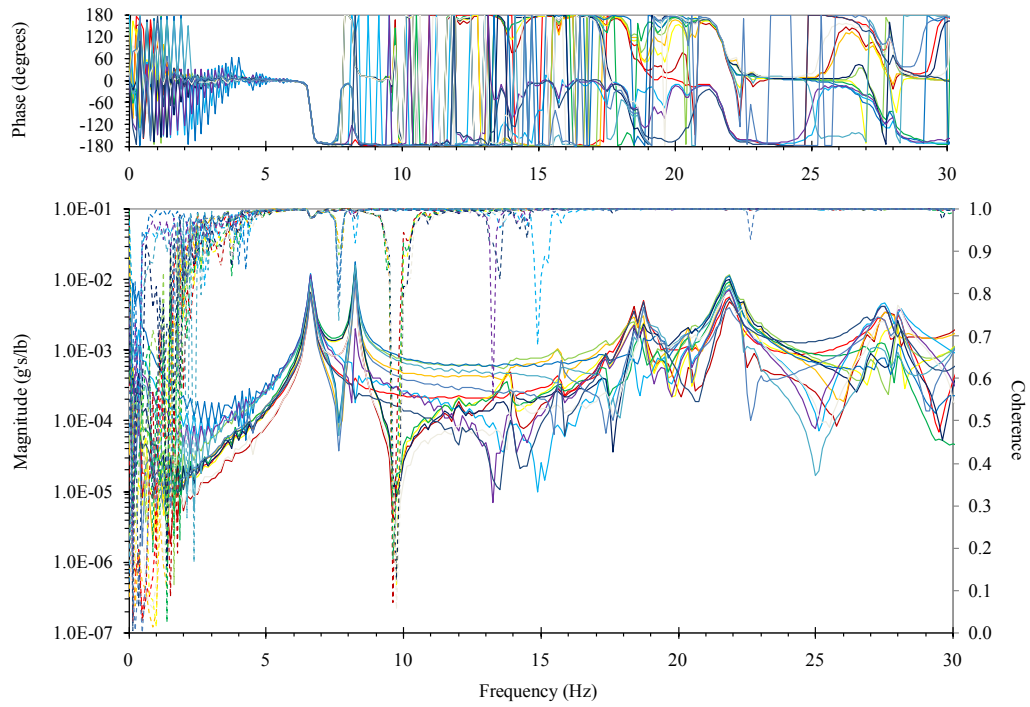
Figure 33: Experimental FRF (mass ratio=0.02, standing-straight knees, dense, test-1).
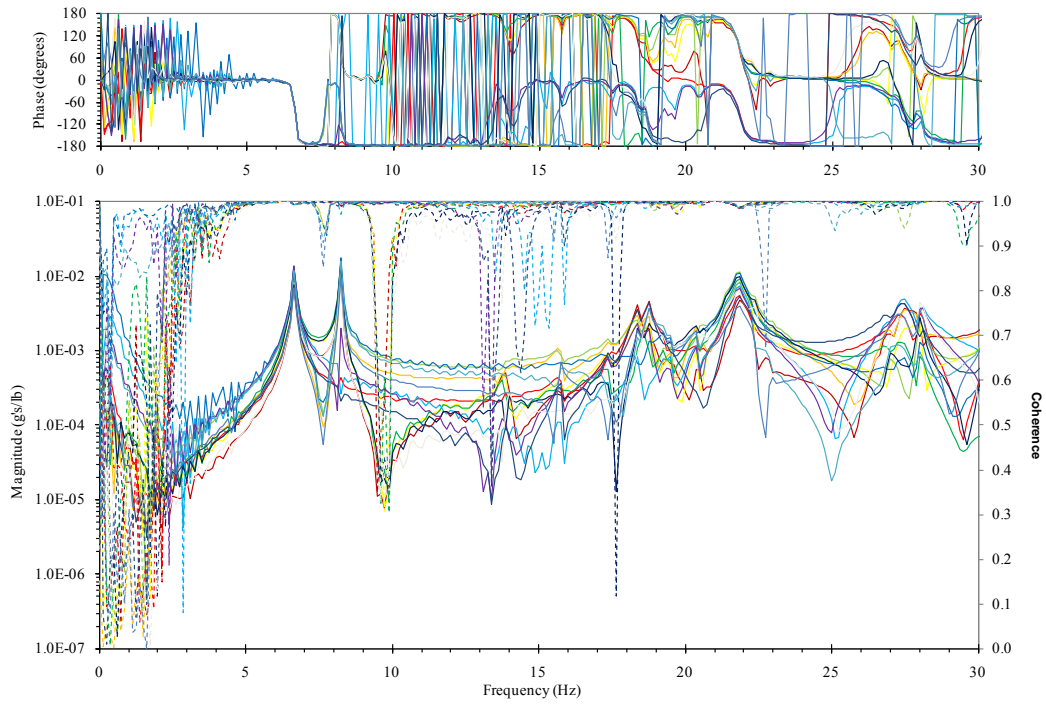
Figure 34: Experimental FRF (mass ratio=0.02, standing-straight knees, dense, test-2).
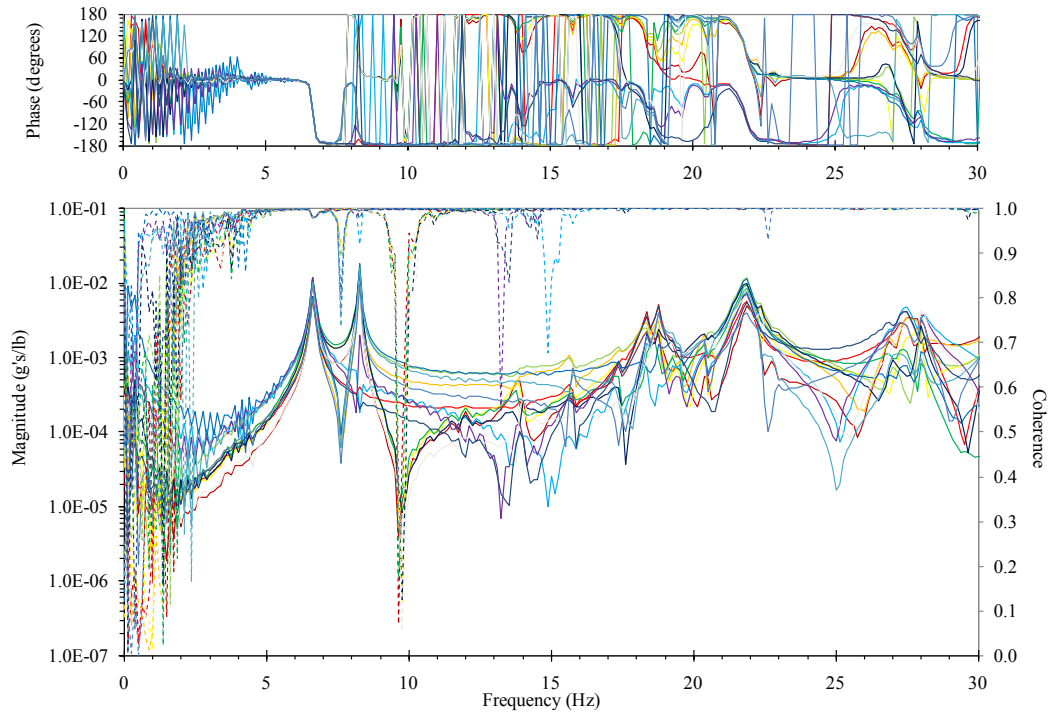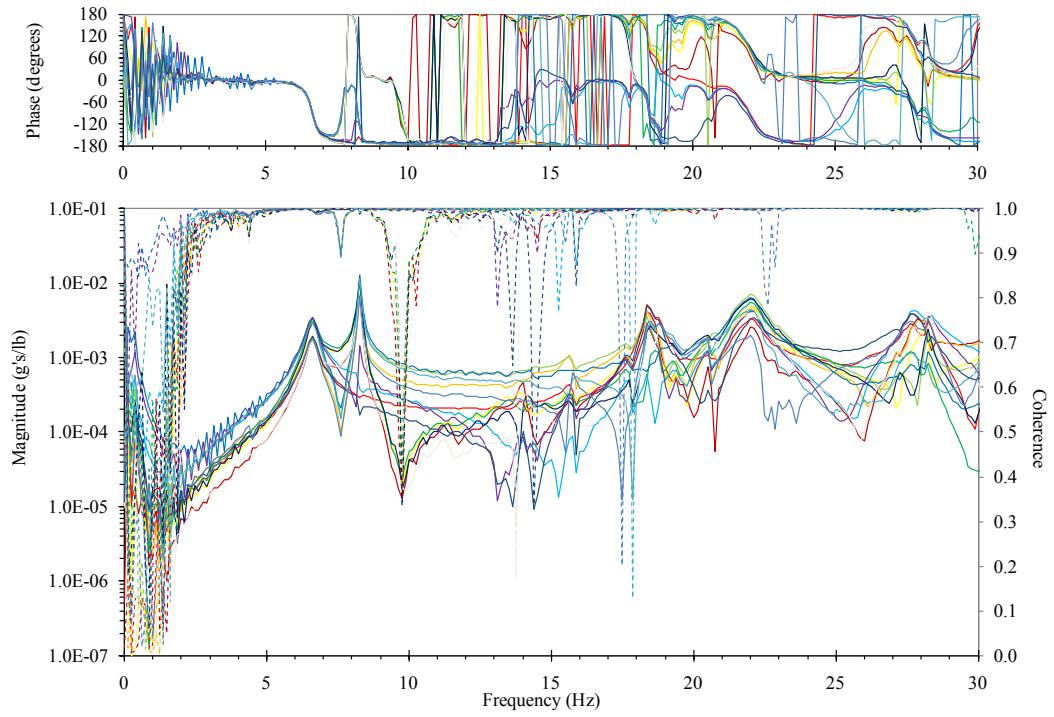
Figure 35: Experimental FRF (mass ratio=0.02, standing-bent knees, dense, test-1).
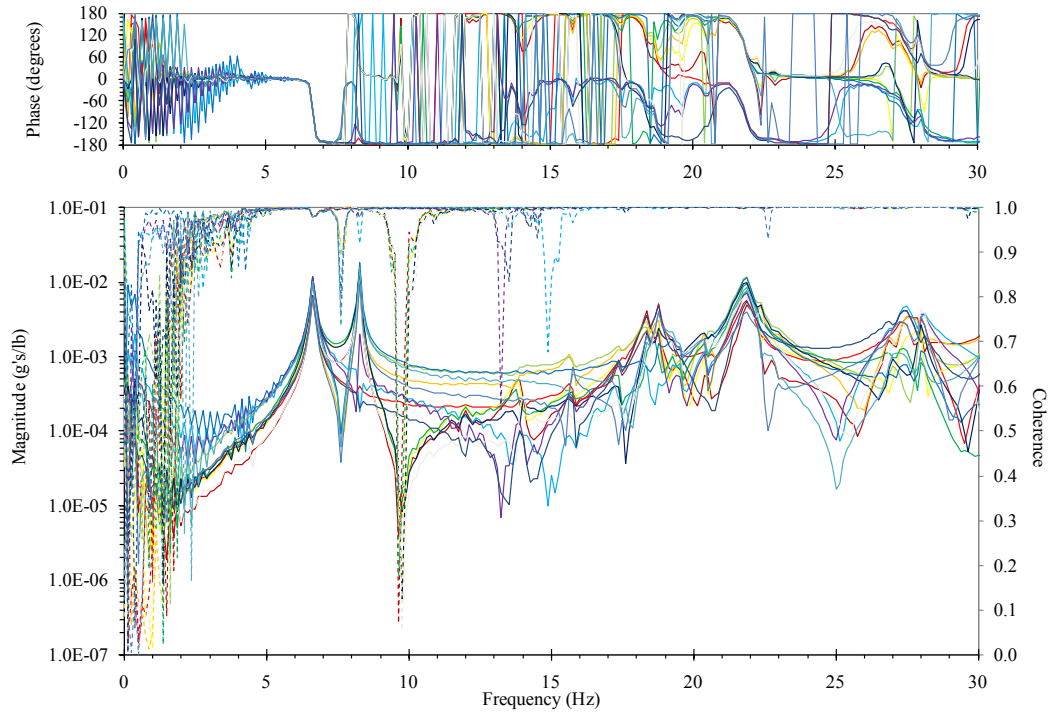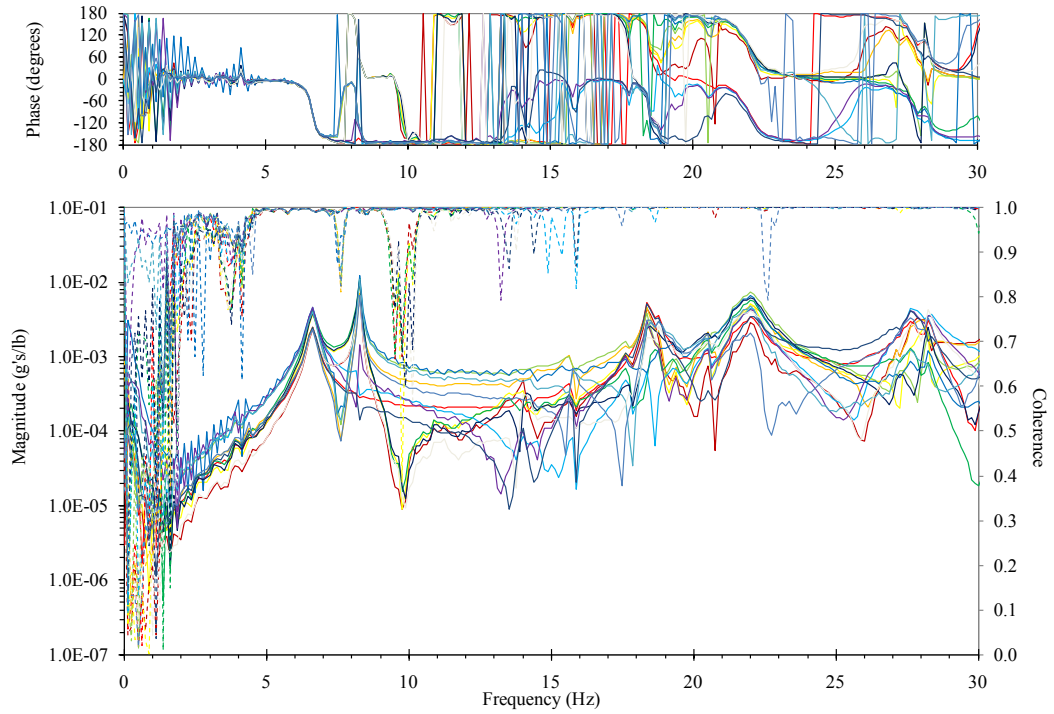

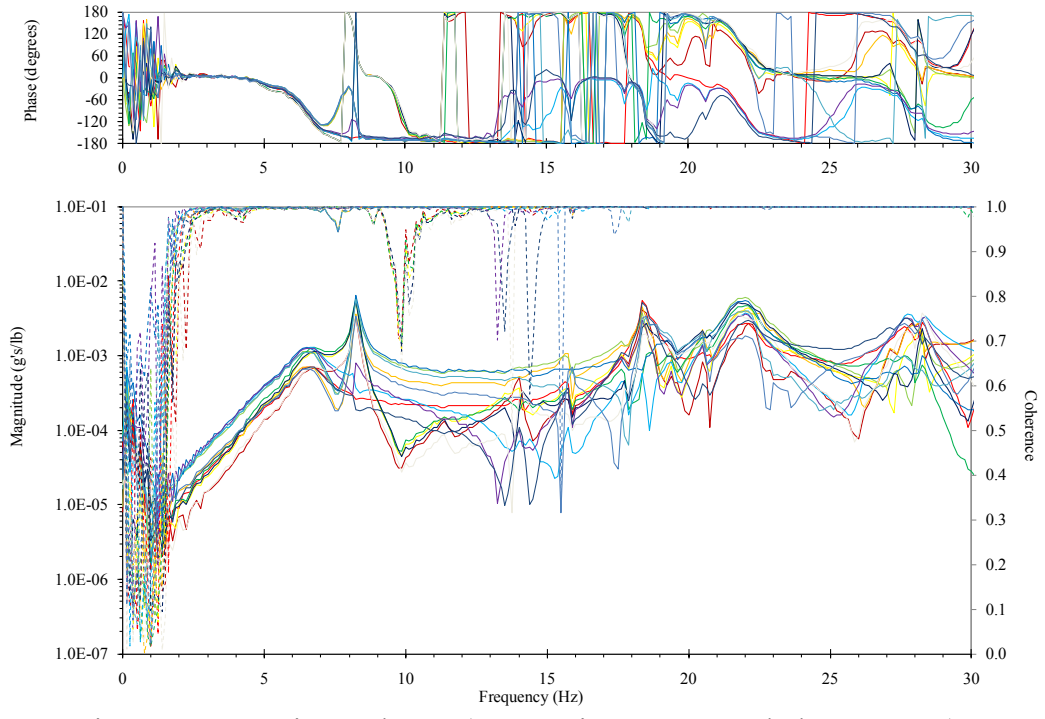Figure 36: Experimental FRF (mass ratio=0.02, standing-bent knees, dense, test-2).
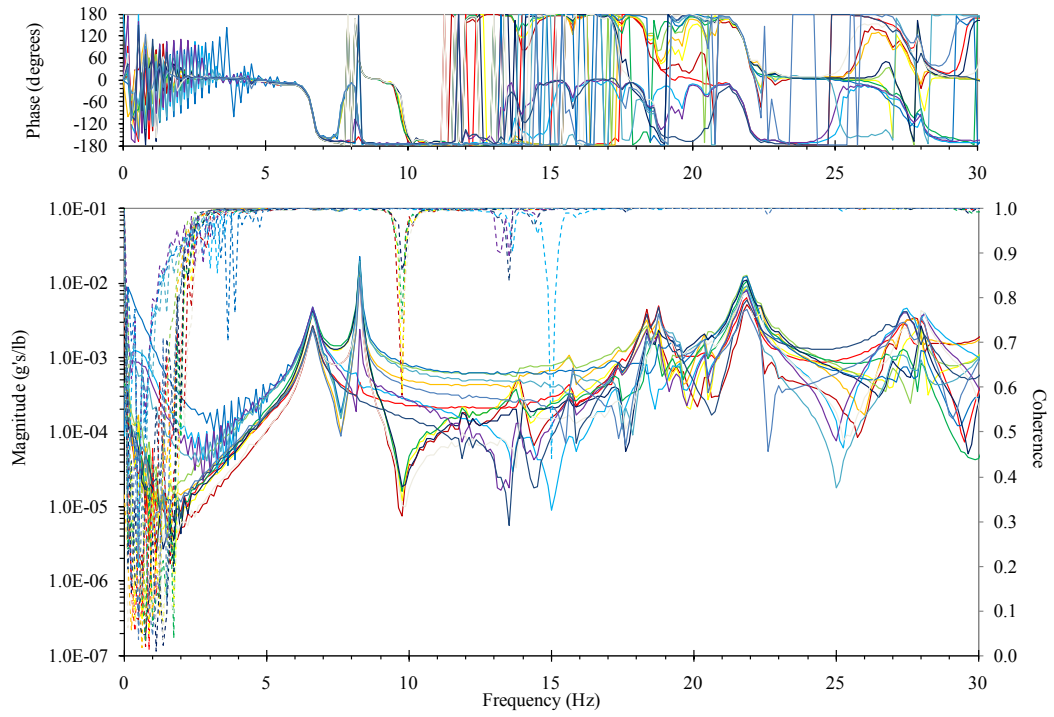
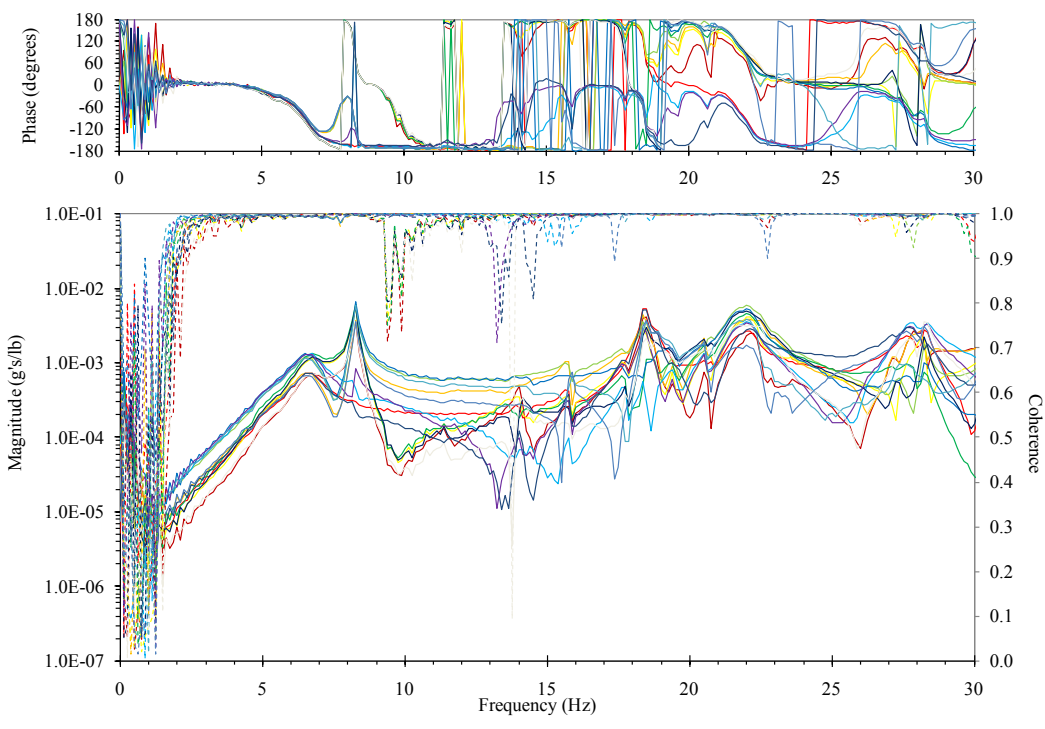Figure 37: Experimental FRF (mass ratio=0.02, seated, dense, test-1).
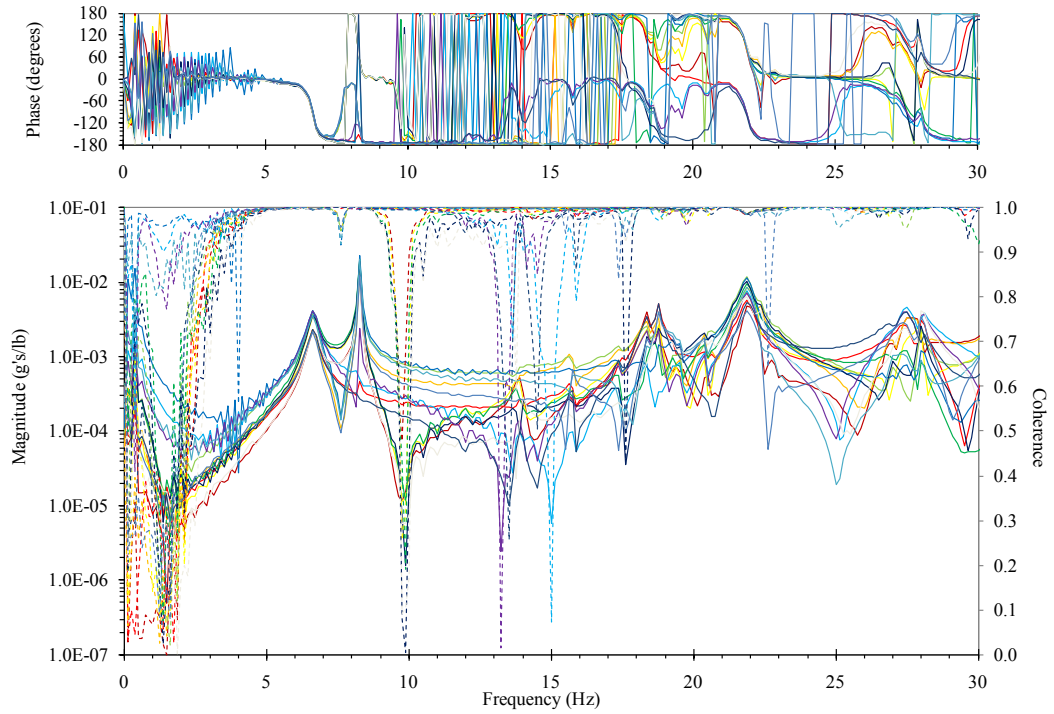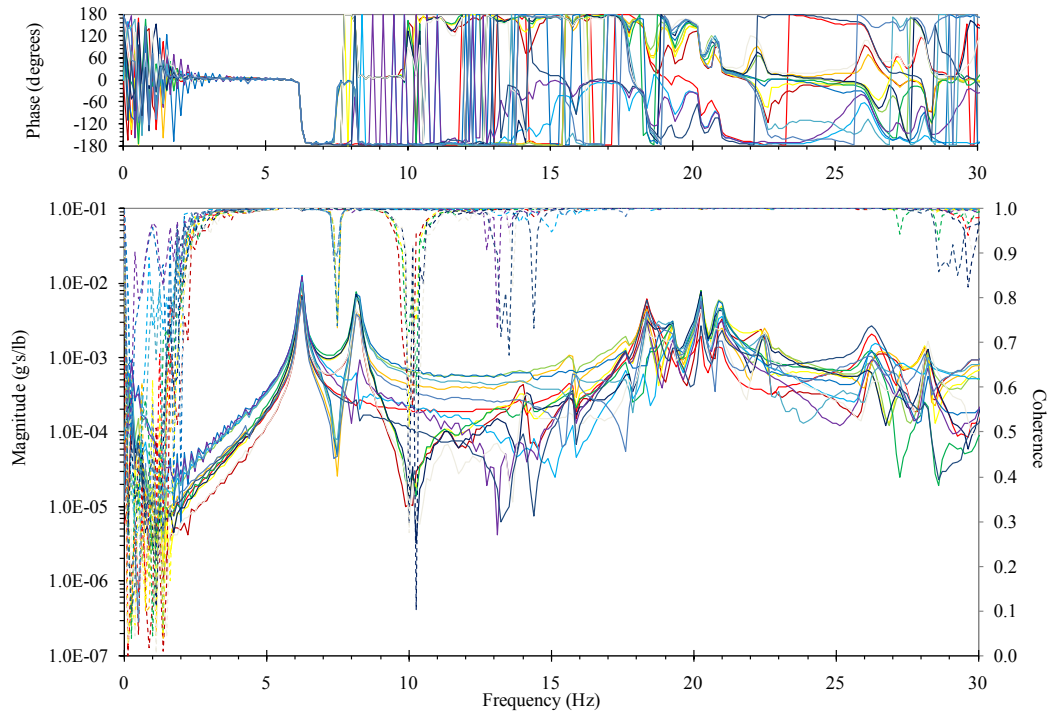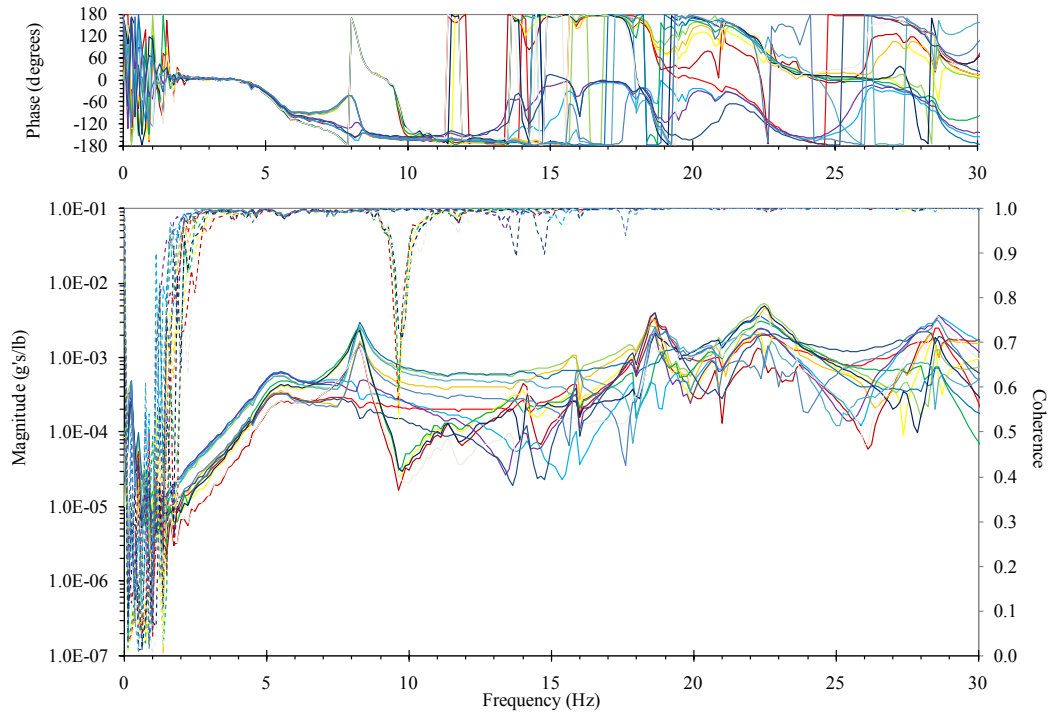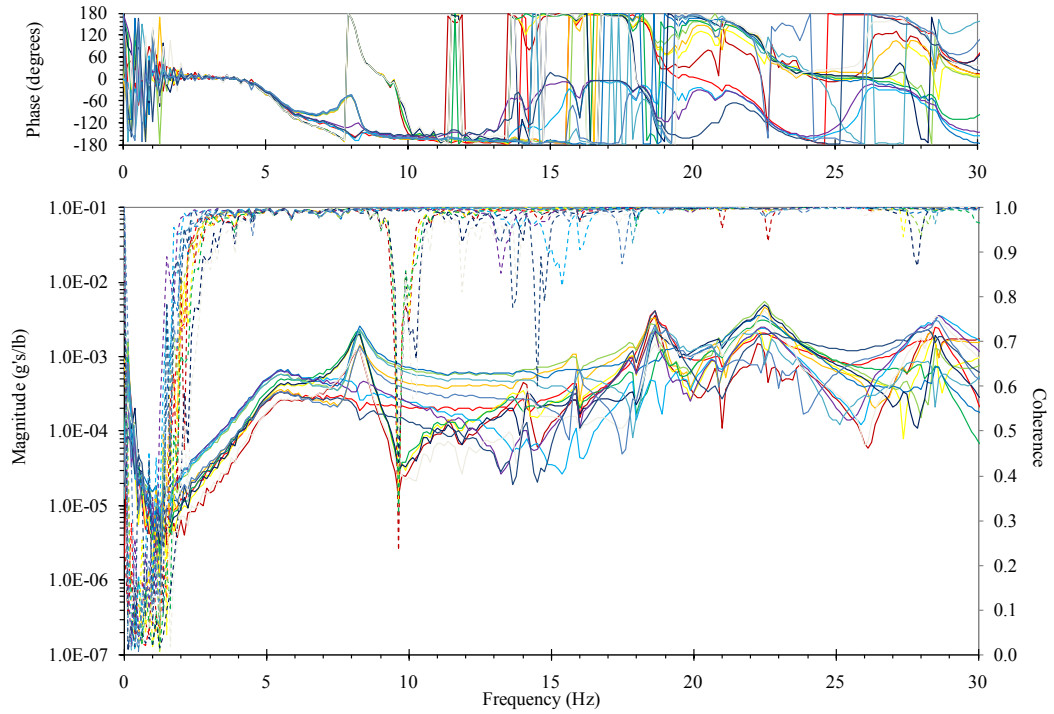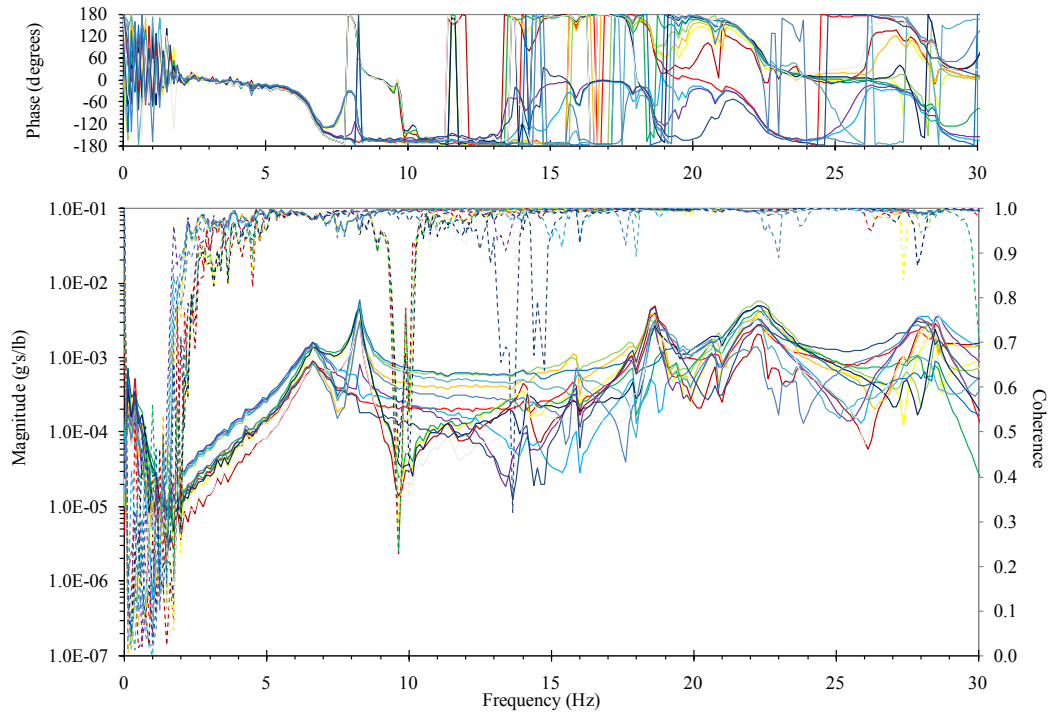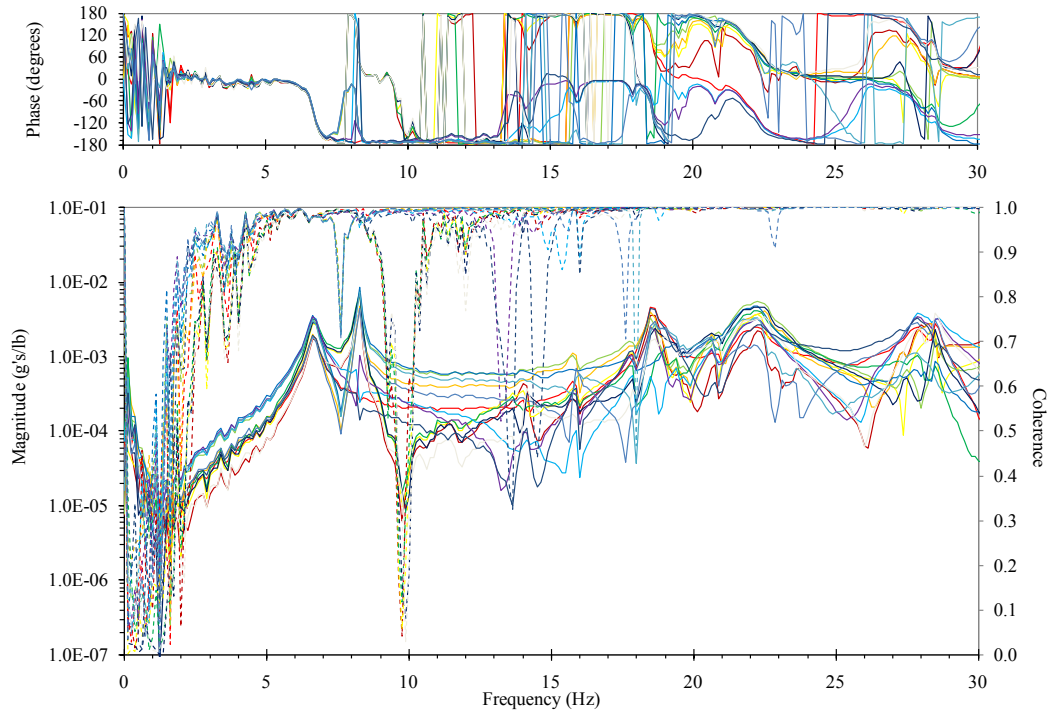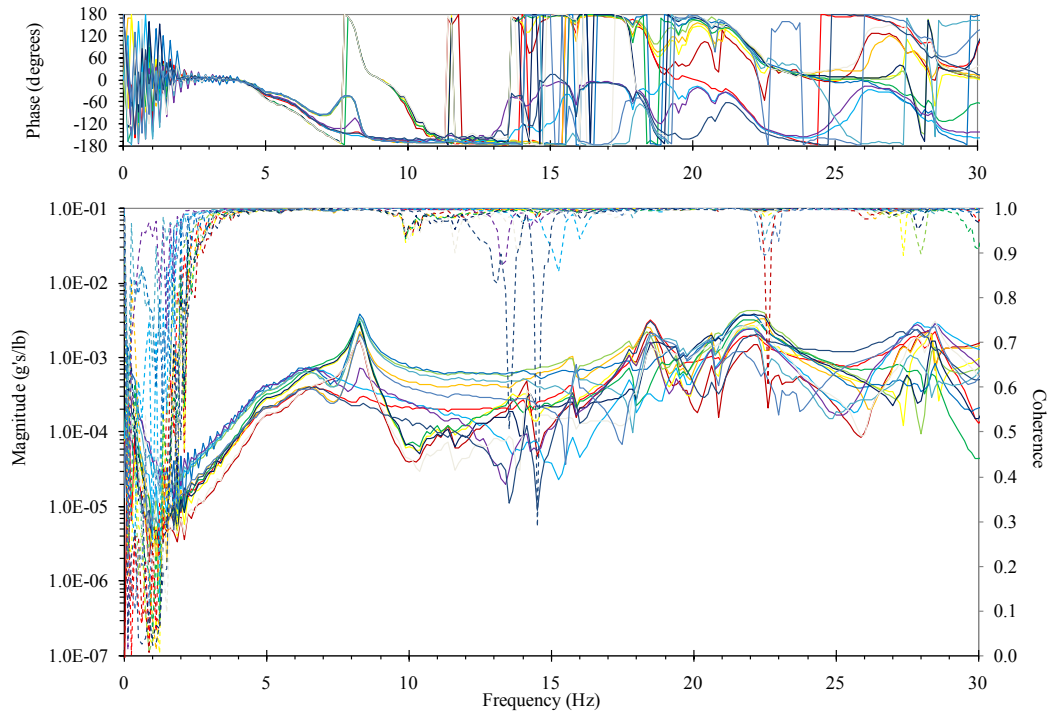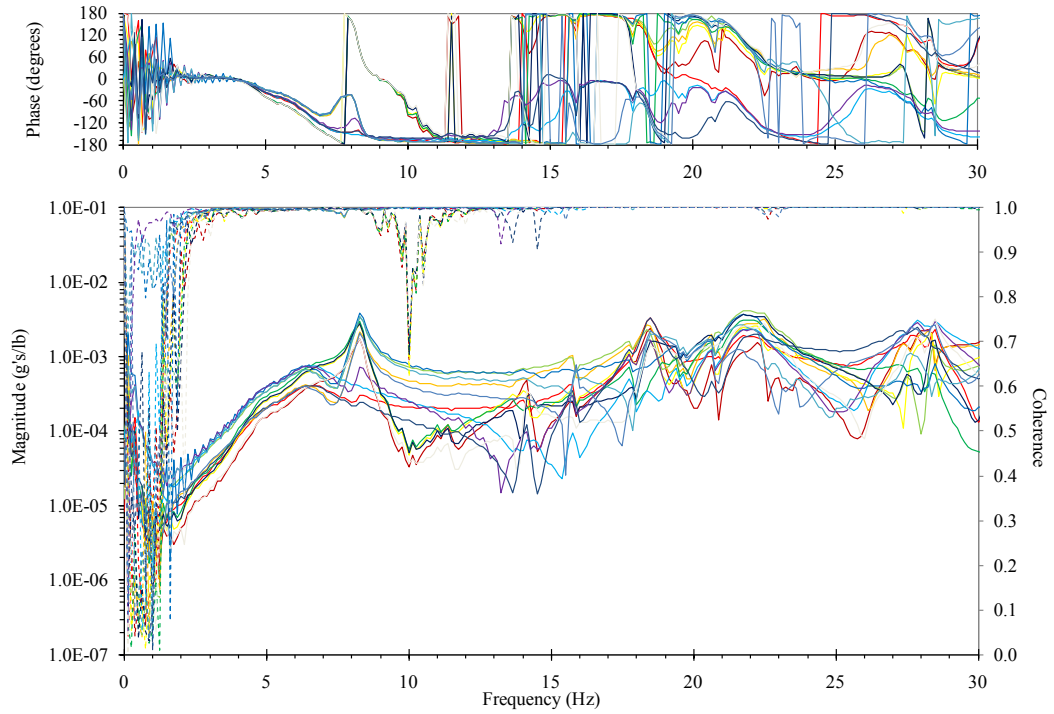

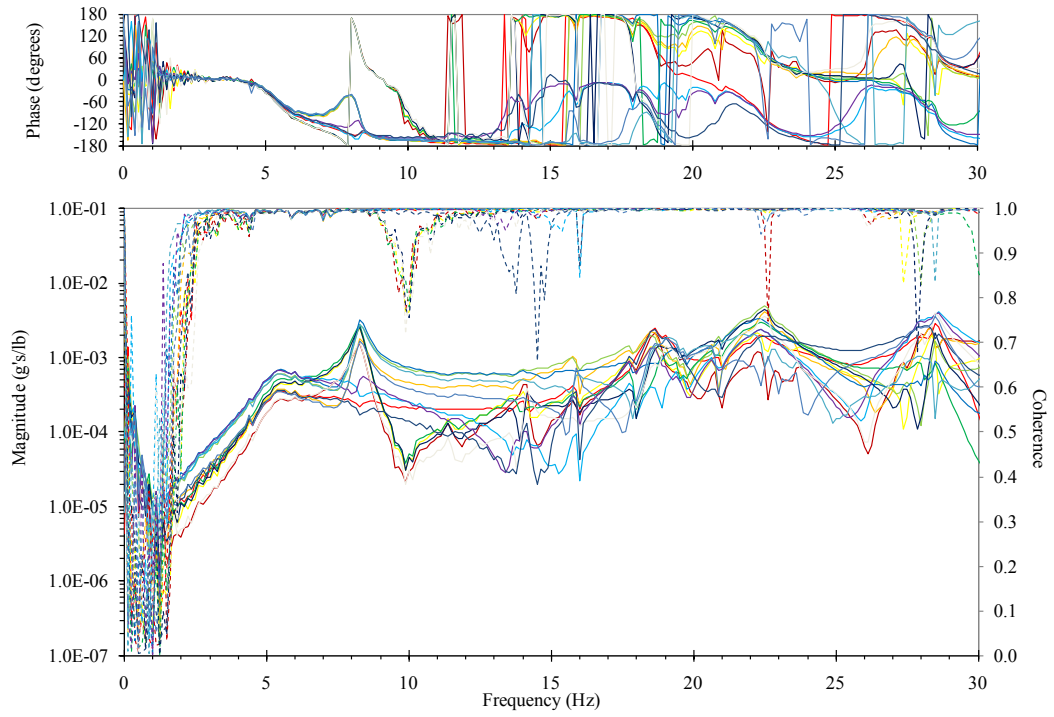Figure 38: Experimental FRF (mass ratio=0.02, seated, dense, test-2).

95
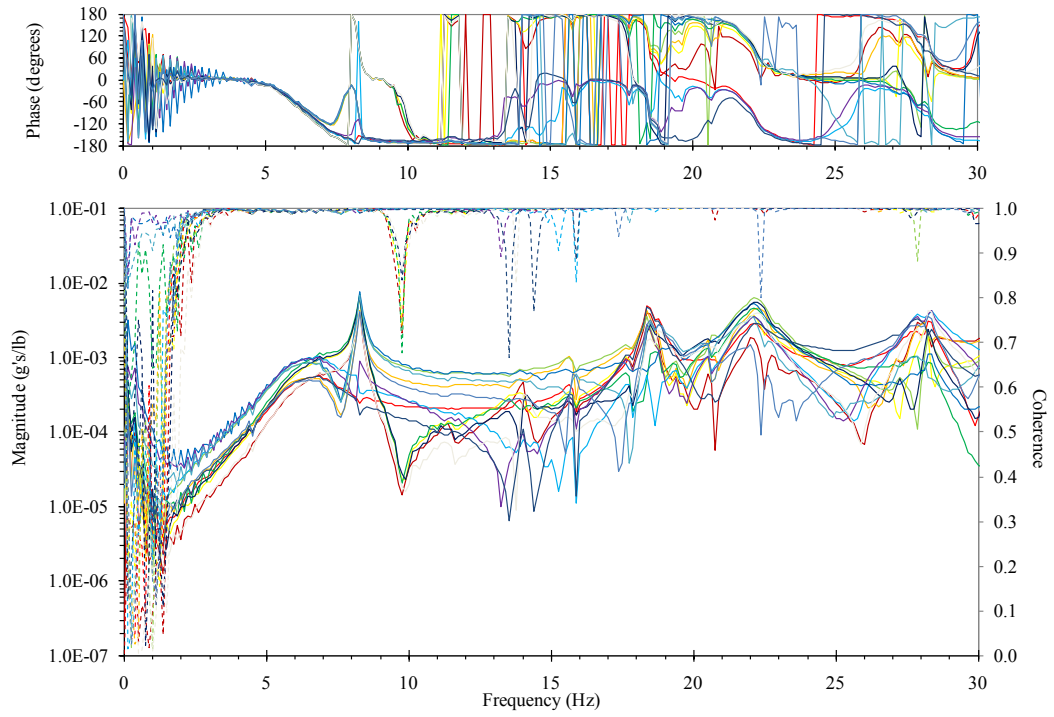
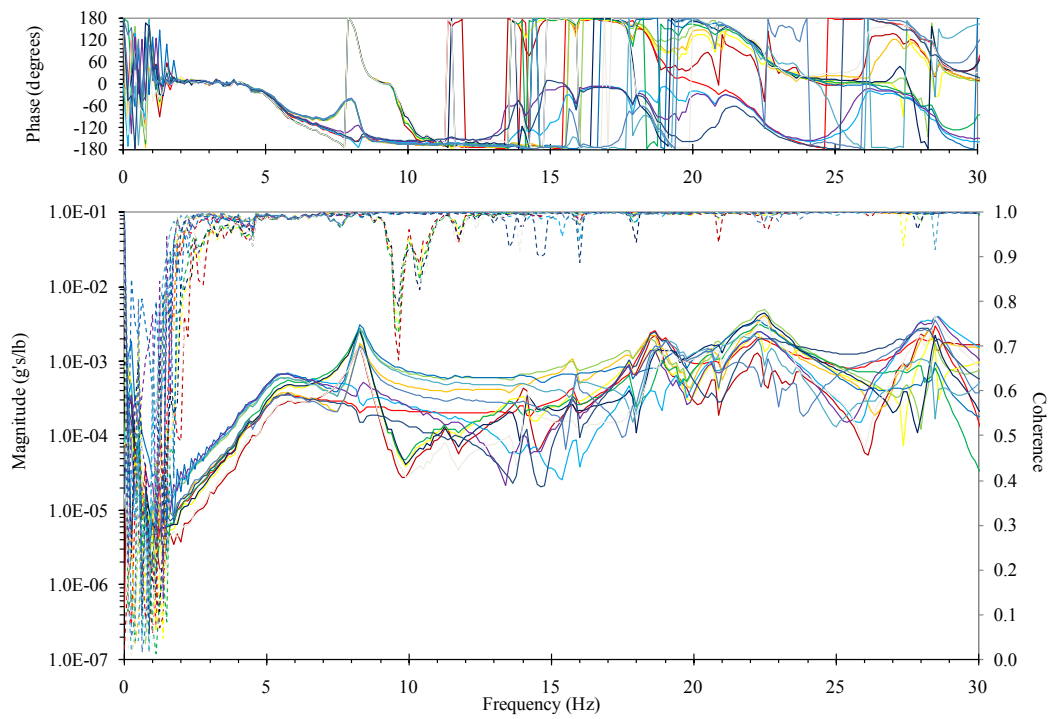Figure 39: Experimental FRF (mass ratio=0.08, standing-straight knees, dense, test-1).
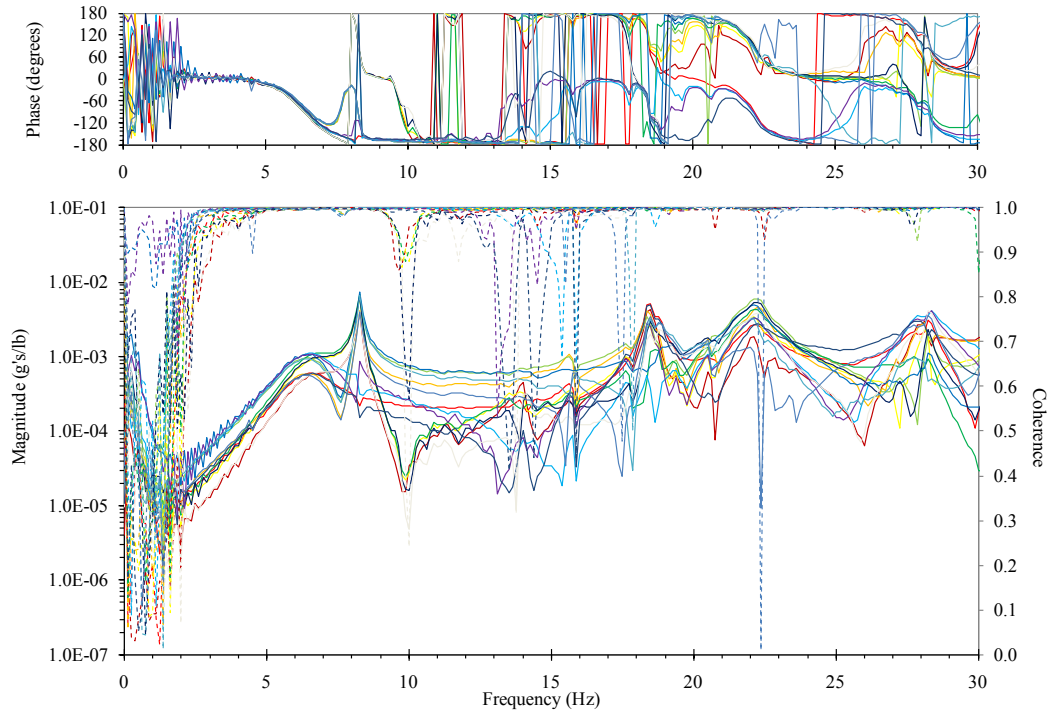
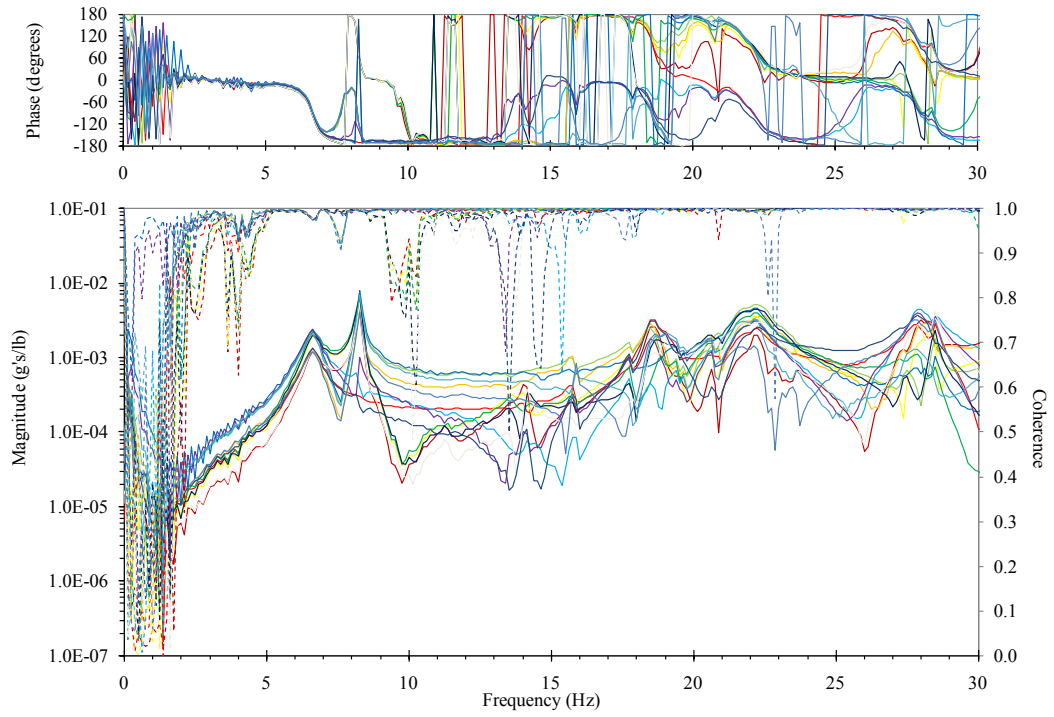Figure 40: Experimental FRF (mass ratio=0.08, standing-straight knees, dense, test-2).

96

Figure 41: Experimental FRF (mass ratio=0.08, standing-bent knees, dense, test-1).
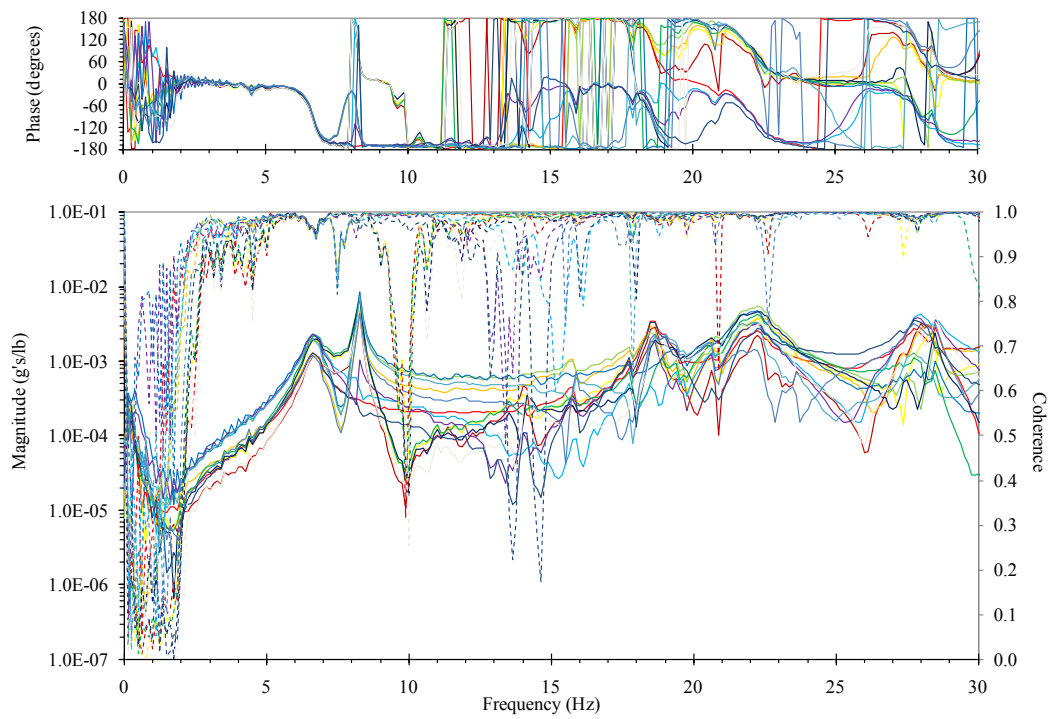

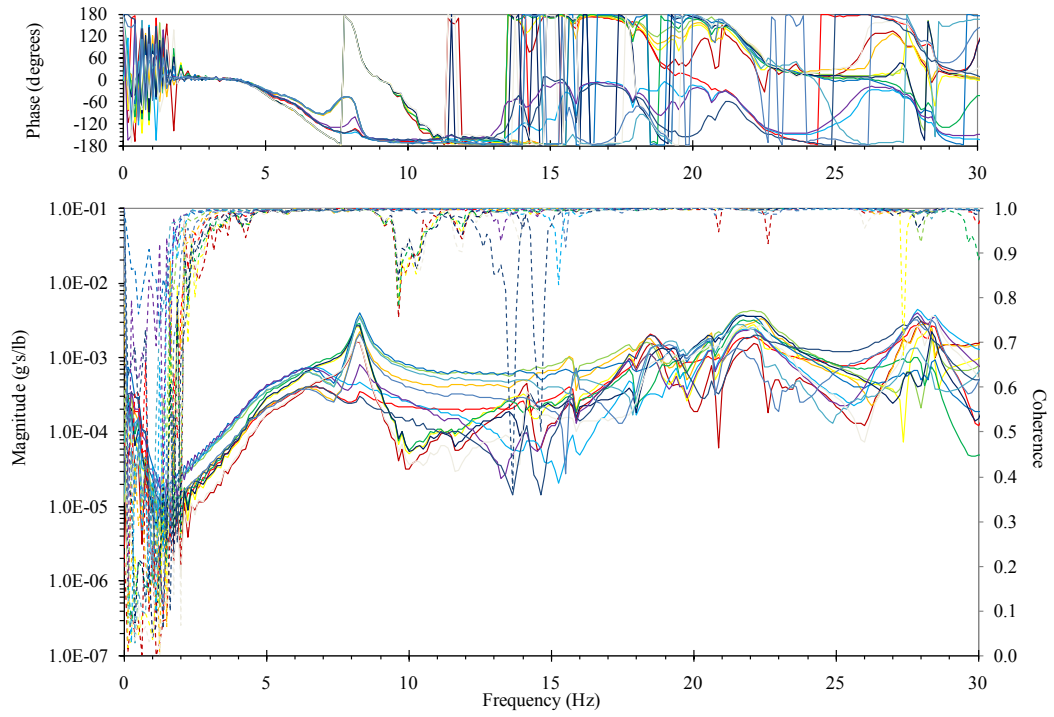Figure 42: Experimental FRF (mass ratio=0.08, standing-bent knees, dense, test-2).

Figure 43: Experimental FRF (mass ratio=0.08, seated, dense, test-1).

Figure 44: Experimental FRF (mass ratio=0.08, seated, dense, test-2).

Figure 45: Experimental FRF (mass ratio=0.08, equivalent mass, dense, test-1).
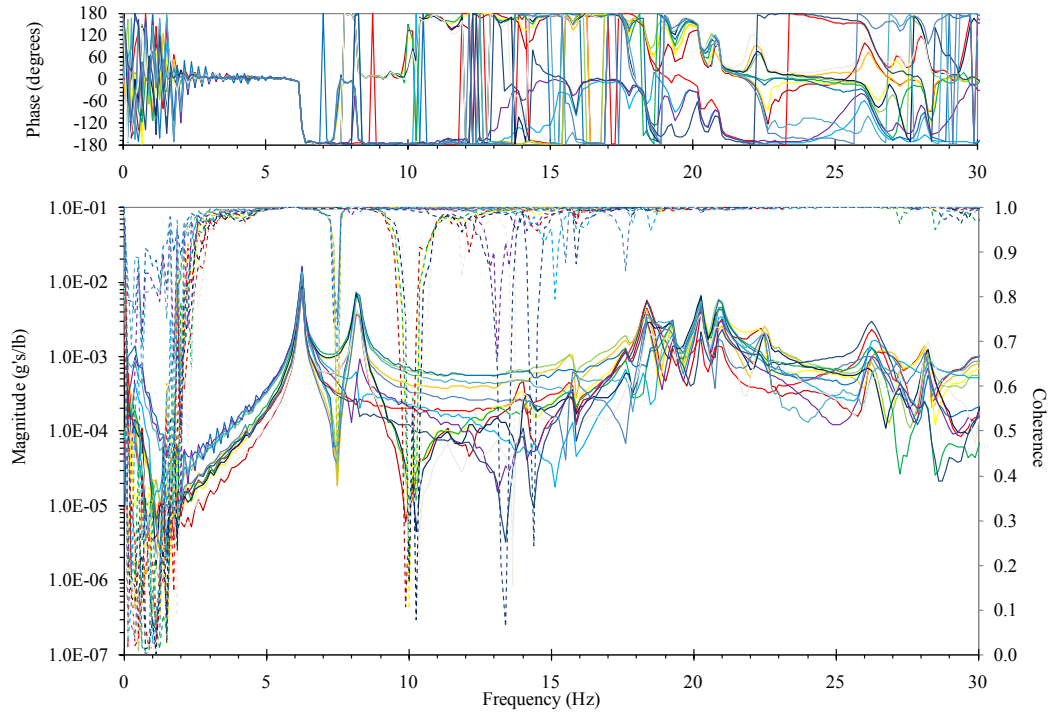
Figure 46: Experimental FRF (mass ratio=0.08, equivalent mass, dense, test-2).

Figure 47: Experimental FRF (mass ratio=0.16, standing-straight knees, dense, test-1).

Figure 48: Experimental FRF (mass ratio=0.16, standing-straight knees, dense, test-2).

Figure 49: Experimental FRF (mass ratio=0.16, standing-bent knees, dense, test-1).

Figure 50: Experimental FRF (mass ratio=0.16, standing-bent knees, dense, test-2).

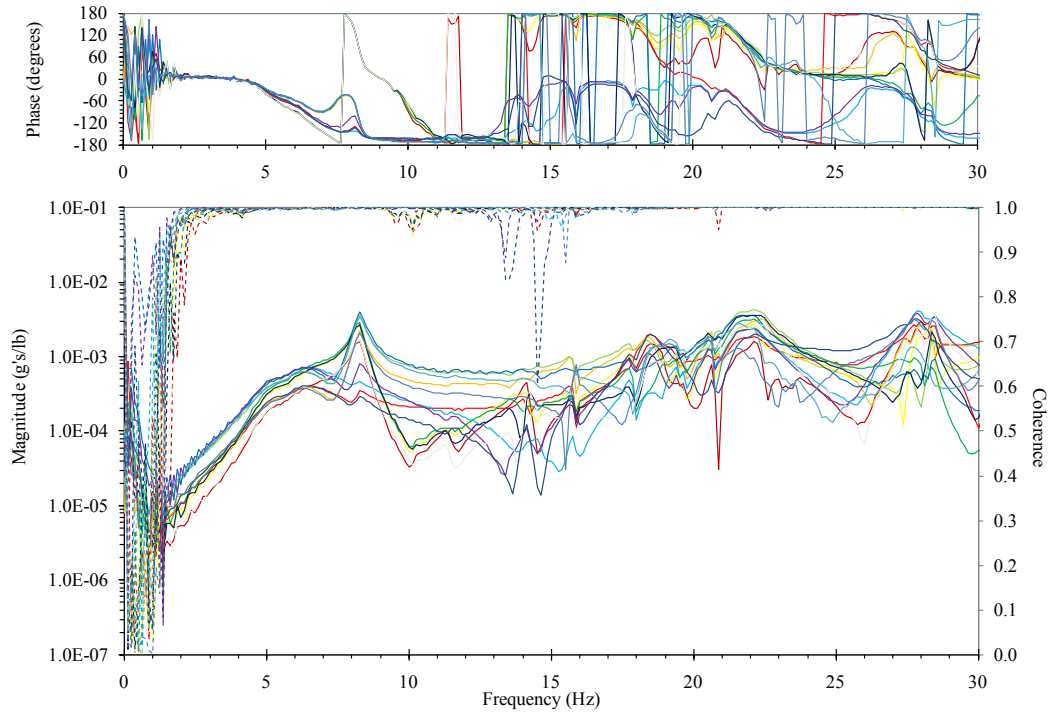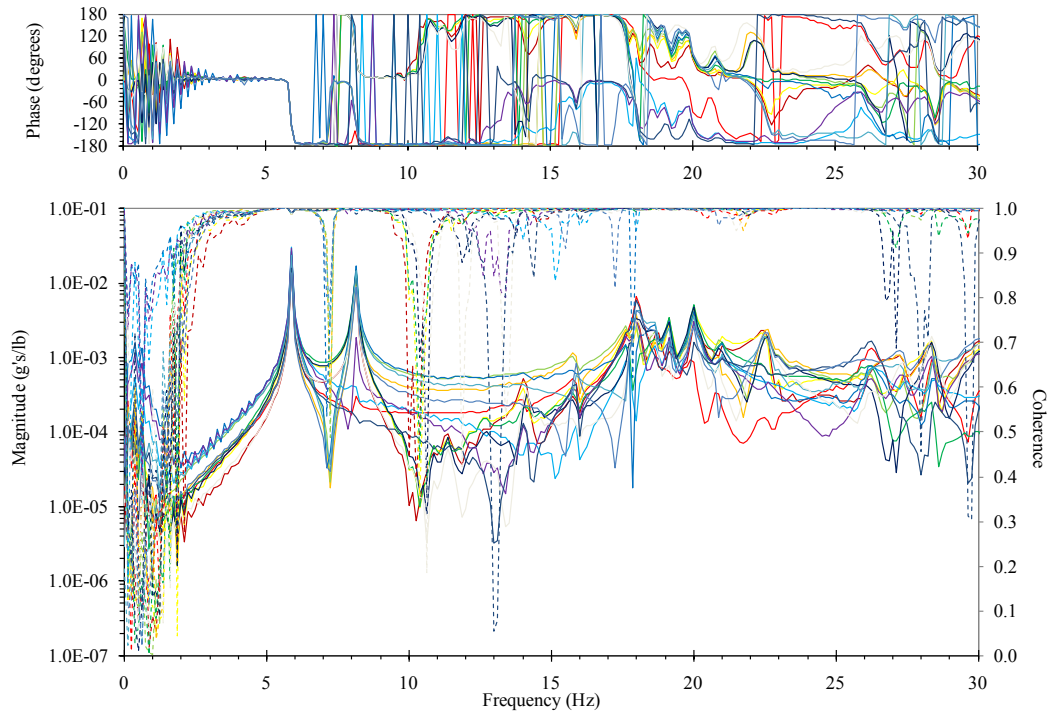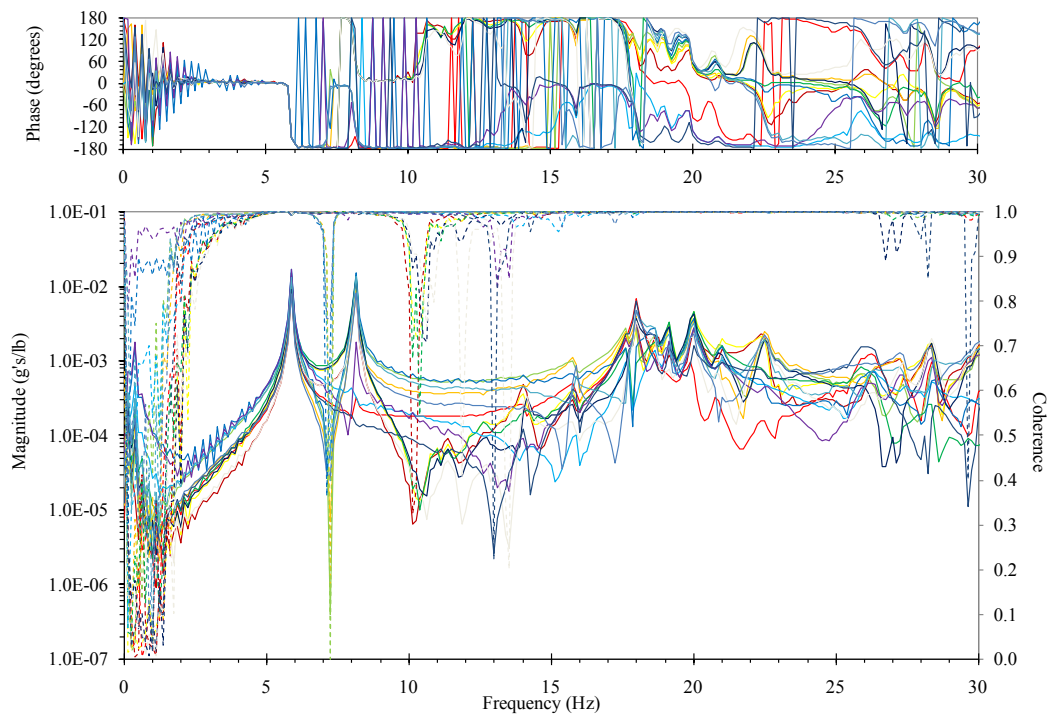Figure 51: Experimental FRF (mass ratio=0.16, seated, dense, test-1).

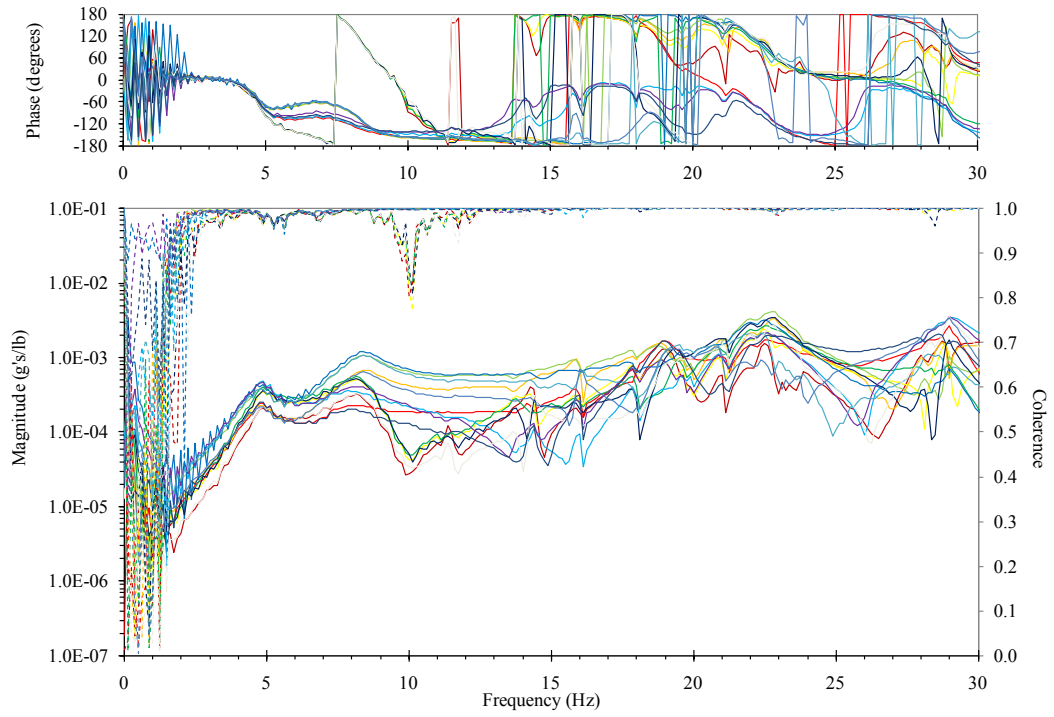Figure 52: Experimental FRF (mass ratio=0.16, seated, dense, test-2).

Figure 53: Experimental FRF (mass ratio=0.16, standing - straight knees, sparse, test-1).

Figure 54: Experimental FRF (mass ratio=0.16, standing - straight knees, sparse, test-2).

Figure 55: Experimental FRF (mass ratio=0.16, standing - bent knees, sparse, test-1).

Figure 56: Experimental FRF (mass ratio=0.16, standing - bent knees, sparse, test-2).

Figure 57: Experimental FRF (mass ratio=0.16, seated, sparse, test-1).

Figure 58: Experimental FRF (mass ratio=0.16, seated, sparse, test-2).

Figure 59: Experimental FRF (mass ratio=0.16, equivalent mass, dense, test-1).

Figure 60: Experimental FRF (mass ratio=0.16, equivalent mass, dense, test-2).

Figure 61: Experimental FRF (mass ratio=0.33, standing - straight knees, dense, test-1).
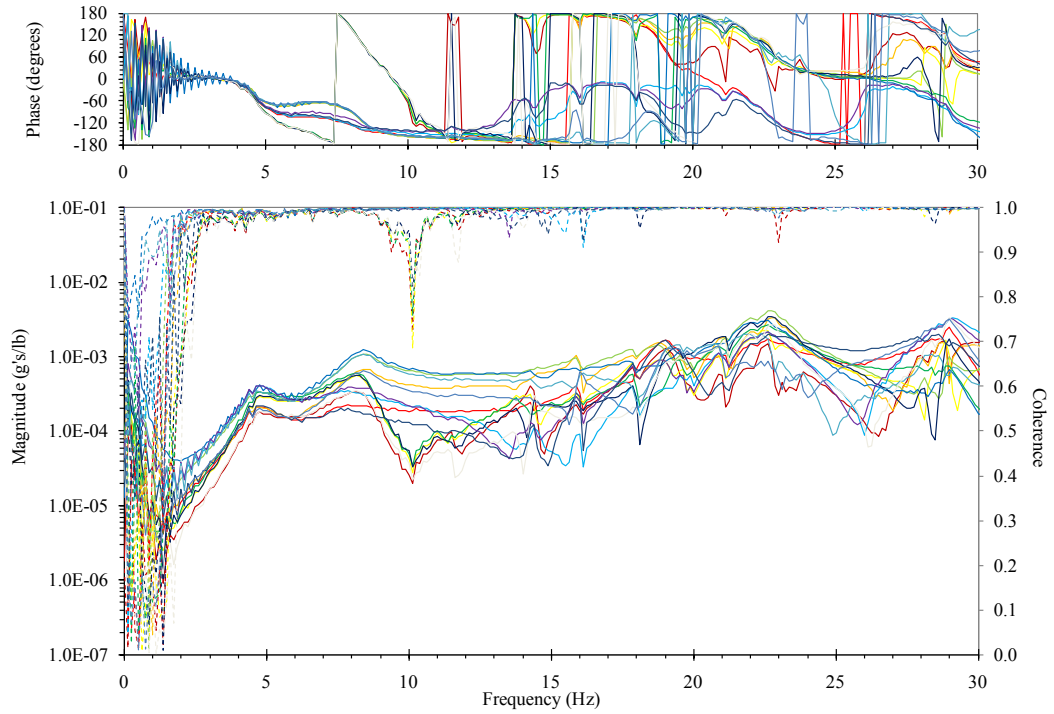

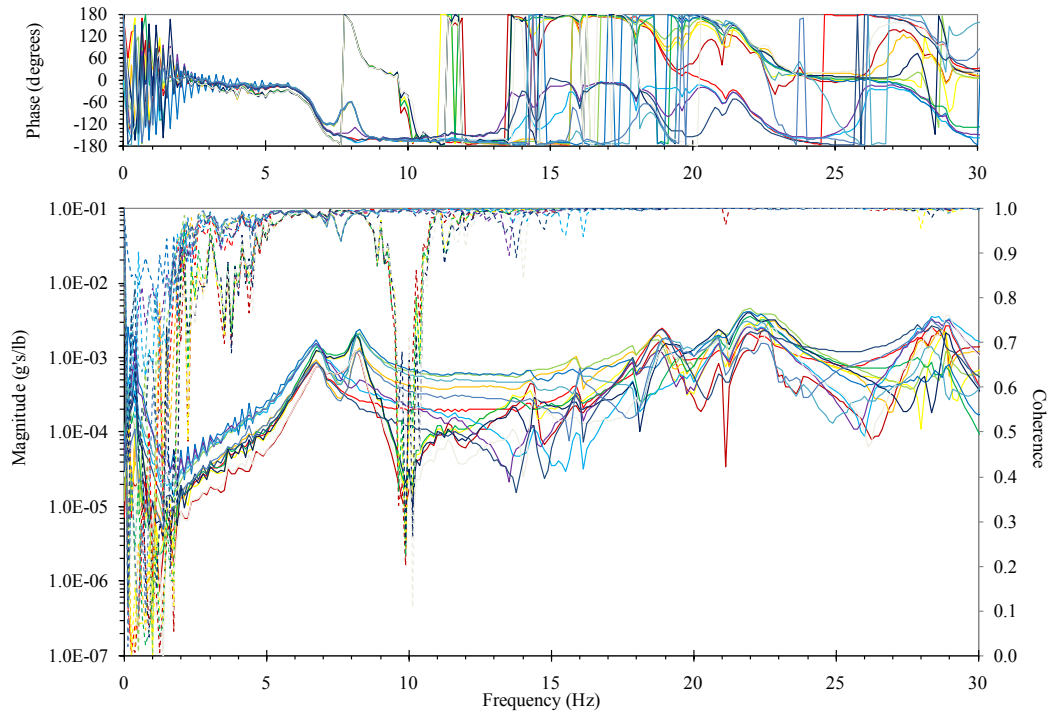Figure 62: Experimental FRF (mass ratio=0.33, standing - straight knees, dense, test-2).

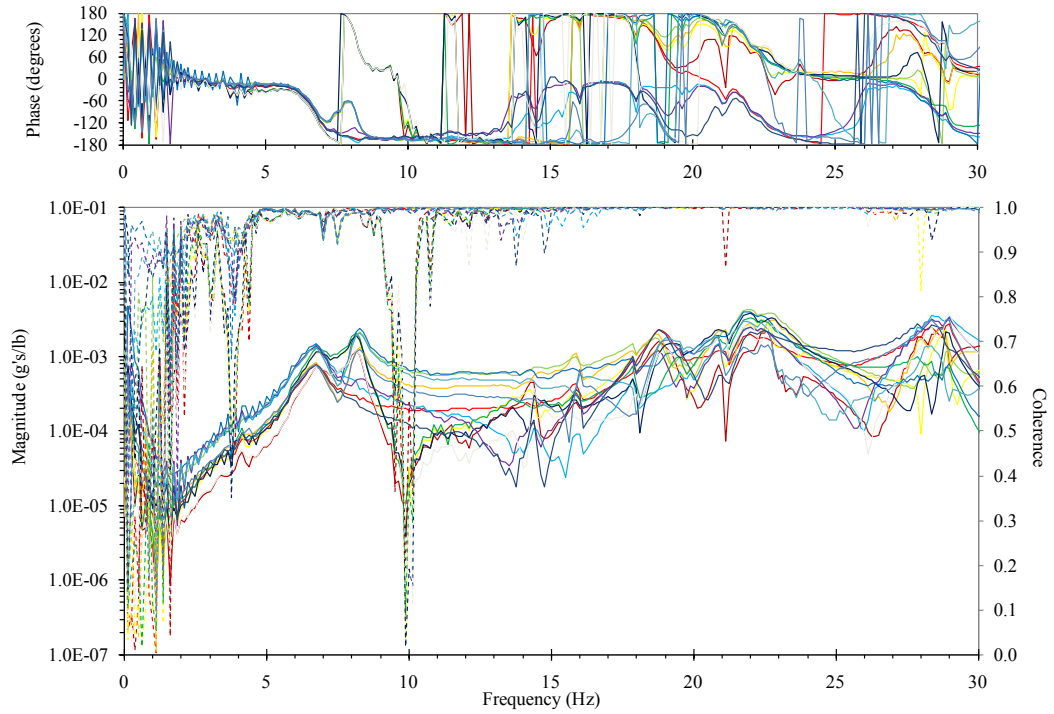Figure 63: Experimental FRF (mass ratio=0.33, standing - bent knees, dense, test-1).

Figure 64: Experimental FRF (mass ratio=0.33, standing - bent knees, dense, test-2).
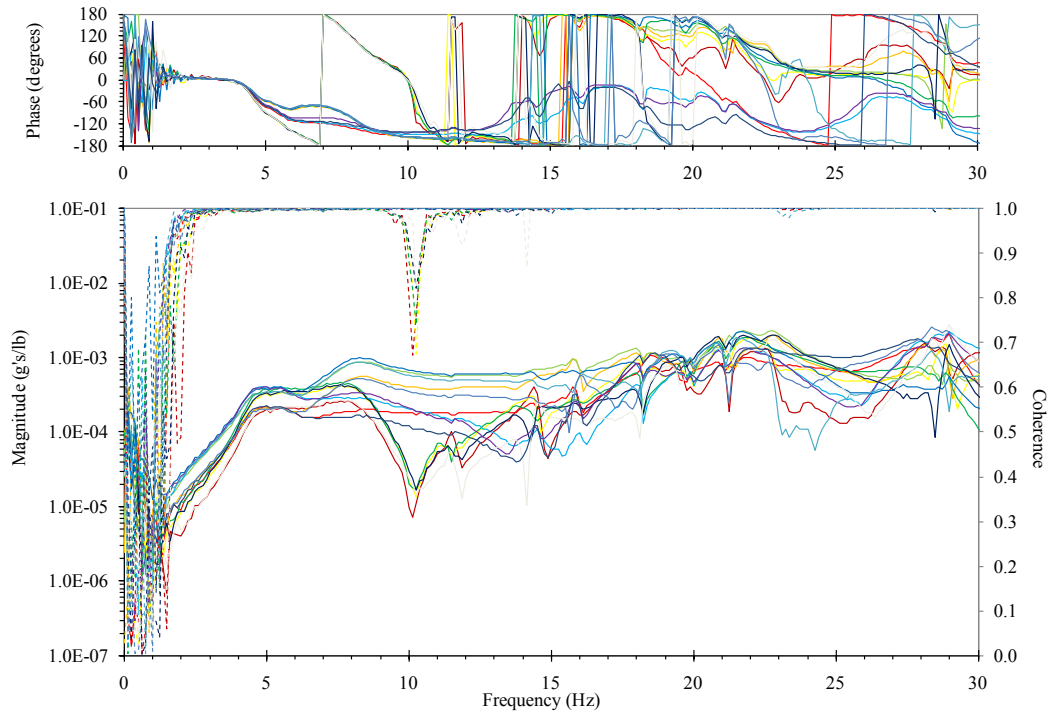
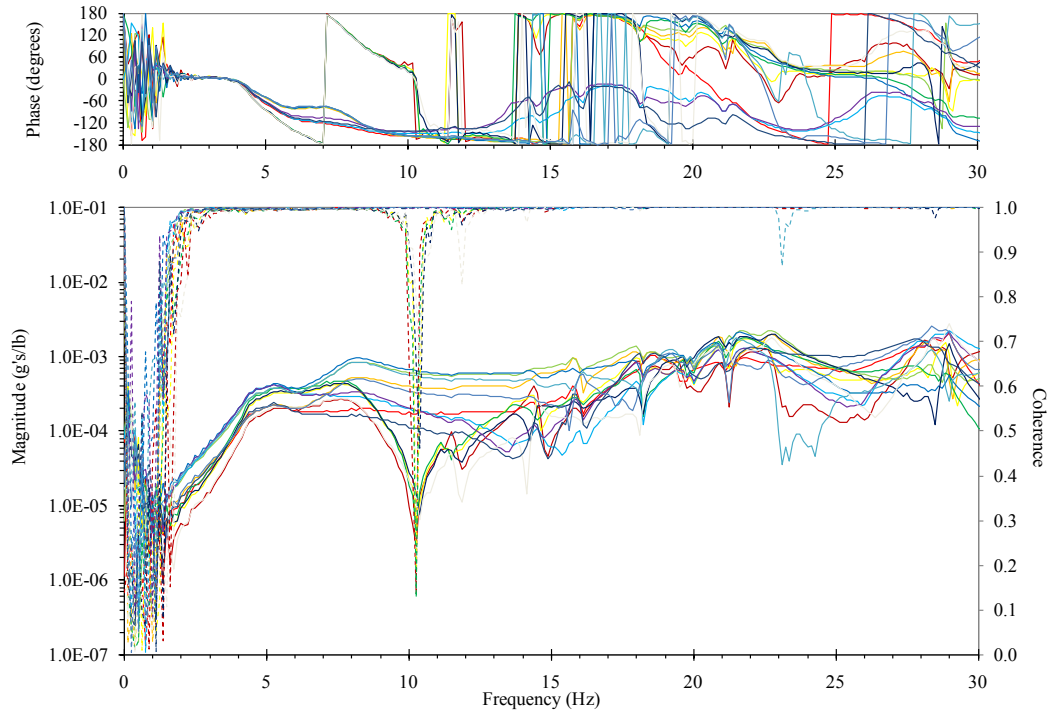Figure 65: Experimental FRF (mass ratio=0.33, seated, dense, test-1).

Figure 66: Experimental FRF (mass ratio=0.33, seated, dense, test-2).
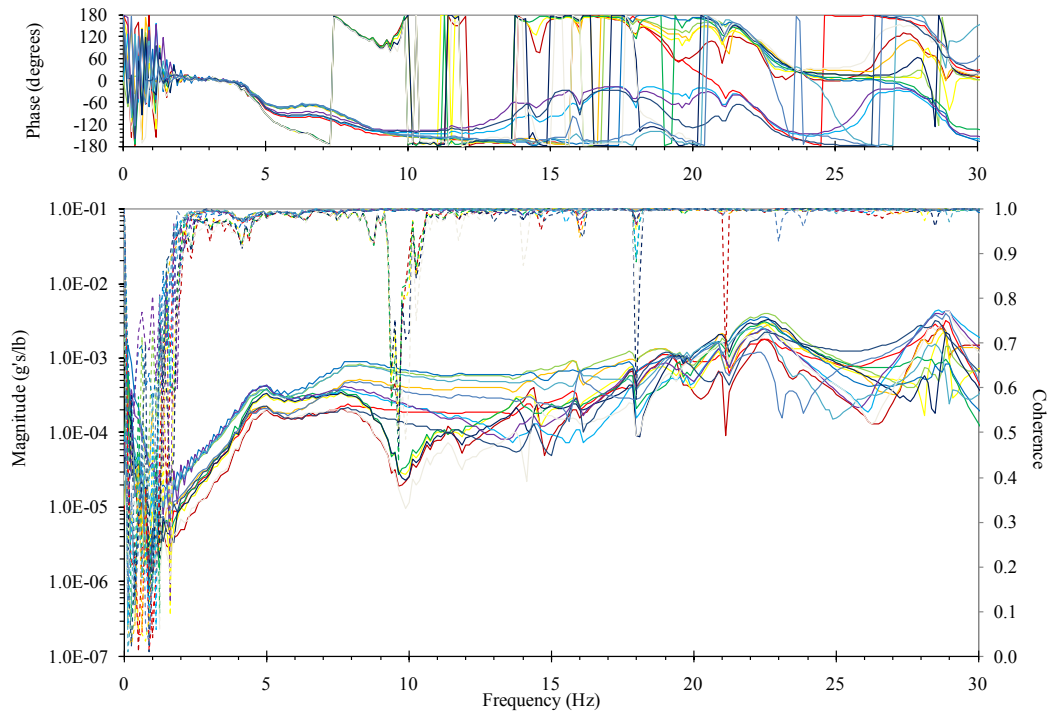
Figure 67: Experimental FRF (mass ratio=0.33, standing - straight knees, sparse, test-1).
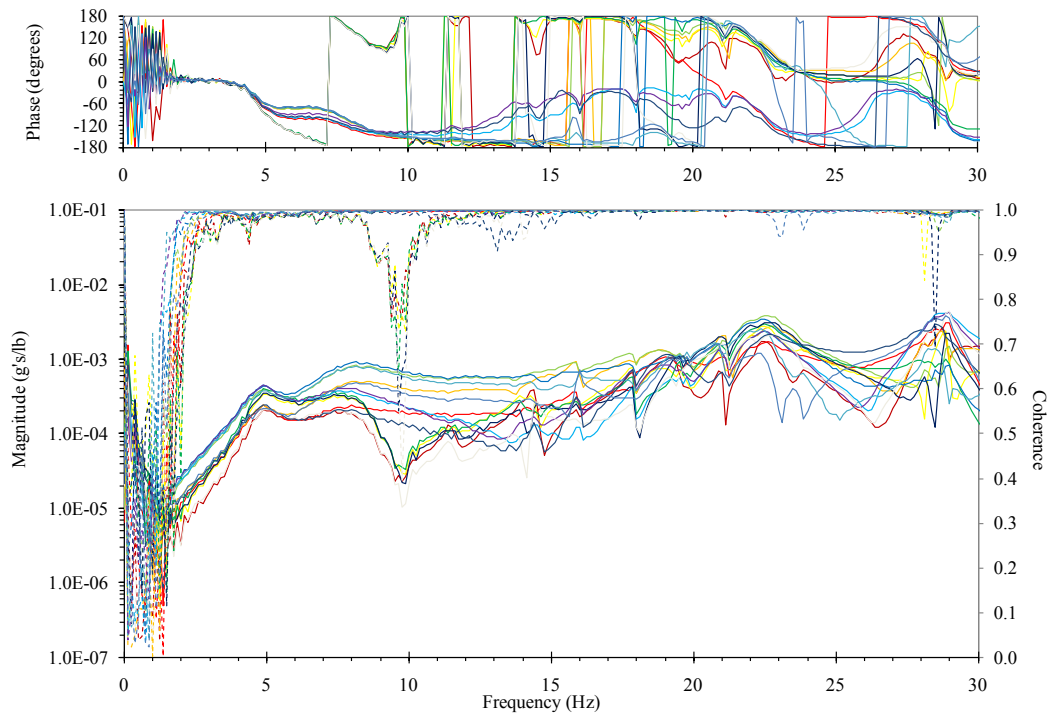

Figure 68: Experimental FRF (mass ratio=0.33, standing - straight knees, sparse, test-2).
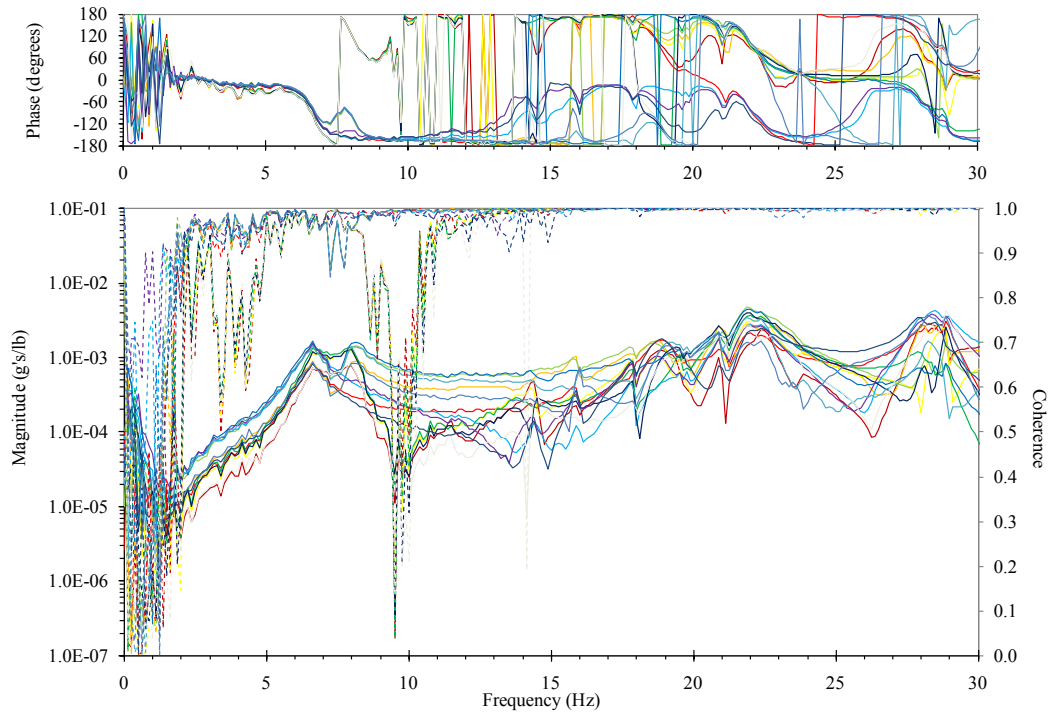
Figure 69: Experimental FRF (mass ratio=0.33, standing - bent knees, sparse, test-1).
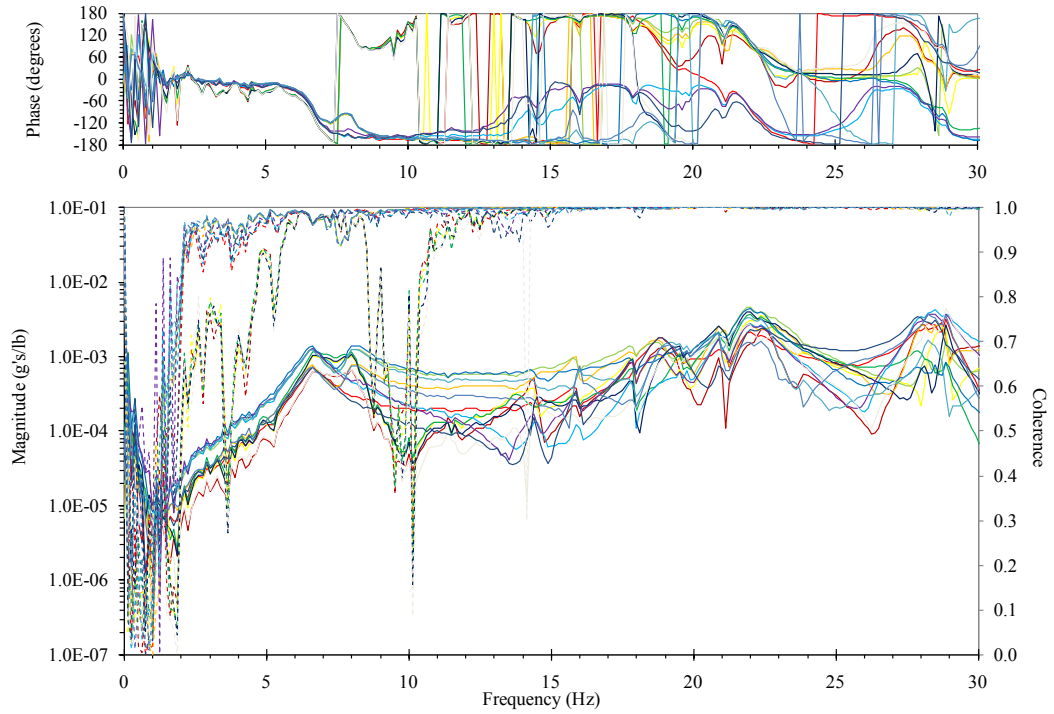

Figure 70: Experimental FRF (mass ratio=0.33, standing - bent knees, sparse, test-2).
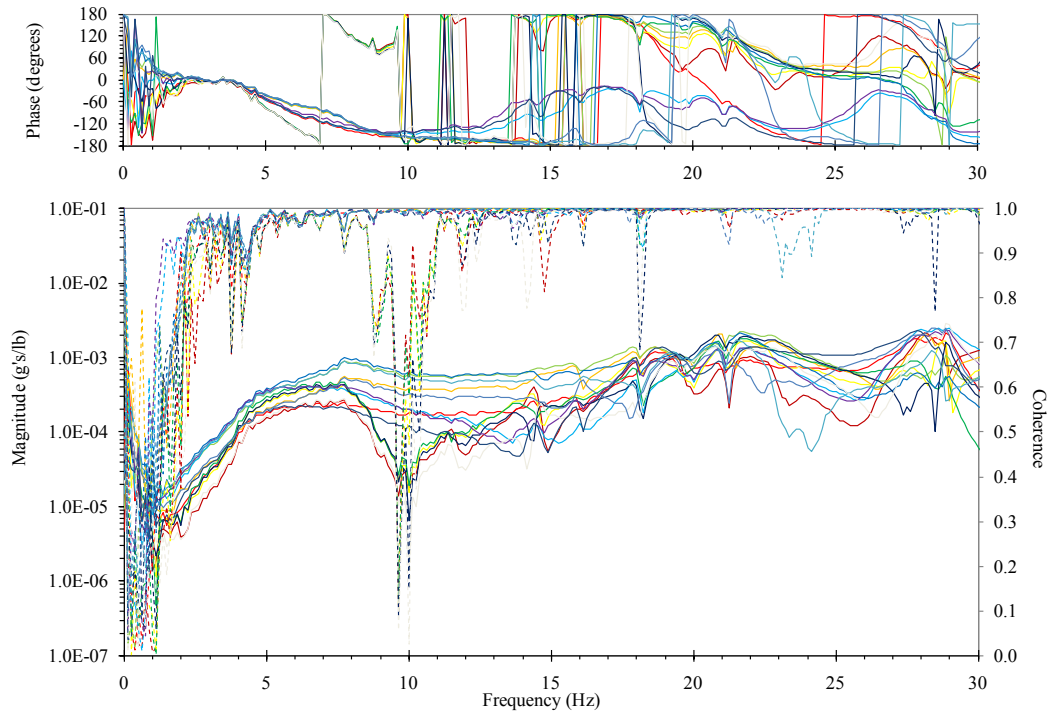
Figure 71: Experimental FRF (mass ratio=0.33, seated, sparse, test-1).

Figure 72: Experimental FRF (mass ratio=0.33, seated, sparse, test-2).
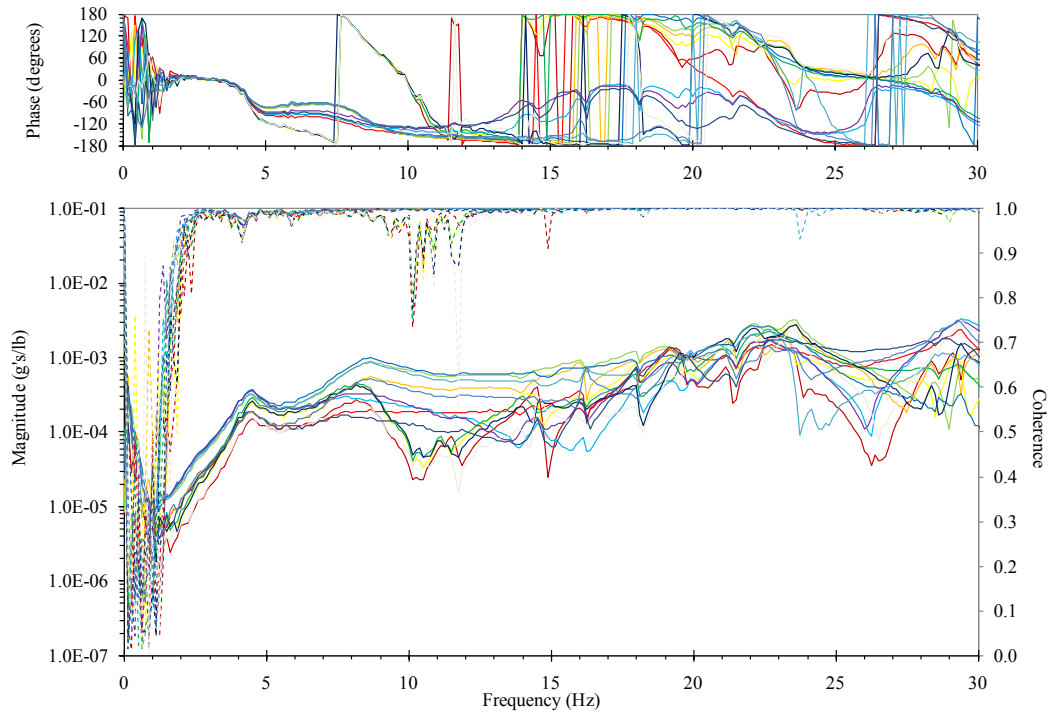
Figure 73: Experimental FRF (mass ratio=0.43, standing - straight knees, dense, test-1).
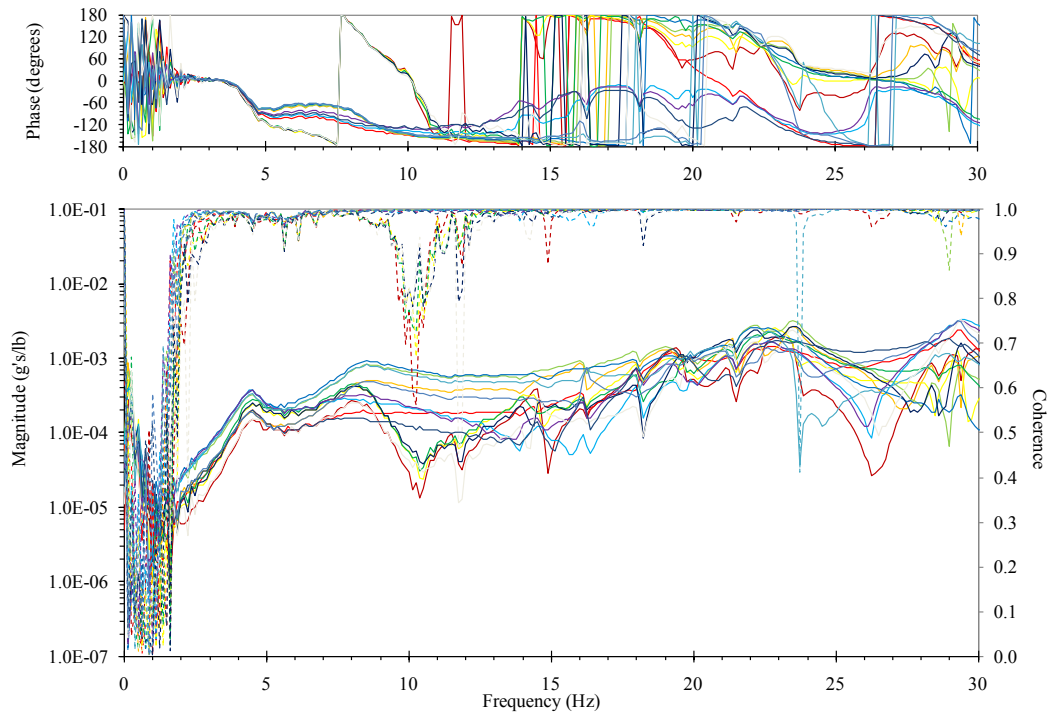
Figure 74: Experimental FRF (mass ratio=0.43, standing - straight knees, dense, test-2).
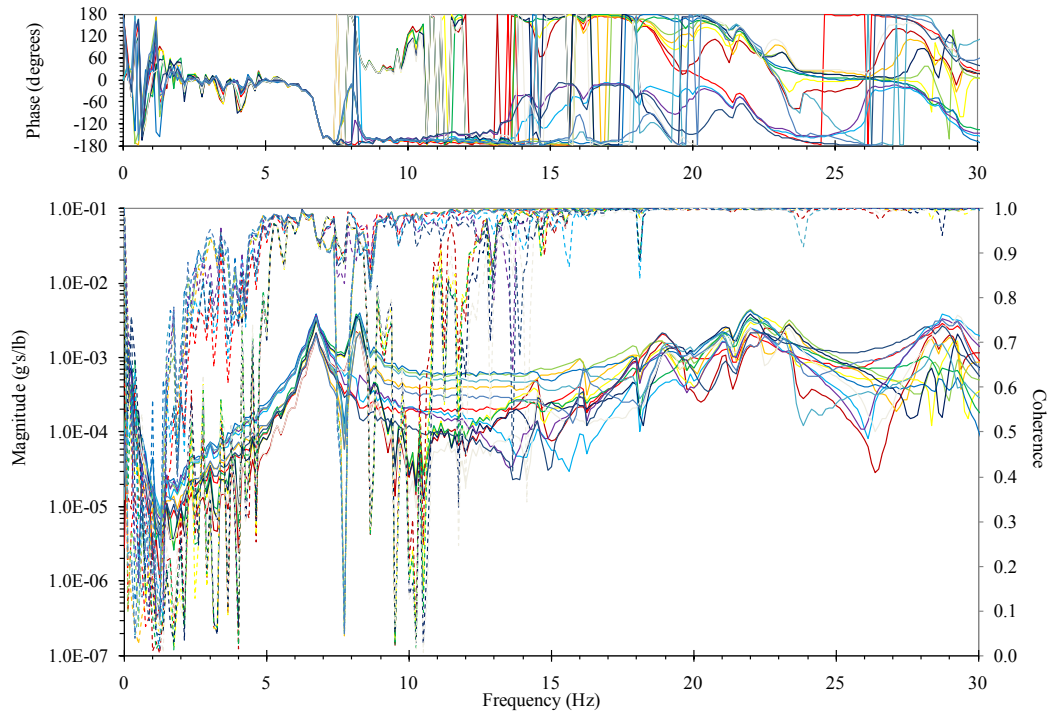
Figure 75: Experimental FRF (mass ratio=0.43, standing - bent knees, dense, test-1).
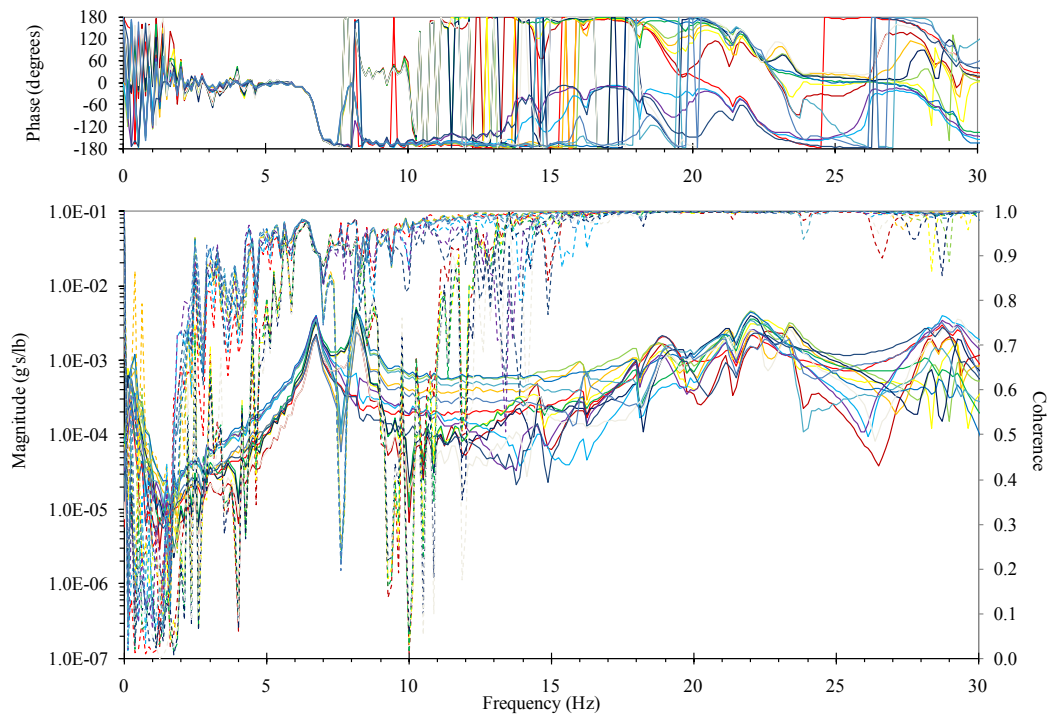
Figure 76: Experimental FRF (mass ratio=0.43, standing - bent knees, dense, test-2).
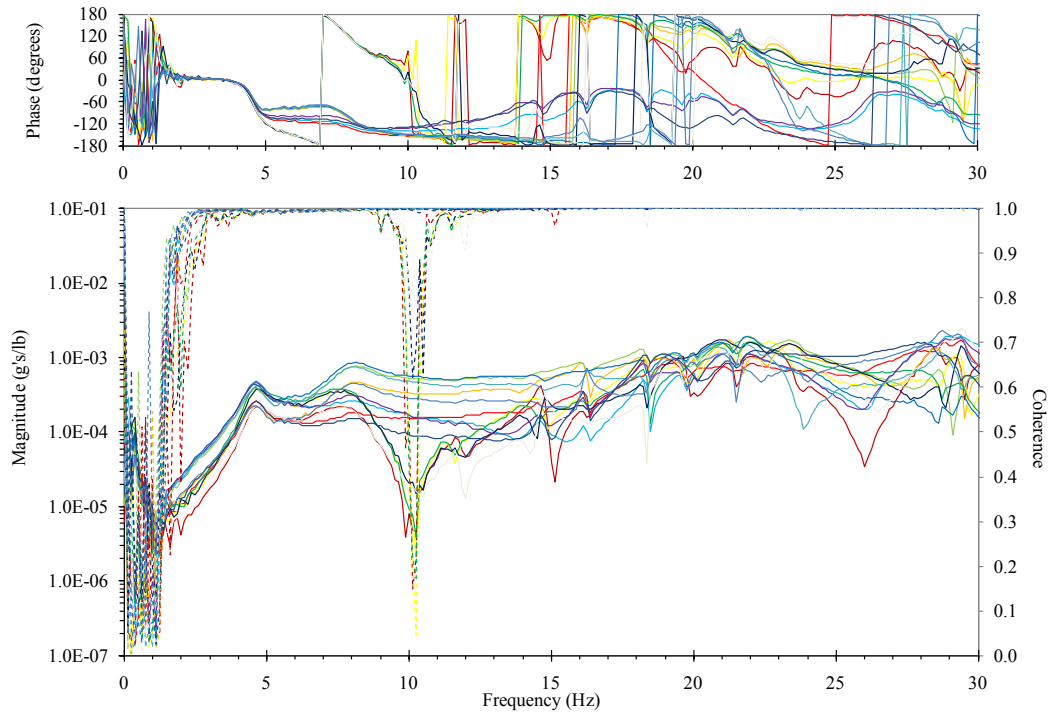
Figure 77: Experimental FRF (mass ratio=0.43, seated, dense, test-1).

Figure 78: Experimental FRF (mass ratio=0.43, seated, dense, test-2).

115

Figure 79: Experimental FRF (mass ratio=0.43, standing - straight knees, sparse, test-1).

Figure 80: Experimental FRF (mass ratio=0.43, standing - straight knees, sparse, test-2).

Figure 81: Experimental FRF (mass ratio=0.43, standing - bent knees, sparse, test-1).

Figure 82: Experimental FRF (mass ratio=0.43, standing - bent knees, sparse, test-2).

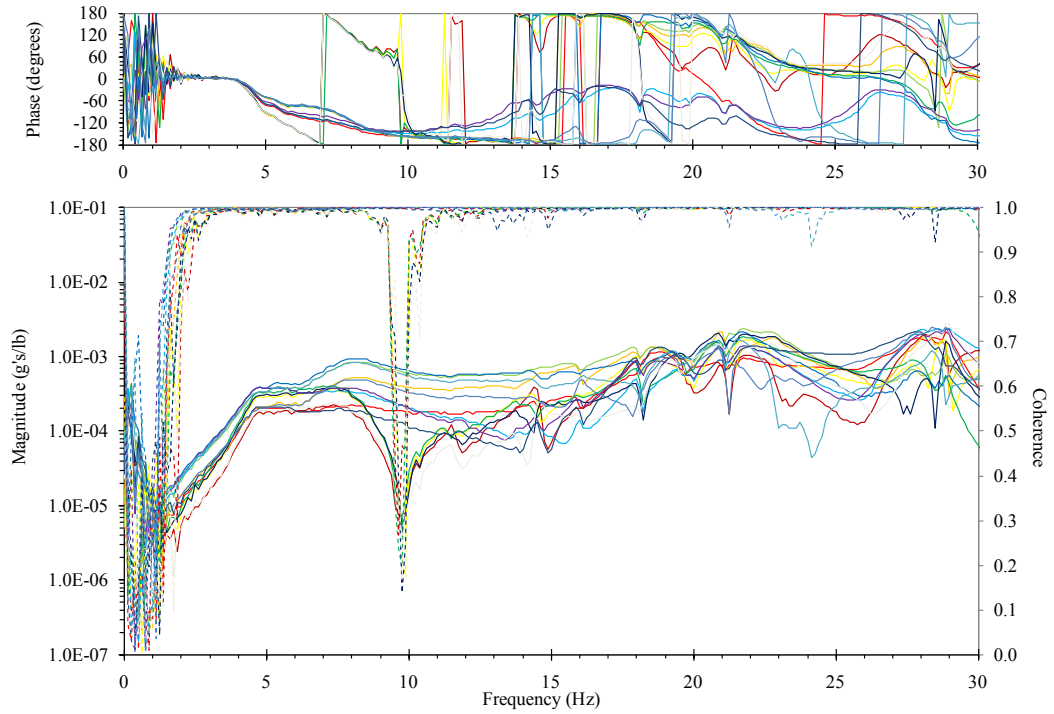Figure 83: Experimental FRF (mass ratio=0.43, seated, sparse, test-1).

Figure 84: Experimental FRF (mass ratio=0.43, seated, sparse, test-2).
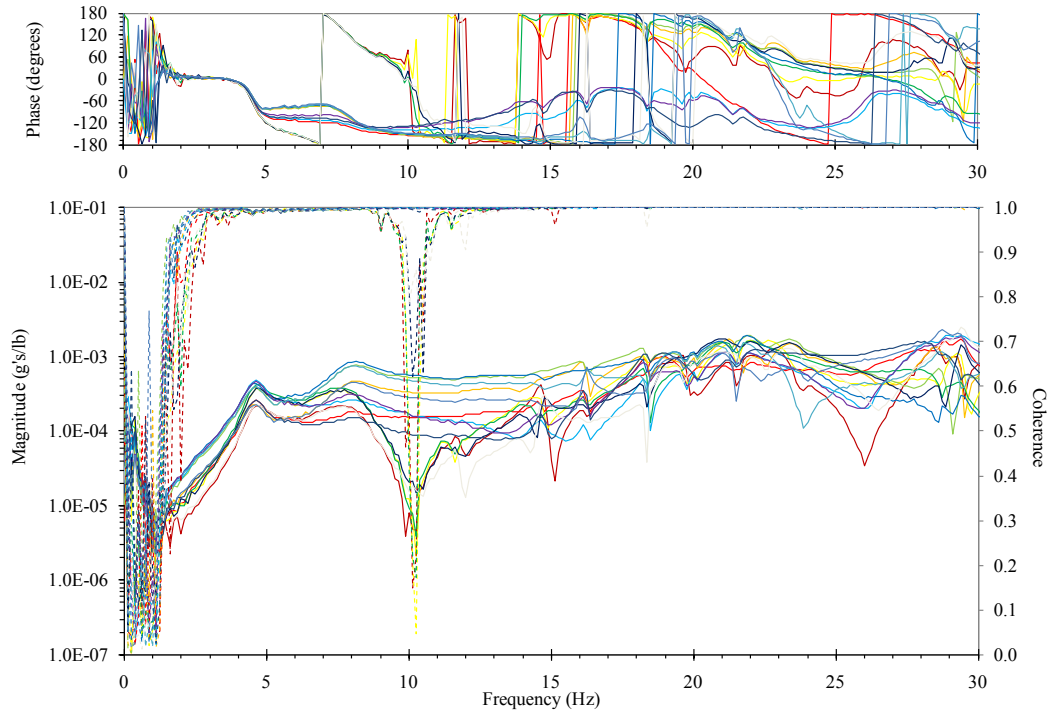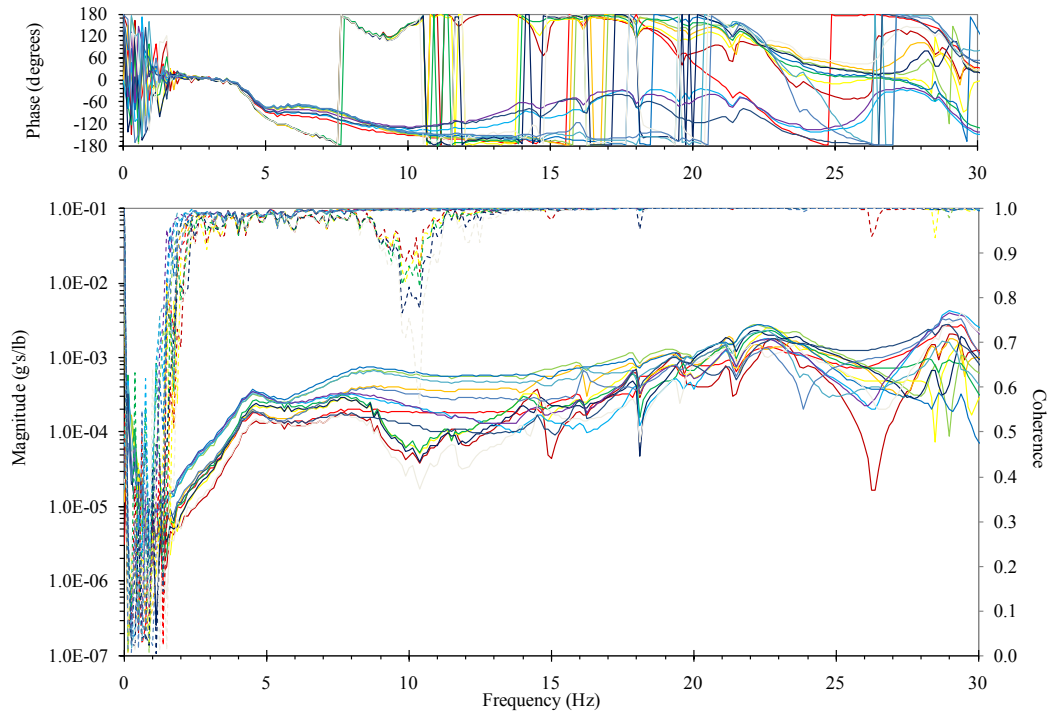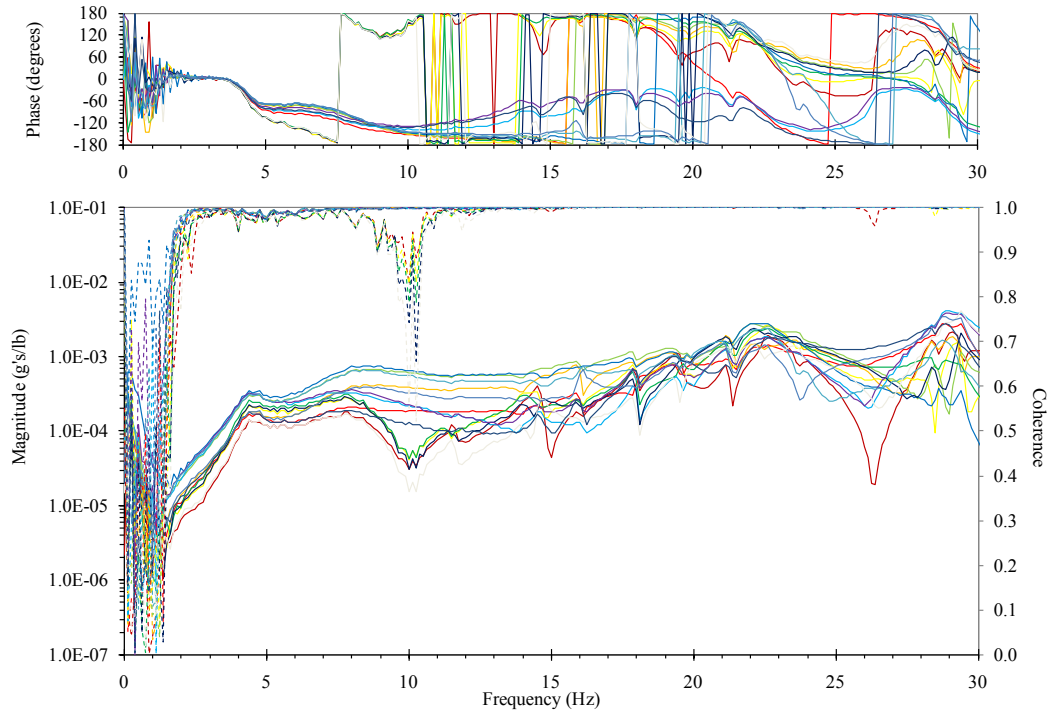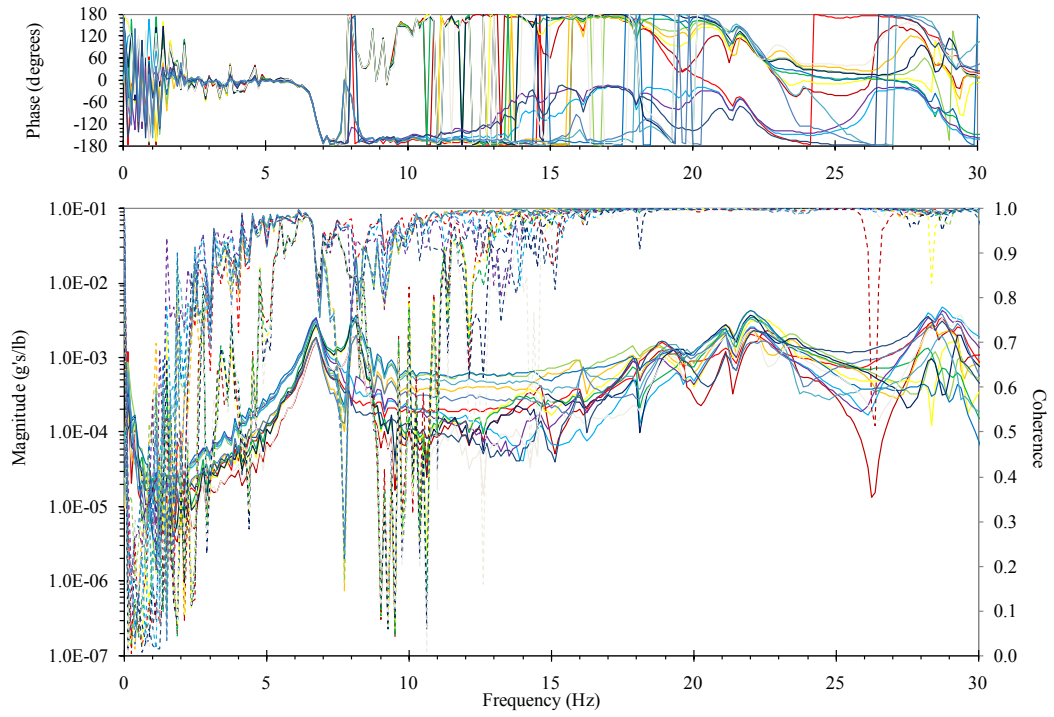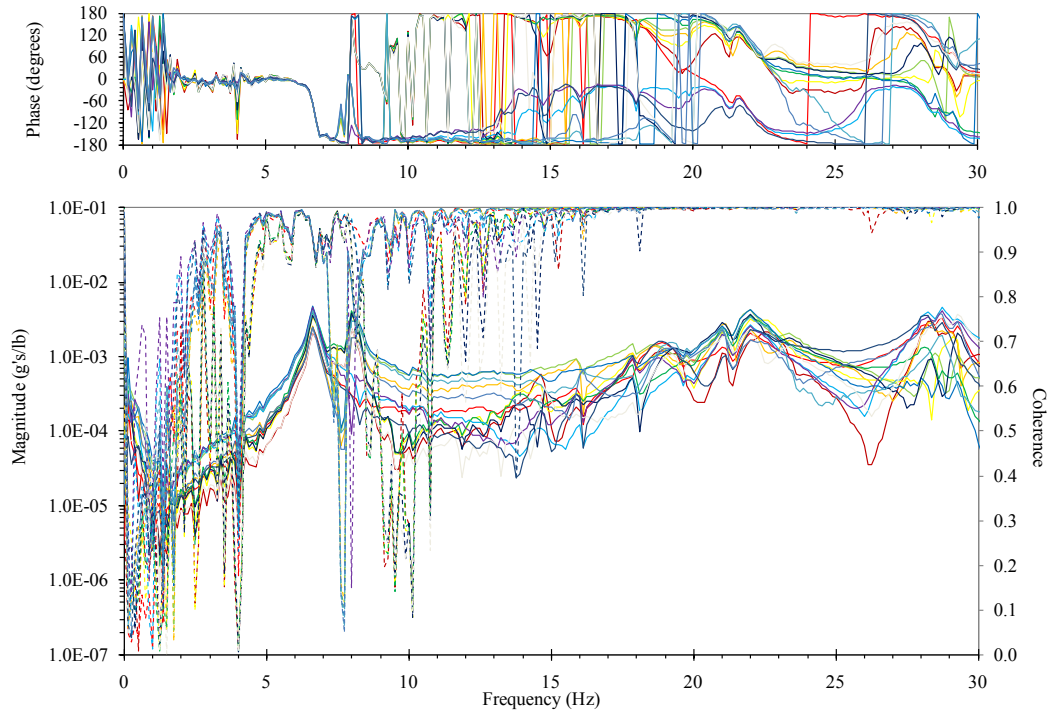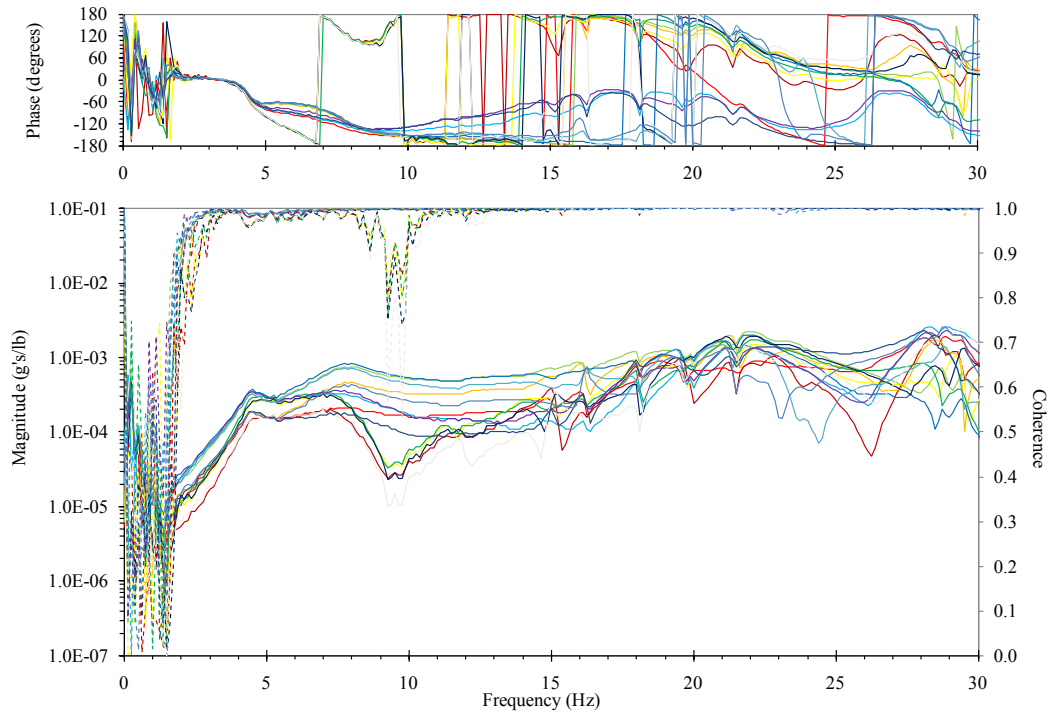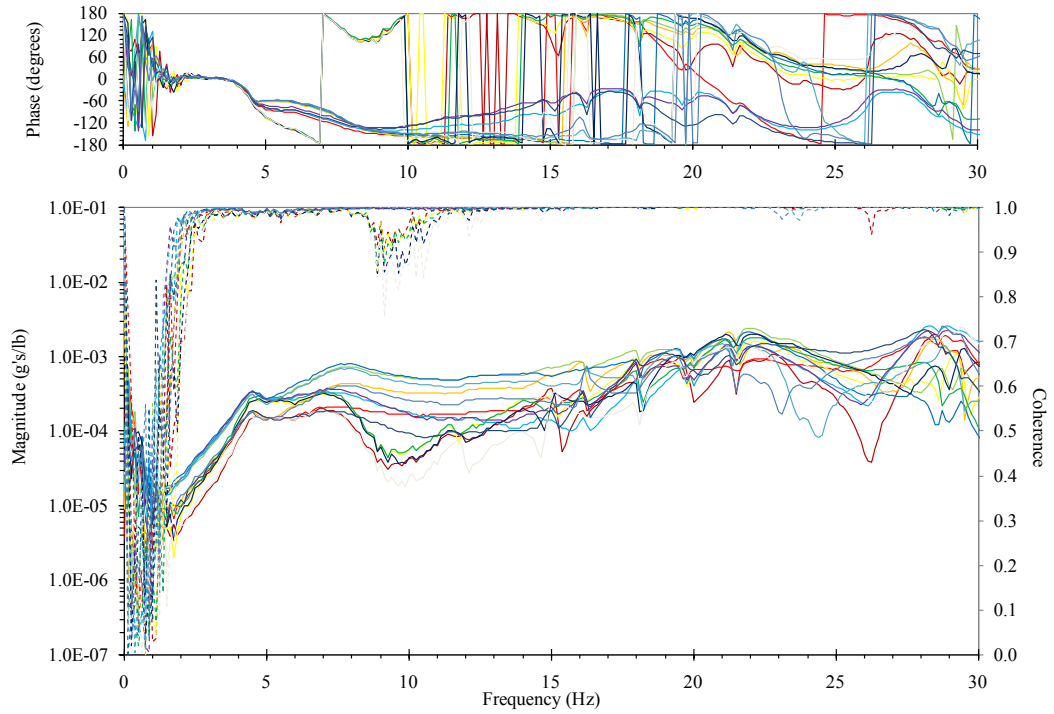
Appendix H: Frequency values obtained from curve fitting experimental FRFs with ME'scope.

Table 9: Frequency data obtained from experimental testing (set-1).

Mass ratio	Dens	Pos	Set	Damped Frequency (Hz)				
			Mode	1	2	3	4	5
			Raebel	7.1	8.9	19.3	23.9	29.5
			DG11	6.8				
			Empty	6.6	8.2	18.4	21.8	27.5
0.02	--	Sta	1	6.6	8.2	18.7	21.7	27.6
0.02	--	Sta	2	6.6	8.2	18.7	21.9	27.4
0.02	--	Ben	1	6.6	8.2	18.7	21.8	27.3
0.02	--	Ben	2	6.6	8.2	18.7	21.8	27.5
0.02	--	Sea	1	6.6	8.2	18.4	21.8	27.5
0.02	--	Sea	2	6.6	8.2	18.7	21.9	27.5
0.02	Eq. mass		1	6.5	8.2	18.3	21.4	27.1
0.08	D	Sta	1	6.6	8.3	18.5	22.1	28.0
0.08	D	Sta	2	6.6	8.2	18.5	22.1	28.0
0.08	D	Ben	1	6.6	8.2	18.5	22.0	27.9
0.08	D	Ben	2	6.6	8.2	18.5	22.0	27.7
0.08	D	Sea	1	6.7	8.3	18.5	21.9	27.8
0.08	D	Sea	2	6.7	8.2	18.4	22.0	27.8
0.08	Eq. mass		1	6.2	8.2	18.4	19.2*	26.3
0.08	Eq. mass		2	6.2	8.2	18.4	19.1*	26.3
0.16	D	Sta	1	5.5	8.2	18.7	22.4	28.6
0.16	D	Sta	2	5.7	8.2	18.6	22.5	28.4
0.16	D	Ben	1	6.7	8.2	18.6	22.2	28.3
0.16	D	Ben	2	6.7	8.2	18.6	22.2	28.5
0.16	D	Sea	1	6.8	8.3	18.5	22.0	28.0
0.16	D	Sea	2	6.7	8.3	18.5	21.9	27.9
0.16	S	Sta	1	5.6	8.3	18.6	22.4	28.5
0.16	S	Sta	2	5.8	8.3	18.7	22.4	28.1
0.16	S	Ben	1	6.6	8.2	18.6	22.1	28.0
0.16	S	Ben	2	6.7	8.2	18.7	22.1	28.0
0.16	S	Sea	1	6.8	8.2	18.7	22.0	27.9
0.16	S	Sea	2	6.7	8.2	18.7	21.9	28.1
0.16	Eq. mass		1	5.9	8.1	18.0	18.5*	26.2
0.16	Eq. mass		2	5.9	8.1	18.0	18.5*	26.1

(Note: D – dense, S – sparse, Sta – standing with straight knees, Ben – standing with bent knees, Seat – seated, Eq. mass – equivalent mass, * - multiple frequencies with the same mode shape)

Table 10: Frequency data obtained from experimental testing (set-2).

Mass ratio	Dens	Pos	Set	Damped Frequency (Hz)				
				1	2	3	4	5
0.33	D	Sta	1	4.9	8.3	19.0	22.6	29.0
0.33	D	Sta	2	5.0	8.2	19.1	22.4	29.0
0.33	D	Ben	1	6.8	8.2	18.9	21.9	28.4
0.33	D	Ben	2	6.8	8.2	18.9	22.0	28.4
0.33	D	Sea	1	5.0*	8.1	18.5	21.9	28.8
0.33	D	Sea	2	5.0	8.0	18.9	20.8*	28.3
0.33	S	Sta	1	5.0	8.1	19.2	22.4	28.6
0.33	S	Sta	2	5.0	8.0	19.2	22.5	28.6
0.33	S	Ben	1	6.7	8.0	18.9	22.1	28.5
0.33	S	Ben	2	6.7	8.0	19.0	22.2	28.5
0.33	S	Sea	1	5.9	7.7	19.0	20.8*	28.1*
0.33	S	Sea	2	5.6	7.9	19.0	21.8	28.3
0.43	D	Sta	1	4.4	8.4	19.3	22.4	29.4
0.43	D	Sta	2	4.5	8.3	19.3	22.4	29.4
0.43	D	Ben	1	6.8	8.2	19.0	22.0	28.9
0.43	D	Ben	2	6.7	8.2	19.0	22.2	28.8
0.43	D	Sea	1	4.6	8.0	18.7	21*	29.1
0.43	D	Sea	2	4.7	8.0	19.1	19.9*	29.3
0.43	S	Sta	1	4.5	8.2	19.4	22.6	29*
0.43	S	Sta	2	4.6	8.0	19.3	22.5	28.6
0.43	S	Ben	1	6.7	8.1	19.0	21.1*	28.4*
0.43	S	Ben	2	6.7	8.1	19.0	22.0	28.3
0.43	S	Sea	1	4.7	7.6	19.2	21.1*	28.4*
0.43	S	Sea	2	4.5	7.6	19.1	21.1*	28.3*

Appendix I: Damping values obtained from curve fitting experimental FRFs with ME'scope.

Table 11: Damping data obtained from experimental testing (set-1).

Mass ratio	Dens	Pos	Set	Damping (%)				
			Mode	1	2	3	4	5
			Raebel	0.20	0.25	0.27	0.35	0.28
			Empty	0.5	0.3	0.7	0.7	0.7
0.02	--	Sta	1	2.5	0.2	0.8	1.1	1.0
0.02	--	Sta	2	2.6	0.2	0.8	1.1	1.0
0.02	--	Ben	1	0.8	0.2	0.8	0.9	1.0
0.02	--	Ben	2	0.7	0.3	0.9	0.9	1.1
0.02	--	Sea	1	2.0	0.3	1.0	0.8	1.1
0.02	--	Sea	2	2.3	0.3	0.7	0.9	1.1
0.02	Eq. mass		1	0.5	0.2	0.6	0.8	0.7
0.08	D	Sta	1	12.2	0.8	0.8	1.9	1.4
0.08	D	Sta	2	10.5	0.8	0.8	2.0	1.0
0.08	D	Ben	1	2.7	0.5	0.8	1.8	1.0
0.08	D	Ben	2	2.2	0.4	0.8	1.7	1.0
0.08	D	Sea	1	7.7	0.9	0.7	1.8	1.1
0.08	D	Sea	2	7.8	0.9	0.7	2.3	1.3
0.08	Eq. mass		1	0.4	0.3	0.7	1.1*	1.0
0.08	Eq. mass		2	0.4	0.3	0.7	0.7*	0.9
0.16	D	Sta	1	11.0	1.8	1.1	2.0	1.4
0.16	D	Sta	2	14.2	2.1	1.1	1.4	0.9
0.16	D	Ben	1	5.6	0.9	0.9	2.0	1.2
0.16	D	Ben	2	2.4	0.5	0.9	1.9	0.4
0.16	D	Sea	1	13.6	1.8	1.3	2.3	1.3
0.16	D	Sea	2	12.3	1.8	1.3	2.6	1.7
0.16	S	Sta	1	11.7	1.9	1.5	1.1	0.7
0.16	S	Sta	2	16.5	1.8	1.6	2.5	1.0
0.16	S	Ben	1	3.8	0.7	1.4	2.4	1.2
0.16	S	Ben	2	3.3	0.6	1.3	2.1	1.2
0.16	S	Sea	1	12.7	2.0	2.0	2.5	1.0
0.16	S	Sea	2	14.1	2.0	2.0	2.5	1.1
0.16	Eq. mass		1	0.2	0.4	0.5	1.0*	1.2
0.16	Eq. mass		2	0.3	0.4	0.5	0.7*	1.4

Table 12: Damping data obtained from experimental testing (set-2).

Mass ratio	Dens	Pos	Set	Damping (%)				
				1	2	3	4	5
0.33	D	Sta	1	8.8	7.2	2.1	1.9	1.0
0.33	D	Sta	2	13.6	6.5	2.2	2.9	1.5
0.33	D	Ben	1	5.2	2.2	1.6	2.7	1.0
0.33	D	Ben	2	6.0	2.4	1.7	2.3	1.5
0.33	D	Sea	1	15.1*	10.0	0.8	2.5	0.7
0.33	D	Sea	2	17.7	9.7	2.2	2.2*	3.3
0.33	S	Sta	1	11.9	12.7	2.9	2.8	1.6
0.33	S	Sta	2	15.0	13.2	2.9	2.8	1.6
0.33	S	Ben	1	5.3	3.9	2.3	2.4	1.0
0.33	S	Ben	2	6.3	4.6	2.0	0.5	0.8
0.33	S	Sea	1	18.0	8.9	2.8	2.2*	2.1*
0.33	S	Sea	2	22.5	11.2	2.6	2.5	1.4
0.43	D	Sta	1	14.8	8.1	2.5	2.9	1.9
0.43	D	Sta	2	11.5	8.0	2.6	3.0	2.4
0.43	D	Ben	1	2.3	1.1	2.0	2.2	1.0
0.43	D	Ben	2	2.0	0.9	2.0	1.9	1.2
0.43	D	Sea	1	9.6	10.1	0.6	2.8*	1.0
0.43	D	Sea	2	9.0	10.7	2.5	0.4*	0.5
0.43	S	Sta	1	11.3	12.2	1.9	3.0	1.3*
0.43	S	Sta	2	15.2	11.3	2.3	2.9	1.4
0.43	S	Ben	1	2.0	1.2	2.5	1.4*	1.1*
0.43	S	Ben	2	1.8	0.8	2.6	2.2	1.2
0.43	S	Sea	1	13.2	12.1	3.3	2.6*	1.9*
0.43	S	Sea	2	12.5	11.2	3.1	2.1*	1.9*

Appendix J: Sample calculation used for SDOF model.

SDOF Calculations

Given:

Structure mass (calculate) $m_{st} := 271.18 \dfrac{lb \cdot s^2}{ft}$

Structure frequency (from experimental) $f_{st} := 6.65 Hz$

Structure damping (from experimental) $c_{st\_percent} := 0.5$

Calculations:

1. Calculate structure stiffness

$$k := f_{st}^2 \cdot m_{st} = 1.199 \times 10^4 \frac{lb}{ft}$$

2. Calculate structure critical damping

$$c_{c\_st} := 2 \cdot m_{st} \cdot f_{st} = 3.607 \times 10^3 \frac{lb \cdot s}{ft}$$

3. Calculate damping

$$c_{st} := c_{c\_st} \cdot \frac{c_{st\_percent}}{100} = 18.033 \frac{lb \cdot s}{ft}$$

Appendix K: Matlab scripts used for SDOF model.

```matlab
%%%%%%%%%%%%%%%%%%%%%%%%%%%%%%%%%%%%%%%%%%%%%%%%%%%%%%%%%%%%%%%%%%%%%%%%%%%%%%%%% ⤶
%%%%
% two_dof
%
% This is a script file that curve fits an experimental FRF based on ⤶
varied
% occupant properties including stiffness, damping, and frequency.  The
% output includes all possible combinations of properties that meet the
% tolerance levels assigned
%
%
%%%%%%%%%%%%%%%%%%%%%%%%%%%%%%%%%%%%%%%%%%%%%%%%%%%%%%%%%%%%%%%%%%%%%%%%%%%%%%%%% ⤶
%%%%
%
% Author: Robert J. Firman
% Date: 31-Mar-10
% Bucknell University
%
%%%%%%%%%%%%%%%%%%%%%%%%%%%%%%%%%%%%%%%%%%%%%%%%%%%%%%%%%%%%%%%%%%%%%%%%%%%%%%%%% ⤶
%%%%

clc
clear
format compact
tic

% Define variable ranges
occ_stiff=(50:100:8050);
occ_damp_perc=(10:5:70);
occ_freq=(3:0.2:6);

l_occ_s=length(occ_stiff);
l_occ_d=length(occ_damp_perc);
l_occ_f=length(occ_freq);

% Define tolerance level
tol=0.05;

% Define constants
structf=4.88;
min_f=structf-structf*tol/2.5;
max_f=structf+structf*tol/2.5;

pk_frf=0.00048;
min_pk_frf=pk_frf-pk_frf*tol*30;
max_pk_frf=pk_frf+pk_frf*tol*30;
```

126

```matlab
% Define curve fitting limits
lower_ratio=4;
upper_ratio=1.548;

min_lr=lower_ratio-lower_ratio*tol*5;
max_lr=lower_ratio+lower_ratio*tol*5;

min_ur=upper_ratio-upper_ratio*tol*5;
max_ur=upper_ratio+upper_ratio*tol*5;

x=1;
q=1;
check1=0;
check2=0;
check3=0;




for i=1:l_occ_f
    for j=1:l_occ_d
        for k=1:l_occ_s
            occ_s=occ_stiff(k);
            occ_d=occ_damp_perc(j);
            occ_f=occ_freq(i);
            [freq,frf]=mystery_frf(occ_s,occ_d,occ_f);
            fn_mag=max(frf(1,901:1101));
            for m=901:1101
                if frf(m)==fn_mag
                    loc=m;
                end
            end
            fn=freq(loc);
            lower=fn_mag/frf(701);
            upper=fn_mag/frf(1101);
            %Check peak frequency
            if fn>=min_f && fn<=max_f
                check1=check1+1;
                %Check peak magnitude
                if fn_mag>=min_pk_frf && fn_mag<=max_pk_frf
                    check2=check2+1;
                    %Check lower point
                    if lower>=min_lr && lower<=max_lr
                        check3=check3+1;
                        %Check upper point
                        if upper>=min_ur && upper<=max_ur
                            ans(x,:)=frf;
```

127

```
                              prop(x,1)=fn;
                              prop(x,2)=fn_mag;
                              prop(x,3)=(fn-structf)/structf;
                              prop(x,4)=(lower-lower_ratio)/lower_ratio;
                              prop(x,5)=(upper-upper_ratio)/upper_ratio;
                              prop(x,6)=(prop(x,3)+prop(x,4)+prop(x,5))↙
/3;
                              prop(x,7)=occ_s;
                              prop(x,8)=occ_d;
                              prop(x,9)=occ_f;
                              x=x+1;
                        end
                    end
                end
            else
                %disp 'sorry, try again'
            end
            q=q+1;
        end
    end
end
toc
```

```matlab
function [f,xf_abs] = sdof_frf(os,odp,of)
%%%%%%%%%%%%%%%%%%%%%%%%%%%%%%%%%%%%%%%%%%%%%%%%%%%%%%%%%%%%%%%%%%%%%%%%%% ↙
%%%%
% SDOF FRF
%
% This is a script file to solve a 2 DOF system given the mass, ↙
damping,
% and stiffness matrices in dimensionless units.  The output includes
% poles, residues (modal coefficients) and frequency response ↙
functions.
%
%
%%%%%%%%%%%%%%%%%%%%%%%%%%%%%%%%%%%%%%%%%%%%%%%%%%%%%%%%%%%%%%%%%%%%%%%%%% ↙
%%%%
%
% Original Author: Randall J. Allemang
% Date: 18-Apr-94
% Structural Dynamics Research Lab
% University of Cincinnati
%
%%%%%%%%%%%%%%%%%%%%%%%%%%%%%%%%%%%%%%%%%%%%%%%%%%%%%%%%%%%%%%%%%%%%%%%%%% ↙
%%%%
%
% Revised: Robert J. Firman
% Date: 31-Mar-10
% Bucknell University
%
%%%%%%%%%%%%%%%%%%%%%%%%%%%%%%%%%%%%%%%%%%%%%%%%%%%%%%%%%%%%%%%%%%%%%%%%%% ↙
%%%%


pi=3.14159265;

% Define constants
stm=271;
sts=11992;
std=18;
om=90;

% Convet damping ratio from percentage
od=odp/100*(2*om*of);



mass=[stm,0;0,om];
stiff=[sts+os,-os;-os,os];
damp=[std+od,-od;-od,od];
```

```matlab
null=[0,0;0,0];

% For 2n x 2n state space equation.
a=[null,mass;mass,damp];
b=[-mass,null;null,stiff];
[x,d]=eig(-inv(a)*b);

% Sort modal frequencies
orig_lambda=diag(d);
[Y,I]=sort(imag(orig_lambda));
lambda=orig_lambda(I);
xx=x(:,I);

% Normalize x matrix
for ii=1:4
    xx(1:4,ii)=xx(1:4,ii)./xx(3,ii);
end

% Extract modal vectors from state-space formulation
psi(1:2,1)=xx(3:4,1);
psi(1:2,2)=xx(3:4,2);

% Calculate modal mass matrix
mm=psi.'*mass*psi;

% Calculate modal scaling value (Q)
Q(1)=1./(2*j*imag(lambda(1))*mm(1,1));
Q(2)=1./(2*j*imag(lambda(2))*mm(2,2));

% Calculate residue matrices
A1=Q(1).*psi(1:2,1)*psi(1:2,1).';
A2=Q(2).*psi(1:2,2)*psi(1:2,2).';

% Formulate H(1,2) FRF as Default
resp=1;
inp=2;

residu(1)=A1(resp,inp);
residu(2)=A2(resp,inp);
A1;A2;

magA1=abs(A1);
phaseA1=angle(A1).*360.0./(2.0*pi);
magA2=abs(A2);
phaseA2=angle(A2).*360.0./(2.0*pi);
magA1;phaseA1;
magA2;phaseA2;
```

130

```
lambda;residu;


f=linspace(0,50,10001);
xf1=residu(1)./(j.*f-lambda(1))+residu(1)'./(j.*f-lambda(1)');
xf2=residu(2)./(j.*f-lambda(2))+residu(2)'./(j.*f-lambda(2)');
xf=xf1+xf2;
xf_abs=abs(xf);
```

Appendix L: FRFs comparing experimental results and 2DOF models.
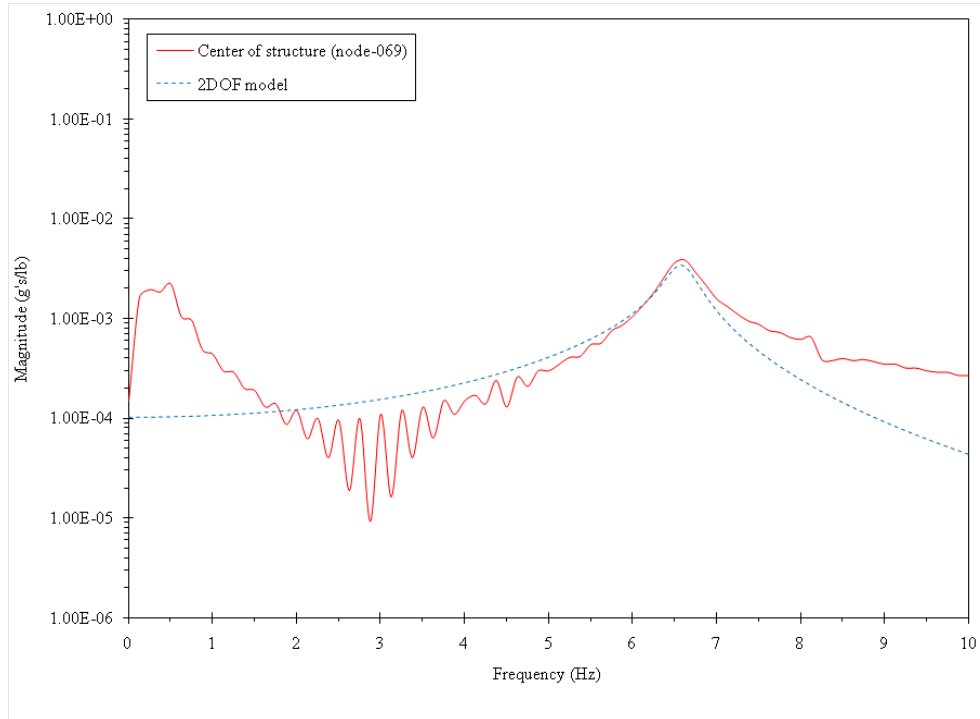

Figure 85: FRF comparison between experimental results and 2DOF model for a mass ratio of 0.02.
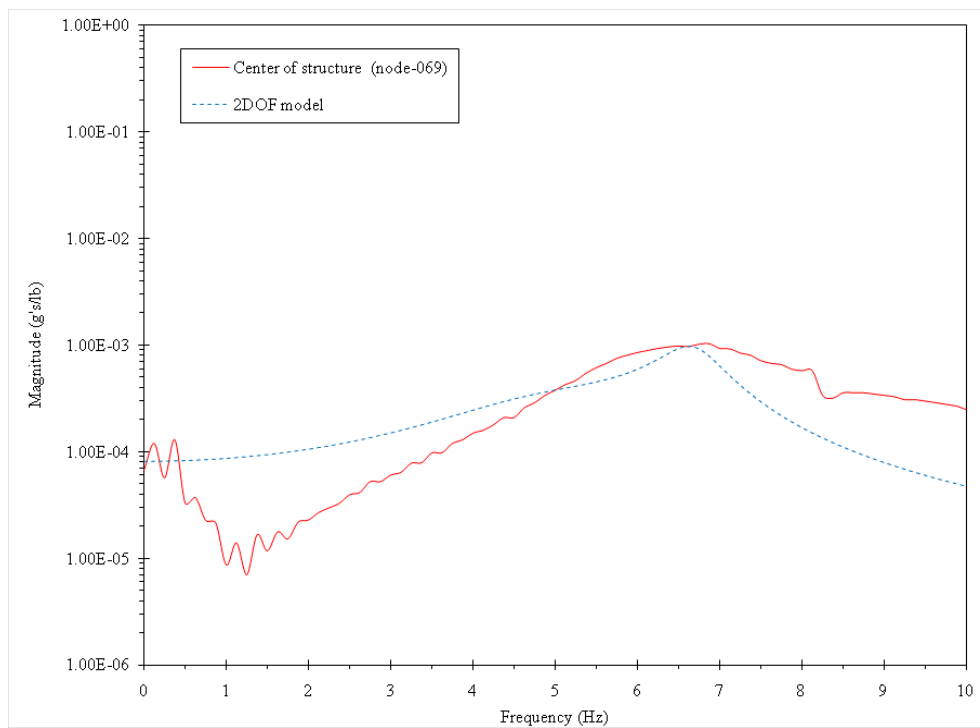

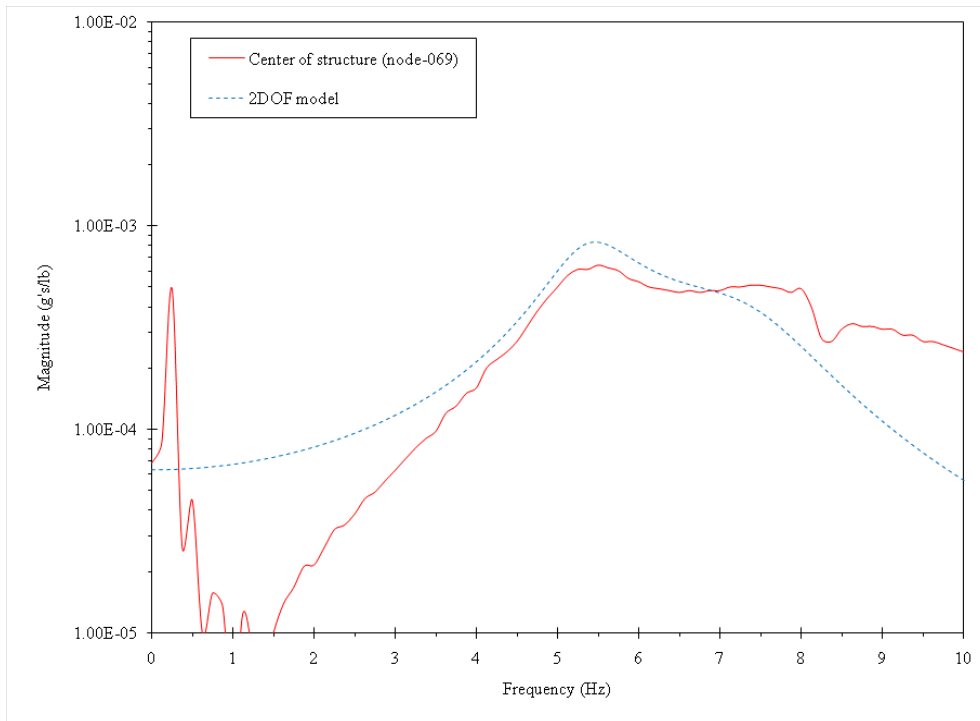Figure 86: FRF comparison between experimental results and 2DOF model for a mass ratio of 0.08.

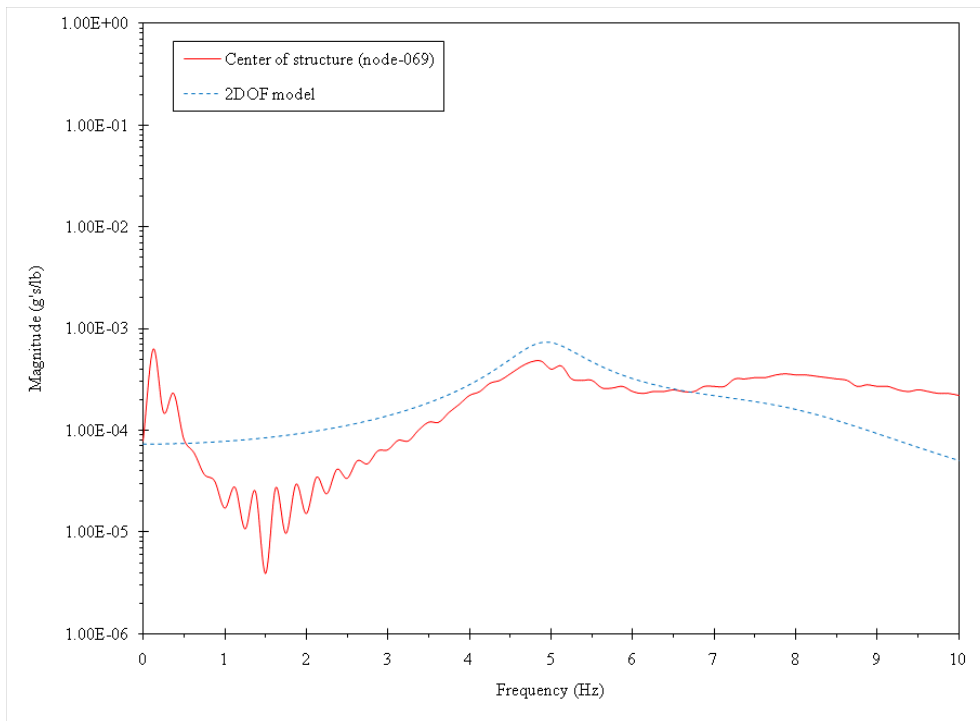Figure 87: FRF comparison between experimental results and 2DOF model for a mass ratio of 0.16.

Figure 88: FRF comparison between experimental results and 2DOF model for a mass ratio of 0.33.

REFERENCES

Allemang, Randall J. "ME 554 Experimental Modal Analysis: Supplemental Notes." The Pennsylvania State University Department of Mechanical and Nuclear Engineering, 1994. Print.

APS Dynamics - Systems for Generating Controlled Vibration (APS). Web. 07 Apr. 2010. <http://www.apsdynamics.com/>.

Avitabile, Peter. "Basics of Modal Analysis for the New/young Engineer." Presented at IMAC-XXVIII, Jacksonville, FL, 2010.

Avitabile, Peter. "Experimental Modal Analysis: A Simple Non-Mathematical Presentation." *Sound and Vibration* (2001): 1-11. Print.

Beavers, Timothy A. "Fundamental Natural Frequency of Steel Joist Supported Floors." Thesis. Virginia Polytechnic Institute and State University, 1998. Print.

Bernan. *Guide to Safety at Sports Grounds - Fifth Edition*. Stationery Office Books (TSO), 2008. Print.

Brownjohn, J.M.W. *Energy Dissipation in One-way Slabs with Human Participation*. Proc. of Asia-Pacific Vibration Conference 1999, Nanyang Technological University, Singapore. Vol. 1. 1999. Print.

Computers and Structurs, Inc. (2005), SAP2000 Manual: Linear and Nonlinear Static and Dynamic Analysis and Design of Three-dimensional Structures.

Dougill, J.W. *Recommendations for Design of Grandstands Subject to Dynamic Crowd Excitation*. Proc. of 6th European Conf. on Structural Dynamics (EURODYN 2005). Munich, Germany: European Association for Structural Dynamics (EASD), 2005. 491-96. Print.

Duarte, Ernesto, and Tianjian Ji. "Action of Individual Bouncing on Structures." *Journal of Structural Engineering* (2009): 818-27. Print.

Ebrahimpour, Arya, and Ronald L. Sack. "A Review of Vibration Serviceability Criteria for Floor Structures." *Computers and Structures* 83 (2005): 2488-494. Print.

Ellis, B.R., and T. Ji. *Human-structure Interaction in Vertical Vibrations*. Proc. of ICE: Structures and Buildings. Vol. 122, No.1. 1997. 1-9. Print.

Ewins, D. J. *Modal Testing: Theory, Practice, and Application*. Baldock, Hertfordshire, England: Research Studies, 2000. Print.

Falati, S. "The Contribution of Non-structural Components to the Overall Dynamic Behavior of Concrete Floor Slabs." Thesis. University of Oxford, 1999. Print.

Geschwindner, Louis F. *Unified Design of Steel Structures*. Hoboken, New Jersey: J. Wiley & Sons, 2008. Print.

Harrison, R.E., S. Yao, J.R. Wright, A. Pavic, and P. Reynolds. "Human Jumping and Bobbing Forces on Flexible Structures: Effect of Structural Properties." *Journal of Engineering Mechanics* (2008): 663-75. Print.

Hothan, S. "Einfluβ Der Verkehrslast - Mensch - Auf Das Eigen-schwingungsverhalten Von Fuβgängerbrücken und Die Auslegung Linearer Tilger." Thesis. University of Hannover, 1999. Print.

The Institution of Structural Engineers (IStructE). *Dynamic Performance Requirements for Permanent Grandstands Subject to Crowd Action: Interim Guidance on Assessment and Design*. Institution of Structural Engineers, 2001. Print.

Kappos, Andreas J. *Dynamic Loading and Design of Structures*. London: Spon, 2002. Print.

Lenzen, K.H. "Vibration of Steel Joist-concrete Slab Floors." *American Institute of Steel Construction (AISC) Engineering Journal* 6th ser. 3.133 (1966). Print.

Littler, J.D. "Retractable Grandstands: Dynamic Response." *Information Paper 4/00, Building Research Establishment (BRE)* (2000). Print.

MASTAN2. Web. 02 May 2010. <http://www.mastan2.com/index.html>.

Measurement Computing - The Value Leader in Data Acquisition (IOtech). Web. 07 Apr. 2010. <http://www.mccdaq.com/>.

Murray, T.M., D.E. Allen, and E.E. Ungar. *Floor Vibrations Due to Human Activity*. American Institute of Steel Construction (AISC), 1997. Print. Steel Design Guide Series, No.11.

PCB Piezotronics, Inc.- Sensors That Measure Up! (PCB) Web. 07 Apr. 2010. <http://www.pcb.com/>.

Raebel, Christopher H. "Development of an Experimental Protocol for Floor Vibration Assessment." Thesis. The Pennsylvania State University, 2000. Print.

Sachse, R., A. Pavic, and P. Reynolds. "Human-Structure Dynamic Interaction in Civil Engineering Dynamics." *The Shock and Vibration Digest* 35 (2003): 3-18. Print.

Sim, Jackie H. "Human-Structure Interaction in Cantilever Grandstands." Thesis. University of Oxford, 2006. Print.

Vibrant Technology, Inc. - Modal Analysis, ODS, Acoustic, and Finite Element Analysis Software (ME'scope). Web. 07 Apr. 2010. <http://www.vibetech.com/go.cfm/en-us/content/index>.

Wasserman, D.E., and J.M. Wasserman. "The Nuts and Bolts of Human Exposure to Vibration." *Sound and Vibration* 36 (2002): 40-41. Print.